

# Polarization Measurements on Nuclear Gamma Rays\*

LAWRENCE W. FAGG,† *Nucleonics Division, U. S. Naval Research Laboratory, Washington, D. C.*

AND

STANLEY S. HANNA,† *Physics Division, Argonne National Laboratory, Lemont, Illinois*

## TABLE OF CONTENTS

<p>I. Theoretical Survey . . . . . 711</p> <p>  A. Introduction . . . . . 711</p> <p>  B. Linear Polarization Distribution . . . . . 712</p> <p>  C. Circular Polarization Distribution . . . . . 717</p> <p>II. Polarization-Sensitive Processes . . . . . 719</p> <p>  A. Compton Effect . . . . . 719</p> <p>    (a) Sensitivity to Plane Polarization . . . . . 719</p> <p>    (b) Sensitivity to Circular Polarization . . . . . 720</p> <p>  B. Photodisintegration of the Deuteron . . . . . 722</p> <p>  C. Photoelectric Effect . . . . . 724</p> <p>  D. Other Polarization-Sensitive Processes . . . . . 725</p> <p>    (a) Pair Production . . . . . 725</p> <p>    (b) Nuclear Photoeffect . . . . . 726</p> <p>    (c) Photofission . . . . . 726</p> <p>III. Measurements of Polarization of Nuclear Gamma Rays . . . . . 726</p> <p>  A. Measurement of Plane Polarization by Means of the Compton Effect . . . . . 726</p> <p>    (a) Early Experiments on Annihilation Radiation . . . . . 727</p> <p>    (b) Direction-Polarization Correlation . . . . . 727</p> <p>    (c) Experiments of Metzger and Deutsch . . . . . 728</p> <p>    (d) Other Measurements with Radioactive Sources . . . . . 730</p> <p>    (e) Measurements on Gamma Rays from Nuclear Reactions and Coulomb Excitation . . . . . 733</p> <p>    (f) Measurements on Gamma Rays from Aligned Nuclei . . . . . 734</p> <p>  B. Measurement of Plane Polarization by Means of the Photodisintegration of the Deuteron . . . . . 735</p> <p>    (a) Experimental Considerations . . . . . 735</p> <p>    (b) Experiments Using Nuclear Emulsions . . . . . 736</p> <p>  C. Measurement of Plane Polarization by Means of the Photoelectric Effect . . . . . 737</p> <p>  D. Measurement of Circular Polarization by Means of the Compton Effect . . . . . 737</p>	<p>    (a) Experimental Considerations . . . . . 738</p> <p>    (b) Measurements on Gamma Rays from Nuclei (Parity Conserving Reactions) . . . . . 739</p> <p>    (c) Beta-Gamma Circular Polarization Correlation . . . . . 741</p> <p>  E. Tabulation of Polarization Experiments on Nuclear Gamma Rays . . . . . 744</p> <p>  Bibliography . . . . . 756</p> <p style="text-align: center;"><b>I. THEORETICAL SURVEY</b></p> <p style="text-align: center;"><b>A. Introduction</b></p> <p>THE investigation of gamma radiation has encompassed all the important properties of electromagnetic radiation: energy, intensity as a function of energy and direction of propagation, multipolarity, and polarization. The emission of gamma rays of discrete and characteristic energies was associated early with the existence of sharp, well-defined energy levels in nuclei, whose properties determine the intensities (transition probabilities) of the radiations. Of equal interest are the radiation patterns (angular distributions) of emitting nuclei which have been oriented in some prescribed fashion, for the spatial distribution is intimately connected to the multipole character of the radiation (My 38, Ha 40). By relatively simple measurements, therefore, it is often possible to establish the multipolarity of a gamma ray, at least in the case of a pure multipole.</p> <p>There still remains an essential ambiguity, since the radiation may be either electric or magnetic. This property is associated with the parity of the radiation. The ambiguity in the parity is immediately resolved if the linear polarization of the radiation is known (Fa 48, Ha 48). Moreover, a knowledge of the polarization can be used to untangle the results in the case of mixed multipoles (Zi 50). It is sometimes possible to resolve such ambiguities with indirect arguments based on observations of associated phenomena. The measurement of polarization, however, provides a direct means of attack on such problems.</p> <p>The radiation from nuclei may also be circularly polarized and a measurement of this polarization provides valuable additional information (Go 46, Fa 49, Ha 51, To 52, St 53). In a discussion of linear and circular polarization two types of nuclear orientation are distinguished, <i>alignment</i> and <i>polarization</i>. In the</p>
--	--

\* Work performed partly under the auspices of the U. S. Atomic Energy Commission.

† LWF now at Atlantic Research Corporation, 901 N. Columbus Street, Alexandria, Virginia. SSH—Visiting Guggenheim Fellow (1958–1959), Clarendon Laboratory, Oxford, England.

TABLE I. Summary of conditions which produce nuclear alignment or polarization, and the corresponding types of correlations. The abbreviations dir, pol, circ, and align stand for direction, (linear) polarization, circular polarization, and alignment, respectively. The symbol LT(B) represents a low temperature orientation of the Bleaney type which produces alignment, LT(RG) represents a method of the Rose-Gorter type which leads to polarization. In each case only the most complex condition or correlation is listed. Thus if the circular polarization of the initial gamma ray is measured, its direction also is measured and one may have a dir-dir or dir-pol correlation as well as a circ-circ correlation.

Initial particle	Initial condition	Type of orientation	Type of correlation
$p, n$ , etc.	dir	align	$p$ - $\gamma$ dir-pol
$p, n$ , etc.	pol	pol	$p$ - $\gamma$ pol-circ
$\beta$	dir	pol	$\beta$ - $\gamma$ dir-circ
$\gamma$	dir	align	$\gamma$ - $\gamma$ dir-pol
$\gamma$	pol	align	$\gamma$ - $\gamma$ pol-pol
$\gamma$	circ	pol	$\gamma$ - $\gamma$ circ-circ
...	LT(B)	align	"align"-pol
...	LT(RG)	pol	"pol"-circ

case of *alignment* an axis of rotational symmetry is established, but the sense of this axis is not determined. In the case of *polarization* an axis is established which provides a single preferred direction in space. If the spin of the nuclear state is  $j$  and its component along the axis is  $m$  and if the (relative) population of the  $m$ th sublevel is  $w(m)$ , then the condition for alignment is  $w(m) = w(-m)$  and that for polarization is  $w(m) \neq w(-m)$ . If the  $w(m)$  are all equal, the nuclei are not oriented.

From an assemblage of aligned nuclei the radiation can show linear polarization but not circular polarization (Ha 48). Only if there is nuclear polarization will there be a component of circular polarization. Moreover, the processes which produce nuclear orientation can be classified according to the type of orientation which is produced, either alignment or polarization. In Table I the various processes are summarized and classified in this manner and the possible polarization correlation for each case is listed (in addition to the references already cited, see Si 51, Wo 49, To 52a, Si 53a, Le 56). This tabulation illustrates the formal way of designating a correlation. For example, a  $\gamma$ - $\gamma$  direction-polarization correlation represents the measurement made on a  $\gamma$ - $\gamma$  cascade in which the (linear) polarization of one gamma ray is determined relative to the direction of the other gamma ray. Two general methods are available for producing orientation. In one a nuclear particle is observed with or without polarization, and in the other an external or atomic field is employed at very low temperature.

The literature on the theory of direction-direction correlations is voluminous and detailed (see the comprehensive list of references given in De 57a). In the present survey, the theoretical results are presented (without derivation) in a manner which stresses the application to polarization experiments in order to provide a basis for the discussion in Part III.

## B. Linear Polarization Distribution

The general expression for the intensity distribution of linearly polarized radiation has been given in several different forms by many authors (Ha 48, Zi 50, Ll 52, St 53, To 53, Sa 53, Si 53a, Bi 53, Sa 55b, Ma 58). The various expressions are equivalent and differ only superficially to cover different experimental situations or degrees of complexity. In this review we give three forms, two of which are generally appropriate for the direction-polarization correlation but differ enough to make one or the other preferable in certain problems, while the other is designed specifically for the case of nuclear orientation at low temperature. It is convenient to make such a classification, partly for historical reasons, although in many instances the differences are hardly more than a matter of nomenclature.

The direction-direction correlation for two radiations in a nuclear process is given in a concise form by (Co 53, Bi 53, De 57a)

$$W(\theta) = \sum_{\nu} A_{\nu}(1)A_{\nu}(2)P_{\nu}(\cos\theta). \quad (\text{I-1})$$

Here  $P_{\nu}(\cos\theta)$  is the ordinary Legendre polynomial,  $\theta$  is the angle between the directions of the two radiations, and 1 and 2 stand for sets of quantum numbers for the first and second radiations, respectively. The summation over  $\nu$  is over all integral values (including zero) for which the coefficient of  $P_{\nu}(\cos\theta)$  does not vanish. If we let  $1 \rightarrow L_1 L_1' j j'$  and  $2 \rightarrow L_2 L_2' j j'$  and sum the expression over all allowed sets of values of these quantum numbers, we can treat problems in which both the intermediate state and the radiations are of a mixed nature. The quantities  $L_n$  and  $L_n'$  represent possible values of the total angular momentum (multipolarity) of the  $n$ th radiation, while  $j$  and  $j'$  are possible total angular momenta for the intermediate state. Because of their great complexity, problems of this general type have not been studied extensively, especially in connection with polarization studies of gamma rays.

In most of the cases which have been studied experimentally, the intermediate state is characterized by unique spin and parity and the radiations are mixtures involving not more than two components. With these restrictions Eq. (I-1) is greatly simplified, not so much in form as in the complexity of the computation. We adhere to the notation which seems to provide the greatest ease in calculation through the use of published tables. The summation in Eq. (I-1) is now restricted to the even integers (including zero) and, after setting  $j = j'$  for the intermediate state, the factorization of the coefficient of  $P_{\nu}(\cos\theta)$  is complete. Hence, writing out the summation over the  $L$ 's explicitly, we have (Bi 53, Fe 55)

$$A_{\nu}(n) = F_{\nu}(L_n L_n j_n j) + 2\delta_n F_{\nu}(L_n L_n' j_n j) + \delta_n^2 F_{\nu}(L_n' L_n' j_n j), \quad (\text{I-2})$$

which is the expression that is applicable to gamma radiation. The intensity ratio of the  $L_n$  and  $L_n'$  radiation is denoted by  $\delta_n^2$  ( $\delta_n$  is real) and  $j_n$  is the total angular momentum of the  $n$ th state, i.e., either the initial (1) or the final (2) state. Equation (I-1), is normalized so that  $A_0(n)=1+\delta_n^2$ . The most complete compilation of the functions  $F_\nu(L_n L_n' j_n j)$  is that given in Fe 55 which covers all cases of apparent interest for even  $\nu$ .

If the  $n$ th radiation is a material particle (e.g., an alpha particle), then it is only necessary to replace each  $F_\nu(L_n L_n' j_n j)$  in Eq. (I-2) by  $F_\nu(L_n L_n' j_n j) b_\nu(L_n L_n')$  and  $\delta_n$  by  $\delta_n \cos \xi$  (leaving  $\delta_n^2$  unchanged, however), where the "particle factor" (Bi 53) is

$$b_\nu(LL') = \frac{2[L(L+1)L'(L'+1)]^{\frac{1}{2}}}{L(L+1)+L'(L'+1)-\nu(\nu+1)}, \quad (\text{I-3})$$

and  $\xi$  is an appropriate phase angle. If, in addition, the particle has a spin, it is convenient to employ the channel spin formalism. The total correlation function is then an incoherent superposition of the functions corresponding to each value of the channel spin obtained by compounding the spins of the two interacting particles. In beta decay and in Coulomb excitation the particle factors are more complex in that they involve specific features of the interactions. These factors are discussed in Al 56 (Coulomb excitation) and Bi 53 (beta decay). The  $\beta$ - $\gamma$  circular polarization correlation is discussed in Sec. C following.

If unobserved intervening radiations are present, (I-1) is generalized (Sa 54), for transitions between nuclear states of well-defined spin and parity, to

$$W(\theta) = \sum_\nu A_\nu(1)U_\nu(2) \cdots U_\nu(n-1)A_\nu(n)P_\nu(\cos\theta). \quad (\text{I-1}')$$

The function

$$U_\nu(m) = (-1)^{im+1-im-L_m} [(2j_{m+1}+1)(2j_m+1)]^{\frac{1}{2}} \times W(j_m j_m j_{m+1} j_{m+1}; \nu L_m)$$

is inserted for each unobserved transition  $j_m(L_m)j_{m+1}$ . The quantity  $W(j_m j_m j_{m+1} j_{m+1}; \nu L_m)$  is the Racah coefficient. For mixed radiation  $U_\nu(L_m) + \delta_m^2 U_\nu(L_m')$  (nor-

TABLE II(a). Numerical values of  $P_\nu^{(2)}(\cos\theta)$ .

$\nu \backslash \cos\theta$	2	3	4	5	6
0	3.00	0	-7.50	0	13.12
0.1	2.97	1.49	-6.90	-5.05	10.70
0.2	2.88	2.88	-5.18	-8.87	4.19
0.3	2.73	4.10	-2.52	-10.46	-4.21
0.4	2.52	5.04	0.76	-9.18	-11.41
0.5	2.25	5.62	4.22	-4.92	-14.15
0.6	1.92	5.76	7.30	1.61	-10.11
0.7	1.53	5.35	9.30	8.81	0.69
0.8	1.08	4.32	9.40	13.90	14.16
0.9	0.57	2.56	6.65	12.82	20.13
1.0	0	0	0	0	0

TABLE II(b). Numerical values of the coefficients  $\kappa_\nu(LL')$ .

$LL' \backslash \nu$	2	3	4	5	8
11	-1/2				
12	-1/6	-1/6			
13	-1/12	-1/12	-1/12		
22	1/2	0	-1/12		
23	-1/4	1/4	-1/60	-1/20	
33	1/3	0	1/3	0	-1/30

malized to  $1+\delta_m^2$ ) is used. The intervening radiation may be any kind of particle.

The prescription for obtaining the linear polarization distribution in a direction-polarization experiment can now be stated simply as follows. In each term of (I-1) characterized by  $(L_2 L_2')$  and  $\nu$ , replace  $P_\nu(\cos\theta)$  by the expression (Ll 52, Sa 55b, De 57a),

$$P_\nu(\cos\theta) + (\pm)_{L_2'} \cos 2\gamma \kappa_\nu(L_2 L_2') P_\nu^{(2)}(\cos\theta). \quad (\text{I-4})$$

Without loss of generality it is assumed that the linear polarization is observed for the second radiation. The direction of the linear polarization is specified by  $\gamma$ , the angle between the polarization vector and the plane of the reaction. In practice only two values of  $\gamma$  (0 and  $90^\circ$ ) are usually considered, so that  $\cos 2\gamma = \pm 1$ . In the discussion of the experiments, the intensities of polarized radiation for these two directions is designated by  $J_0$  and  $J_{90}$  or  $J_{11}$  and  $J_1$  ( $J_\theta, J_\phi$  are also used in the literature). The quantity often given is the ratio  $J_0/J_{90}$ , although theoretically the polarization excess or difference ( $J_0 - J_{90}$ ) is the more natural quantity, as pointed out by Fano (Fa 49). Thus we write

$$P_1 W(\theta) = (J_0 - J_{90}) = \sum (\pm)_{L_2'} A_\nu \kappa_\nu(L_2 L_2') P_\nu^{(2)}(\cos\theta), \quad (\text{I-5})$$

which may be normalized to the total unpolarized intensity

$$W(\theta) = (J_0 + J_{90}) = \sum A_\nu P_\nu(\cos\theta) \quad (\text{I-6})$$

if so desired. In these expressions the coefficient  $A_\nu(1)A_\nu(2)$  or  $A_\nu(1)U_\nu(2) \cdots A_\nu(n)$  has been shortened to  $A_\nu$  and the sum is over  $\nu$  and whatever quantum numbers are appropriate. The  $P_\nu^{(2)}(\cos\theta)$  appearing in the polarization distribution is the unnormalized associated Legendre function. Numerical values for  $P_\nu^{(2)}(\cos\theta)$  are given in Table II(a). The other quantity  $\kappa_\nu(LL')$  appearing in (I-4) depends on the multipolarity of the radiation. It is given by (Ll 52)

$$\kappa_\nu(LL') = - \left[ \frac{(\nu-2)!}{(\nu+2)!} \right]^{\frac{1}{2}} \frac{C(LL'\nu, 11)}{C(LL'\nu, 1-1)}, \quad (\text{I-7})$$

where  $C(LL'\nu, 11)$  is the familiar vector addition coefficient. Numerical values for these coefficients are presented in Table II(b). Finally, in (I-4) the + or -

TABLE III(a). Numerical values of the coefficients in the series  $a_\nu(LL) = \sum_n \alpha_n A_n(LL)$ . For odd  $\nu$ , all  $\alpha_n = 0$ .

$L$	$\nu$	$\alpha_2$	$\alpha_4$	$\alpha_6$
1	0	-1		
	2	1		
2	0	1	-1/6	
	2	-1	-5/6	
	4	0	1	
3	0	2/3	2/3	-1/15
	2	-2/3	10/3	-1/3
	4	0	-4	-9/15
	6	0	0	1

sign is to be employed according as the  $2L_2'$ -pole radiation is electric or magnetic in character.†

For the case of mixed radiation from a single intermediate level the polarization distribution can be written more explicitly as

$$W(\theta, \gamma) = W(\theta) + (\pm)_{L_2'} \cos 2\gamma \sum_\nu A_\nu(1) \mathcal{Q}_\nu(2) P_\nu^{(2)}(\cos \theta). \quad (\text{I-8})$$

The sum is over even  $\nu$  (excluding zero). The coefficient  $A_\nu(1)$  is given by (I-2) or a suitable modification, if the first radiation is not a gamma ray or there are intervening radiations. The new coefficient  $\mathcal{Q}_\nu(2)$  differs only in the inclusion of the  $\kappa$ 's with appropriate signs [so as to leave unchanged the sign convention in (I-8)]. Thus

$$\begin{aligned} \mathcal{Q}_\nu(2) = & -\kappa_\nu(L_2 L_2') F_\nu(L_2 L_2' j_2 j) \\ & + 2\delta_2 \kappa_\nu(L_2 L_2') F_\nu(L_2 L_2' j_2 j) \\ & + \delta_2^2 \kappa_\nu(L_2' L_2') F_\nu(L_2' L_2' j_2 j). \end{aligned} \quad (\text{I-9})$$

In this case  $L_2' = L_2 + 1$ .

In a number of the problems studied experimentally, the complexity of the direction-direction correlation is limited to  $\nu = 0$  and 2. The direction-polarization correlation then becomes [with  $\mathcal{Q}_2 = A_2(1) \mathcal{Q}_2(2)$ ]

$$W = A_0 + A_2 P_2 \pm \cos 2\gamma \mathcal{Q}_2 P_2^{(2)}. \quad (\text{I-10})$$

Unless the directional correlation is nearly isotropic, a measurement of the polarization easily determines the correct sign in this expression and hence the parity of the radiation. The measurement can also be decisive in removing an ambiguity regarding the mixture of the radiation, as can be seen by inspecting (I-9) and Table II(b). There is one interesting exception in this particular example, namely, the case of pure dipole or pure quadrupole radiation. For both  $L = 1$  and  $L = 2$  we have, using (I-9) and Table II(b)

$$W = 1 + A_2 P_2 \pm \frac{1}{2} \cos 2\gamma A_2 P_2^{(2)} \quad (\text{I-10}')$$

† Most authors give this condition in more elegant fashion by defining a quantity  $\sigma$  equal to 0 or 1 depending on the character of the radiation. Since there is no unanimity in the definition of this quantity, we prefer the foregoing statement (De 57a) in the hope of reducing confusion. The sign convention depends on the direction chosen for  $\gamma = 0$  and on the sign used in (I-7).

and for  $\theta = 90^\circ$ , we have

$$\frac{J_0}{J_{90}} = \frac{1 - \frac{1}{2} A_2 \pm \frac{3}{2} A_2}{1 - \frac{1}{2} A_2 \mp \frac{3}{2} A_2}. \quad (\text{I-10}'')$$

However, this expression does not hold for a dipole-quadrupole mixture. It is a quite general result that the polarization measurement can provide vital information on mixtures in addition to the determination of parity.

The earliest development of the theory (Ha 48, Zi 50) gave a somewhat different but entirely equivalent form for the direction-polarization correlation function, which has been used extensively in experimental work. If the direction-direction correlation is expressed as in (I-6), then the second form of the direction-polarization correlation which we treat is obtained simply by replacing the coefficient  $A_\nu(L_2 L_2')$  in each term by §

$$A_\nu(L_2 L_2') + (\pm)_{L_2'} a_\nu(L_2 L_2') \cos 2\gamma. \quad (\text{I-11})$$

The angle  $\gamma$  and the sign convention are the same as used in the foregoing. In this prescription the new coefficients  $a_\nu$  can be expressed in terms of the old ones  $A_\nu$ . Writing the series in  $\cos^2 \theta$  as well as in  $P_\nu(\cos \theta)$ , we have

$$W(\theta) = \sum A_\nu(L_2 L_2') P_\nu(\cos \theta) = \sum Q_\nu(L_2 L_2') \cos^2 \theta \quad (\text{I-12})$$

$$\begin{aligned} P_1 W(\theta) = & \sum (\pm)_{L_2'} a_\nu(L_2 L_2') P_\nu(\cos \theta) \\ = & \sum (\pm)_{L_2'} q_\nu(L_2 L_2') \cos^2 \theta \end{aligned} \quad (\text{I-13})$$

$$a_\nu(L_2 L_2') = \sum_n \alpha_n A_n(L_2 L_2') \quad (\text{I-14})$$

$$q_\nu(L_2 L_2') = \sum_n \beta_n Q_n(L_2 L_2'). \quad (\text{I-14}')$$

The coefficients  $\alpha_n$  and  $\beta_n$  depend on  $L_2$ ,  $L_2'$ , and  $\nu$ . Numerical values for these coefficients are provided in Table III for pure multipoles, in Table IV for mixed radiation of the same parity, and in Table V for mixed radiation of opposite parity. We note here that  $\alpha_0 = \beta_0 = \alpha_1 = \beta_1 = 0$ . Many examples of the use of this formula-

TABLE III(b). Numerical values of the coefficients in the series  $q_\nu(LL) = \sum_n \beta_n Q_n(LL)$  (cf. Zi 50, Ha 48). For odd  $\nu$ , all  $\beta_n = 0$ .

$L$	$\nu$	$\beta_2$	$\beta_4$	$\beta_6$
1	0	-1		
	2	1		
2	0	1	1	
	2	-1	-2	
	4	0	1	
3	0	2/3	0	-1/3
	2	-2/3	4	19/3
	4	0	-4	-7
	6	0	0	1

§ This substitution is obtained from the one used in the foregoing by expanding the associated Legendre function in terms of the ordinary functions.

tion occur in the literature. We cite here the case of the pure octupole gamma ray in the reaction  $F^{19}(\beta, \alpha)O^{16*}$ ,  $(\gamma)O^{16}$ ,  $E_\gamma = 6.1$  Mev. At  $E_p = 0.33$  Mev it is known that the proton is captured in an  $s$ -state, so that the  $\alpha$ - $\gamma$  emission can be treated as an independent two-stage process. From the measurement of the direction-direction correlation (Ar 50, Ba 50) one selects the theoretical result

$$W(\theta) = 1 + 111 \cos^2\theta - 305 \cos^4\theta + 225 \cos^6\theta. \quad (I-15)$$

With the aid of Table III(b), one finds directly for the direction-polarization correlation for an octupole radiation

$$P_1W(\theta) = \pm \frac{1}{3} [(2Q_2 - Q_6) - (2Q_2 - 12Q_4 - 19Q_6) \cos^2\theta - (12Q_4 + 21Q_6) \cos^4\theta + 3Q_6 \cos^6\theta]. \quad (I-16)$$

Inserting the numerical values of the direction-direction coefficients, one has

$$P_1W(\theta) = \pm [-1 + 131 \cos^2\theta - 355 \cos^4\theta + 225 \cos^6\theta]. \quad (I-17)$$

The linear polarization is complete at  $\theta = 118^\circ$  (or  $62^\circ$ ), i.e., at that angle  $J_0/J_{90} = 0$  or  $\infty$  depending on whether the radiation is magnetic or electric. The measurement of this quantity is discussed in Part III.

A problem frequently encountered is that of the dipole-quadrupole mixture in the radiation from a discrete level. From Tables III(a) and IV(a) we obtain

$$\begin{aligned} a_0(11) &= -A_2(11) & a_0(12) &= -\frac{1}{3}A_2(12) \\ a_0(22) &= A_2(22) - \frac{1}{6}A_4(22) \\ a_2(11) &= A_2(11) & a_2(12) &= \frac{1}{3}A_2(12) \\ a_2(22) &= -A_2(22) - \frac{5}{6}A_4(22) \\ a_4(22) &= A_4(22). \end{aligned} \quad (I-18)$$

TABLE IV(a). Numerical values of the coefficients in the series  $a_\nu(LL') = \sum_n \alpha_n A_n(LL')$  for even  $\nu$ .

L	L'	$\nu$	$\alpha_2$	$\alpha_4$
1	2	0	-1/3	
		2	1/3	
1	3	0	-1/6	-1/6
		2	1/6	-5/6
		4	0	1
2	3	0	-1/2	-1/30
		2	1/2	-1/6
		4	0	1/5

TABLE IV(b). Numerical values of the coefficients in the series  $q_\nu(LL') = \sum_n \beta_n Q_n(LL')$  for even  $\nu$  (cf. Zi 50).

L	L'	$\nu$	$\beta_2$	$\beta_4$
1	2	0	-1/3	
		2	1/3	
1	3	0	-1/6	-1
		2	1/6	1
		4	0	1
2	3	0	-1/2	-2/5
		2	1/2	1/5
		4	0	1/5

TABLE V(a). Numerical values of the coefficients in the series  $a_\nu(LL') = \sum_n \alpha_n A_n(LL')$  for odd  $\nu$ .

L	L'	$\nu$	$\alpha_2$	$\alpha_4$
1	2	1	-1	
		3	1	
1	3	1	-1/2	
		3	1/2	
2	3	1	3/2	-3/10
		3	-3/2	-7/10
		5	0	1

TABLE V(b). Numerical values of the coefficients in the series  $q_\nu(LL') = \sum_n \beta_n Q_n(LL')$  for odd  $\nu$ .

L	L'	$\nu$	$\alpha_2$	$\alpha_4$
1	2	1	-1	
		3	1	
1	3	1	-1/2	
		3	1/2	
2	3	1	3/2	2
		3	-3/2	-3
		5	0	1

Inserting these quantities into (I-13), we find (changing the sign of the dipole term)

$$P_1W(\theta) = \pm [(A_2 - \frac{4}{3}A_2(12) - \frac{1}{6}A_4) - (A_2 - \frac{4}{3}A_2(12) + \frac{5}{6}A_4)P_2 + A_4P_4]. \quad (I-19)$$

In this expression  $A_2$  and  $A_4$  are coefficients of the total correlation function, while  $A_2(12)$  is the mixed coefficient. From this result we obtain at  $\theta = 90^\circ$  and for even parity ( $M1 + E2$ )

$$J_0 = A_0 + A_2 + A_4 - 2A_2(12) \quad (I-20)$$

$$J_{90} = A_0 - 2A_2 - \frac{1}{4}A_4 + 2A_2(12). \quad (I-21)$$

This example is a generalization of the one given above, (I-10').

The third form of the direction-polarization correlation arises because of the convenience of discussing certain problems in terms of the magnetic sublevels of the radiating state as has been recognized by many authors. Because of the obvious physical insight provided by the method in the study of nuclear orientation, it has been the starting point of theoretical developments in this field (St 52a, To 53). Hence, we write

$$W(\theta) = \sum_m w(m) I_m^{LL}(\theta), \quad (I-22)$$

where  $I_m^{LL}(\theta)$  is the intensity distribution of  $2^L$ -pole radiation from the  $m$ th sublevel of the radiating state of angular momentum  $j$ ,  $w(m)$  is the relative population of this sublevel, and the summation over  $m$  is from  $-j$  to  $j$ . If the angular momentum  $j_f$  of the final state is greater than zero, then we have further:

$$I_m^{LL}(\theta) = \sum_M |C(jLj_f; mM)|^2 F_M^{LL}(\theta), \quad (I-23)$$

where the coefficient is the vector addition coefficient

TABLE VI(a). The functions  $F_M^{LL'}(\theta)$  and  $f_M^{LL'}(\theta)$ , both given in the form  $K\sum C_n P_n(\cos\theta)$ . In each case  $F_M^{LL'}(\theta)$  is tabulated on the first line and  $f_M^{LL'}(\theta)$  on the second line. The upper sign corresponds to  $M > 0$ ; the lower to  $M < 0$ .

$L$	$L'$	$ M $	$K$	$C_0$	$C_2$	$C_4$	$C_6$
1	1	1	1	2	1		
				-1	1		
		0	1	2	-2		
				2	-2		
1	2	1	$\pm\frac{1}{3}\sqrt{15}$	0	3		
				-1	1		
		0	...	0	0		
				0	0		
2	2	2	1/21	42	-30	-12	
				-28	40	-12	
		1	1/21	42	15	48	
				7	-55	48	
		0	1/21	42	30	-72	
				42	30	-72	
2	3	2	$\pm(350)^{1/2}/210$	0	-30	30	
				14	-20	6	
		1	$\pm(35)^{1/2}/210$	0	60	150	
				-35	5	30	
		0	...	0	0	0	
				0	0	0	
3	3	3	1/66	132	-165	18	15
				-99	165	-81	15
		2	1/66	132	0	-42	-90
				-22	-110	222	-90
		1	1/66	132	99	6	225
				55	-121	-159	225
		0	1/66	132	132	36	-300
				132	132	36	-300

and  $F_M^{LL}(\theta)$  is the intensity distribution of an  $(L, M)$ -pole. Associated with each  $F_M^{LL}(\theta)$  there is of course a distribution function  $f_M^{LL}(\theta)$  for linear polarization. Then,

$$F_M^{LL}(\theta, \gamma) = F_M^{LL}(\theta) \pm \cos 2\gamma f_M^{LL}(\theta) \quad (\text{I-24})$$

can be inserted in place of  $F_M^{LL}(\theta)$  in (I-23) to produce the direction-polarization distribution (generalized to mixed radiation), namely,

$$W(\theta, \gamma) = \sum_m w(m) \sum_M \sum_{LL'} C(L)C(L')\delta_L \delta_{L'} \times [F_M^{LL'}(\theta) \pm \cos 2\gamma f_M^{LL'}(\theta)]. \quad (\text{I-25})$$

(Agreement with previous notation is obtained if  $\delta_L = 1$ ). The  $F_M^{LL'}(\theta)$  and  $f_M^{LL'}(\theta)$  are given in Table VI.

There are several empirical examples of angular distributions which correspond to a single  $(L, M)$  pole. The reaction  $F^{19}(\phi, \alpha)O^{16}(\gamma)O^{16}$  has already been cited. In Table IV we see that the distributions given in (I-15, I-17) correspond to a pure  $(3, 1)$ -pole. A second example is the capture reaction,  $H^2(\phi, \gamma)He^3$ . The measured directional distribution is fitted very closely by the function  $F_0^{11}(\theta) \sim \sin^2\theta$ . The polarization distribution is, therefore, [Table IV(b)]

$$F_0^{11}(\theta, \gamma) = (1 \pm \cos 2\gamma)(1 - \cos^2\theta). \quad (\text{I-26})$$

At  $\theta = 90^\circ$  the polarization ratio  $J_0/J_{90} = 0$  or  $\infty$  depending on whether the radiation is magnetic or elec-

tric. The measurement of this quantity is discussed in Part III.

For an angular distribution or correlation it is clearly possible to obtain the population numbers  $w(m)$  from a knowledge of the preceding transitions (Li 49). In a nuclear orientation problem the population numbers are functions of the temperature and of the method used to produce orientation. In a given method they can also depend on specific parameters which may vary from one experiment to the next. The calculation of  $w(m)$  has been treated very thoroughly in the literature and, insofar as possible, general formulas have been provided. In Table VII we list the methods of producing orientation which have been generally discussed and in the last column we give references which deal with the computation of  $w(m)$ .

For purposes of computation it is advantageous to retain as much as possible of the formulation which makes use of the functions  $F_\nu(LL'j_nj)$ . In an equation such as (I-1') it is only necessary to replace the coefficient  $A_\nu(1)$  by an orientation parameter  $B_\nu(j)$  which describes the orientation of the initial state. Equation (I-1') retains its generality. The orientation parameter is merely a linear combination of the population numbers (Gr 55a, Bl 57),

$$B_\nu(j) = (2\nu + 1)^{1/2} \sum_m C(j\nu j; m0)w(m). \quad (\text{I-27})$$

For the linear polarization distribution we need only

TABLE VI(b). The functions  $F_M^{LL'}(\theta)$  and  $f_M^{LL'}(\theta)$ , both given in the form  $k\sum b_n \cos^n\theta$ . In each case  $F_M^{LL'}(\theta)$  is tabulated on the first line and  $f_M^{LL'}(\theta)$  on the second line (cf. Ar 50, Zi 50). The upper sign corresponds to  $M > 0$ ; the lower to  $M < 0$ .

$L$	$L'$	$ M $	$k$	$b_0$	$b_2$	$b_4$	$b_6$
1	1	1	3/2	1	1		
				-1	1		
		0	3/2	2	-2		
				2	-2		
1	2	1	$\pm\frac{1}{3}\sqrt{15}$	-1	3		
				-1	1		
		0	...	0	0		
				0	0		
2	2	2	5/2	1	0	-1	
				-1	+2	-1	
		1	5/2	1	-3	4	
				1	-5	4	
		0	5/2	0	6	-6	
				0	6	-6	
2	3	2	$\pm(175/32)^{1/2}$	1	-6	5	
				1	-2	1	
		1	$\pm\frac{1}{3}\sqrt{35}$	1	-18	25	
				-1	-4	5	
		0	...	0	0	0	
				0	0	0	
3	3	3	7/32	15	-15	-15	15
				-15	45	-45	15
		2	7/32	10	-30	110	-90
				10	-110	190	-90
		1	7/32	1	111	-305	225
				-1	131	-355	225
		0	7/32	12	-132	420	-300
				12	-132	420	-300

the even quantities and of these the following will generally suffice:

$$B_0 = 1$$

$$B_2 = [(1/5)j(j+1)(2j-1)(2j+3)]^{-1/2} \times [\sum_m m^2 w(m) - (1/3)j(j+1)]. \quad (\text{I-28})$$

The calculation of these quantities for the various experimental techniques is discussed in the references given in Table VII.

The orientation parameters are given in To 52 in a form which differs from the  $B$ 's only in normalization. The expression for  $\nu=2$  is

$$f_2 = j^{-2} [\sum_m m^2 w(m) - (1/3)j(j+1)]. \quad (\text{I-29})$$

When the directional distribution has been obtained by any one of the foregoing techniques, the polarization distribution can be derived from it in the usual fashion with the substitution indicated by (I-4) or (I-11).

The polarization-polarization correlation has been discussed by several authors (Fa 48, Ma 51, Ll 52, Bi 53) and a general expression for it can be found in Ll 52. This type of correlation has not received much attention experimentally, since it provides very little additional information (Ha 48, Bi 53) to compensate for the increased experimental difficulties.

In a measurement of the  $\gamma$ - $\gamma$  direction-polarization correlation, it has not always been feasible to distinguish the gamma rays in the detectors. It is then necessary to mix the  $\gamma_1$ - $\gamma_2$  direction-polarization function with the  $\gamma_2$ - $\gamma_1$  function according to the respective efficiencies of detection.

### C. Circular Polarization Distribution

The  $\gamma$ - $\gamma$  circular-circular correlation can be written in concise form (Go 46, Al 57) as

$$W(\theta p_1 p_2) = \sum_{\nu} (-p_1)^{\nu} A_{\nu}(1) (-p_2)^{\nu} A_{\nu}(2) P_{\nu}(\cos\theta). \quad (\text{I-30})$$

The summation is over the odd and even integers

TABLE VII. Some methods of producing nuclear orientation at low temperatures.

Method	Type of orientation	Applied field	References
External field (Brute force)	pol	$>10^5$ gauss	Go 34, Ku 35, Si 51, St 53a, Po 54, Kh 55, St 57a, Bl 57
Magnetic hfs (Rose-Gortler)	pol	$\sim 10^2$ gauss	Go 48, Ro 49, Si 51, St 53a, Po 54, Gr 55a, Va 56, St 57a, Bl 57
Electric hfs (Pound)	align	none	Po 49, Si 51, St 53a, St 57a, Bl 57
Magnetic hfs (Bleaney)	align	none	Bl 51a, Si 51, St 53a, Po 54, Gr 55a, St 57a, Bl 57

(including zero), and  $p_n = \pm 1$  according as the circular polarization of the  $n$ th radiation is right or left handed. The coefficient  $A_{\nu}(n)$  can be obtained from (I-2) which is valid for odd  $\nu$ . The coefficients  $F_{\nu}(L_n L_n' j_n j)$  for odd  $\nu$  have been tabulated in Al 57.

If the expression (I-30) is summed over a  $p_n$ , the total intensity of the corresponding gamma ray is obtained. Thus, we find,

$$W(\theta) = \sum_{p_1 p_2} W(\theta p_1 p_2) = 2 \sum_{p_1} W(\theta p_1 p_2) = 2 \sum_{p_2} W(\theta p_1 p_2) = \sum_{\nu \text{ even}} A_{\nu}(1) A_{\nu}(2) P_{\nu}(\cos\theta), \quad (\text{I-31})$$

which is just the direction-direction correlation. Hence there are no direction-circular (or linear-circular) correlations. If, on the other hand, the excess of circular polarization (right handed minus left handed) is measured for either gamma ray or both, one obtains

$$P_3 W(\theta) = \sum_{p_1 p_2} p_1 p_2 W(\theta p_1 p_2) = 2 \sum_{p_1} p_1 p_2 W(\theta p_1 p_2) = 2 \sum_{p_2} p_1 p_2 W(\theta p_1 p_2) = \sum_{\nu \text{ odd}} A_{\nu}(1) A_{\nu}(2) P_{\nu}(\cos\theta). \quad (\text{I-32})$$

The quantity  $P_3$  is the degree of circular polarization, as defined by Fano (Fa 49). It is analogous to the quantity  $P_1$  defined for the linear polarization [see (I-5)]. In addition, it follows that

$$\sum_{p_1 p_2} p_1 W(\theta p_1 p_2) = \sum_{p_1 p_2} p_2 W(\theta p_1 p_2) = 0,$$

which shows again there is no direction-circular correlation.

In the case of nuclear polarization produced by orientation at low temperatures, we merely identify the coefficient  $A_{\nu}(1)$  in (I-32) with the orientation parameter  $B_{\nu}(j)$ . In terms of the population numbers  $w(m)$ , the most important parameter is (To 52, Bl 57)

$$B_1 = 2\sqrt{3} \sum_m m w(m).$$

or

$$f_1 = j^{-1} \sum_m m w(m). \quad (\text{I-33})$$

References which deal with the computation of these parameters are given in Table VII. The most important feature of  $B_1$  is that its sign depends on the sign of the hfs interaction which produces the nuclear polarization. In turn the sign of the interaction depends on the sign of the nuclear magnetic moment. A measurement of the degree of circular polarization gives the sign in (I-32) and thus yields the sign of the magnetic moment.

|| The term "right handed" is used for a photon with its spin in the direction of its momentum. This definition accords with recent practice, but (unfortunately) not with the "optical" definition.

TABLE VIII. The functions  $g_M^{LL'}(\theta) = K \sum C_n P_n(\cos\theta)$  which give the intensity distribution of circularly polarized radiation for an  $(LL', M)$  pole. The + or - sign corresponds to  $M > 0$  or  $M < 0$ , respectively (cf. St 53).

$L$	$L'$	$ M $	$K$	$C_1$	$C_2$	$C_3$
1	1	1	$\pm 3$	1		
		0	...	0		
1	2	1	$(3/5)^\dagger$	3	2	
		0	$3/(5)^\dagger$	2	-2	
2	2	2	$\pm 1$	2	-2	
		1	$\pm 1$	1	4	
		0	...	0	0	
2	3	2	$(14)^\dagger/21$	-12	7	5
		1	$(35)^\dagger/105$	48	7	50
		0	$(280)^\dagger/105$	-18	-7	25
3	3	3	$\pm 1/6$	9	-14	5
		2	$\pm 1/6$	6	14	-20
		1	$\pm 1/6$	3	14	25
		0	...	0	0	0

The degree of circular polarization can be written in terms of the population numbers directly. In analogy to (I-25) for the case of linear polarization, we have

$$P_3 W(\theta) = \sum_m w(m) \sum_{M LL'} C(L) C(L') \delta_L \delta_{L'} g_M^{LL'}(\theta), \quad (\text{I-34})$$

where  $C(L)$  stands for  $C(jLj_f; mM)$ . The function  $g_M^{LL'}(\theta)$  gives the degree of circular polarization for an  $(LL', M)$  pole. A few of these functions are listed in Table VIII.

Circularly polarized radiation may be produced following the capture or emission of a polarized particle such as a neutron or a proton (Ha 51, Bi 51). The only case of importance so far has been the capture of polarized thermal neutrons as discussed in Part III. Since the orbital angular momentum is zero, there is no complication in applying the formalism of this discussion. In this case  $A_1(1)$  in (I-32) becomes  $\frac{1}{2} F_1(\frac{1}{2}\frac{1}{2}j_1j)$ , by analogy with an absorbed gamma ray. The functions  $F_1(\frac{1}{2}\frac{1}{2}j_1j)$  are tabulated in Table IX. As an example, consider  $j_1=0$ ,  $j=\frac{1}{2}$ ,  $j_2=\frac{1}{2}$ , and  $L=1$ . From Table IX we obtain  $F_1(\frac{1}{2}\frac{1}{2}0\frac{1}{2}) = -2.00$  and in Al 57 we find  $F_1(11\frac{1}{2}\frac{1}{2}) = -1.00$ . Thus (I-32) becomes

$$P_3 = +\cos\theta.$$

At  $\theta=0$  (along the direction of the neutron polarization),  $P_3 = +1$  and the gamma rays are completely circularly polarized (right handed).

TABLE IX. Numerical values of  $F_1(\frac{1}{2}\frac{1}{2}j_1j)$ .

$j_1$	$j$	$F_1(\frac{1}{2}\frac{1}{2}j_1j)$	$j_1$	$j$	$F_1(\frac{1}{2}\frac{1}{2}j_1j)$	$j_1$	$j$	$F_1(\frac{1}{2}\frac{1}{2}j_1j)$
0	1/2	-2.000	2	3/2	0.894	7/2	3	1.000
1/2	1	-1.633	2	5/2	-1.366	7/2	4	-1.291
1	1/2	0.667	5/2	2	0.943	4	7/2	1.018
1	3/2	-1.491	5/2	3	-1.333	4	9/2	-1.277
3/2	1	0.816	3	5/2	0.976	9/2	4	1.033
3/2	2	-1.414	3	7/2	-1.309	9/2	5	-1.265

For the  $\beta$ - $\gamma$  direction-circular correlation (Le 56, Al 57, Ga 57, Mo 57) the formal procedure is the same. For the beta particle, we write (Al 57)

$$A_\nu(\beta) = \sum_{L_1 L_1'} F_\nu(L_1 L_1' j_1 j) b_\nu(L_1 L_1'), \quad (\text{I-35})$$

where  $b_\nu(L_1 L_1')$  is the particle factor for the beta ray. The mixing of multipole orders in the beta radiation is governed by the particle factors which are characteristic of the beta process. The particle factors for allowed beta transitions are given in Table X which is an extension of the table given by Alder *et al.* (Al 57). For the degree of circular polarization, we obtain from (I-32)

$$P_3 = -[A_1(\beta)/A_0(\beta)] A_1(\gamma) P_1(\cos\theta),$$

where

$$A_1(\beta) = [F_1(11j_1j) |M_{GT}|^2 S_1^{(11)} + F_1(01j_1j) |M_{GT}| \cdot |M_F| S_1^{(01)}],$$

$$A_0(\beta) = |M_F|^2 S_0^{(00)} + |M_{GT}|^2 S_0^{(11)}.$$

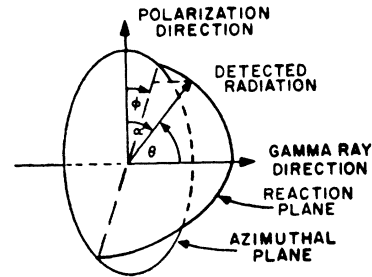


FIG. 1. Angles and vectors involved in a reaction sensitive to the linear polarization of a gamma ray, presented so as to apply to all such reactions discussed. The phrase "detected radiation" can represent a Compton scattered gamma ray, a photoproton from the photodisintegration of the deuteron, etc.

Let

$$S_0^{(00)} = \frac{1}{4} |C_F|^2, \quad S_0^{(11)} = \frac{1}{4} |C_{GT}|^2, \quad a = |C_{GT}/C_F|^2, \quad \text{and } x = a^\dagger M_{GT}/M_F.$$

Then,

$$A_1(\beta)/A_0(\beta) = \frac{2}{3} (p/E) \times [F_1(11j_1j) Gx^2 + F_1(01j_1j) I a^\dagger x] / (1+x^2),$$

where  $\frac{2}{3} (p/E) G = S_1^{(11)}/S_0^{(11)}$  and  $\frac{2}{3} (p/E) I = S_1^{(01)}/S_0^{(11)}$ . This is the form and notation given in Bo 58. The experimental results on the beta-gamma correlation and on the electron distribution from polarized nuclei (Wu 57) have shown that  $G = \pm 1$  for positrons and electrons. As an example, consider the  $\text{Co}^{60}$  decay,  $5(\beta)4(2)2(2)0$ . The beta and gamma radiations are pure. For the first gamma ray, with  $G = -1$ , we find

$$P_3 = \frac{2}{3} (v/c) (0.774) (-0.645) \cos\theta = -\frac{1}{3} (v/c) \cos\theta$$

from the tables in Al 57. For the second gamma ray a factor must be inserted for the unobserved gamma ray [see (I-1')] but the numerical result is the same.



TABLE X. Particle parameters  $b_\nu(LL')$  for allowed beta transitions. The parameter  $b_\nu(LL')$  is the product of the matrix element (ME) and  $S_\nu(LL')$ . The coupling constants are denoted by  $C_S, C_V$ , etc. The energy and momentum of the electron are denoted by  $E$  and  $p$ , and  $\alpha$  is the fine-structure constant. The Fierz interference terms have been put equal to zero (cf. Al 57, Mo 57, Ga 57).

$L$	$L'$	ME	$S_\nu(LL')$
0	0	$ M_F ^2$	$S_0^{(00)} = \frac{1}{4} \{  C_S ^2 +  C_S' ^2 +  C_V ^2 +  C_V' ^2 \}$
1	1	$ M_{GT} ^2$	$S_0^{(11)} = \frac{1}{4} \{  C_T ^2 +  C_T' ^2 +  C_A ^2 +  C_A' ^2 \}$ $S_1^{(11)} = \frac{1}{8} (\rho/E) \{ 2 \operatorname{Re}(C_T C_T'^* - C_A C_A'^*) + (Z\alpha/\rho) \operatorname{Im}(C_T C_A'^* + C_T' C_A^*) \}$
0	1	$ M_F  \cdot  M_{GT} $	$S_0^{(01)} = 0$ $S_1^{(01)} = \frac{1}{8} (\rho/E) \{ \operatorname{Re}(C_S C_T'^* + C_S' C_T^* - C_V C_A'^* - C_V' C_A^*) + (Z\alpha/\rho) \operatorname{Im}(C_S C_A'^* + C_S' C_A^* - C_V C_T'^* - C_V' C_T^*) \}$

## II. POLARIZATION-SENSITIVE PROCESSES

Primary emphasis is given in this part to those processes that have proved the most practicable and useful in the detection of polarization. They are presented in the approximate order of their importance as determined chiefly by the frequency of application. Section D, Part II, contains a brief discussion of some of the processes which have not as yet found use in the study of nuclear gamma rays.

### A. Compton Effect

#### (a) Sensitivity to Plane Polarization

The sensitivity of the Compton effect to the polarization of an incident gamma ray can be obtained from the Klein-Nishina formula (Kl 29, Ni 29) which gives the differential cross section for the process. In almost all cases encountered experimentally the direction of polarization of the scattered photon is not of interest. Thus, for the present discussion the most useful form of the Klein-Nishina expression is the one in which a summation has been made over all directions of polarization of the scattered photon with the result<sup>¶</sup>

$$d\sigma_\phi = \frac{r_0^2 k^2}{2 k_0^2} \left[ \frac{k_0}{k} + \frac{k}{k_0} - 2 \sin^2 \theta \cos^2 \phi \right] d\Omega, \quad (\text{II-1})$$

where  $r_0 = e^2/m_0 c^2$  is the classical radius of the electron,  $d\Omega$  is the element of solid angle into which the photon is scattered,  $\theta$  is the angle through which the incident photon is scattered,  $\phi$  is the angle between the electric vector of the incident photon and the plane of scattering, and  $k_0$  and  $k$  are the energies of the incident and scattered photons, respectively. These energies are related by the expression

$$k = \frac{k_0}{1 + (k_0/m_0 c^2)(1 - \cos\theta)}. \quad (\text{II-2})$$

The angles and vectors involved in a Compton scattering are illustrated in Fig. 1.

The effect of polarization is contained in the  $\cos^2 \phi$  factor of the last term of (II-1) which shows that the

<sup>¶</sup> A more detailed treatment including the derivation of this and other forms of the differential cross section can be found in He 44; see also Ev 55.

scattering is a maximum in the plane normal to the electric vector of the incident photon. As the energy of the incident gamma ray approaches zero the sum of the first two terms in the brackets approaches two. Thus in the limit of zero energy at  $\theta = 90^\circ$  the Compton effect has an ideal response to polarization, i.e., the differential cross section is zero when  $\phi = 0^\circ$  and a maximum when  $\phi = 90^\circ$ . At any given  $\theta$ , an increase in the energy  $k_0$  produces a decrease in the efficiency of analysis as expressed by the asymmetry ratio,  $R = d\sigma_{90}/d\sigma_0$ . Of especial interest is  $\theta_{\max}$ , the value of  $\theta$  which makes  $R$  a maximum for a given energy  $k_0$ . This  $\theta_{\max}$  is  $90^\circ$  for  $k_0 = 0$  and decreases with increasing energy as shown in Fig. 2, which gives values of  $\theta_{\max}$  up to an energy of about 6 Mev. A similar curve for energies up to about 1.5 Mev is given in Me 50.\*\*

Figure 2 also shows the values of  $R$  at  $\theta = \theta_{\max}$  plotted

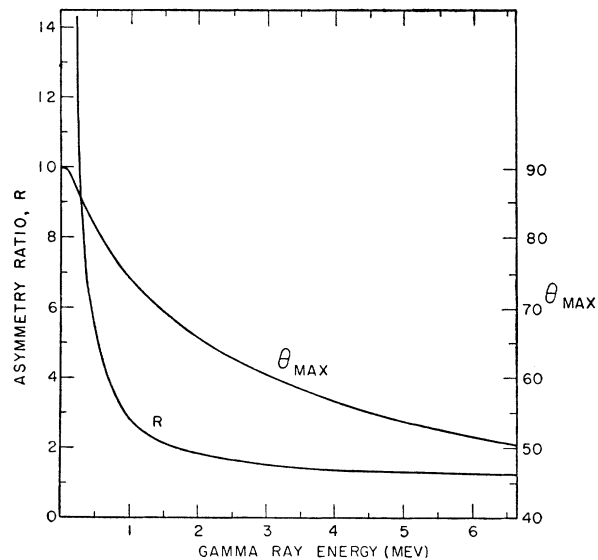


FIG. 2. The Compton scattering angle  $\theta_{\max}$  at which the asymmetry ratio  $R$  is maximum, and the asymmetry ratio  $R$  for  $\theta = \theta_{\max}$  as a function of incident photon energy up to about 6 Mev, the highest energy at which a Compton polarimeter has been used.

\*\* There is disagreement between the latter curve and the one given here, which becomes larger as the energy increases from zero. The reason for this discrepancy is not known: perhaps an approximation valid only in the region of small energy was made in the calculations for the curve in Me 50. In the curve presented here no approximations have been made.

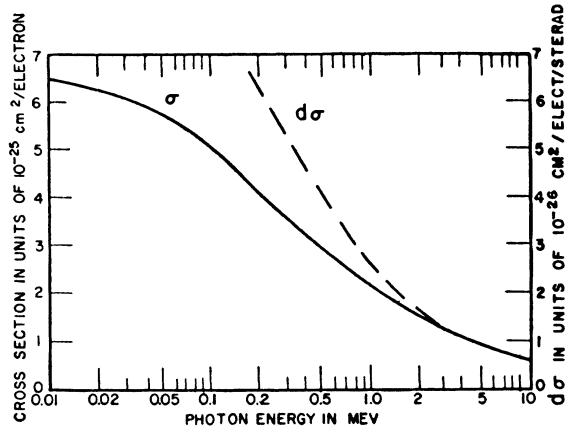


FIG. 3. Total cross section  $\sigma$  for the Compton effect (curve from Da 52a), and the differential cross section  $d\sigma$  at  $\theta=\theta_{\max}$ , as a function of incident photon energy.

as a function of energy. This figure shows that beyond about 2 Mev the value of  $R$  decreases very slowly as it approaches a value of one at infinite energy. Consequently, the Compton effect might in some cases be useful at energies as high as 10 Mev since at least a 10% effect would exist. However, its use at this energy might be somewhat marginal since the values of  $R$  given in Fig. 2 are for an ideal geometry. In any practicable experimental arrangement the value of  $R$  is considerably reduced by the angular spread of the detector apertures. Of course, another consideration involved in the case of the Compton effect at higher energies is the decrease in the cross section with increasing energy as is illustrated in Fig. 3. This decrease is accentuated in the differential cross section at  $\theta=\theta_{\max}$  because of the corresponding increase in the forward peaking in the angular distribution. A discussion of the geometrical considerations associated with the application of the Compton effect to particular polarization experiments is deferred to Part III, Section A(c).

The value of the differential cross section for a Compton scattering at an angle ( $65^\circ$  to  $90^\circ$ ) useful for most polarization analyses is of the order of  $10^{-26}$  cm<sup>2</sup>/sterad/electron for the majority of nuclear gamma rays (see Fig. 3). Figure 2, also shows that the Compton effect furnishes a large efficiency for detection of polarization over quite an extended energy range. The relatively high cross section and large analyzing efficiency, coupled with the relative ease of experimental application, have made the Compton effect the most useful of the polarization-sensitive mechanisms.

#### (b) Sensitivity to Circular Polarization

Interest in the sensitivity of the Compton effect to circular polarization has increased considerably with the recent investigations of nonconservation of parity in weak interactions by means of experiments on the circular polarization of gamma rays following beta

decay. Although the scattering of circularly polarized gamma rays by polarized electrons had been discussed by earlier workers (Bi 51, Ha 51, Cl 52), the first effective experimental study of the effect was made by Gunst and Page (Gu 53). In this work the total cross section is given as  $\sigma=\sigma_0\pm\sigma_1$  where  $\sigma_0$  and  $\sigma_1$  are the parts unaffected and affected, respectively, by circularly polarized gamma rays. Gunst and Page measured the cross section for the effect at  $k_0=2.62$  Mev and found a value of  $\sigma_1/\pi r_0^2=0.089\pm 0.007$  in good agreement with the theoretical value, 0.093, found from expressions calculated by Stehle (see Gu 53). The experiment was done by measuring the difference in intensity of the 2.62-Mev gamma rays from ThC'' which were transmitted through an iron bar 30-cm long when magnetized, and then demagnetized. Although the gamma rays were initially unpolarized, they can be considered as consisting of equal components of right and left circularly polarized radiation. Consequently, when the magnetic field is applied, one of these components is preferentially scattered.

Lipps and Tolhoek (Li 54, Li 54a; see also Fr 38, Fa 49, To 56), have derived the Compton cross section in a general form with all polarizations taken into account,

$$d\sigma=r_0^2(k^2/k_0^2)\Phi(\mathbf{k}_0,\mathbf{k},\xi^0,\xi,\xi^0,\xi)d\Omega, \quad (\text{II-3})$$

where  $\xi^0$ ,  $\xi$ ,  $\xi^0$ , and  $\xi$  are the respective polarization vectors of the incident and scattered photon and of the electron before and after interaction, and  $\Phi(\mathbf{k}_0,\mathbf{k},\xi^0,\xi,\xi^0,\xi)$  is a linear function of these polarization vectors. The function  $\Phi$  can be separated into 16

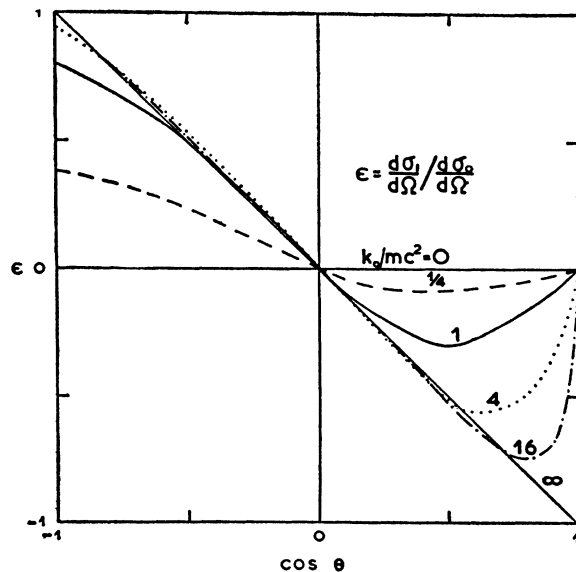


FIG. 4. Polarization-sensitive part  $d\sigma_1$  of the differential Compton cross section for electrons polarized along the axis of incident circularly polarized photons. The curves are normalized to the polarization-insensitive cross section  $d\sigma_0$  and plotted for several energies as a function of  $\cos\theta$ , where  $\theta$  is the angle through which the photon is scattered (figure from Gu 53).

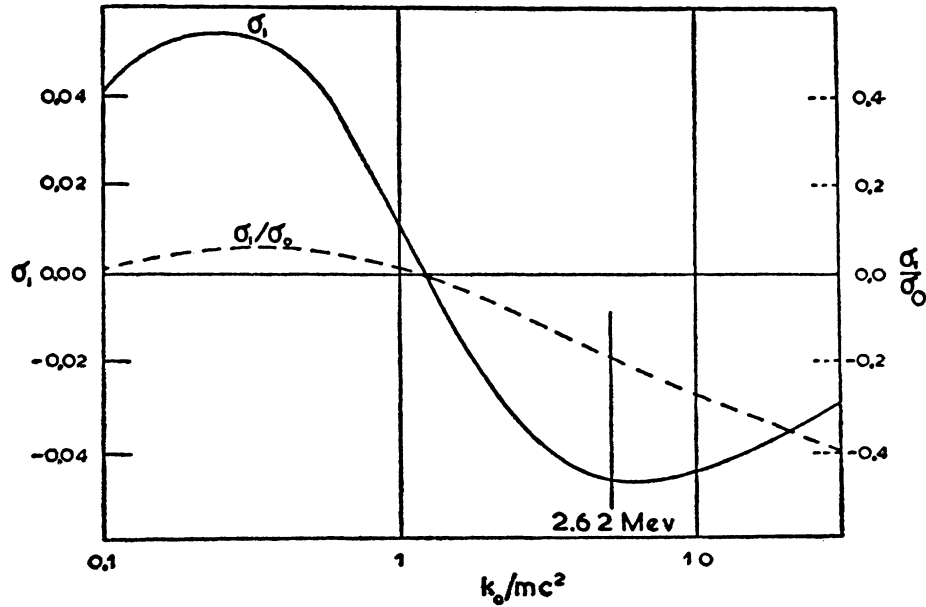


FIG. 5. Polarization-sensitive part  $\sigma_1$  of the total Compton cross section (in units of  $2\pi r_0^2$ ) for the same electron and photon polarizations as in Fig. 4. In the dashed curve  $\sigma_1$  is normalized to  $\sigma_0$ , the polarization-insensitive part of the total cross section. The curves are plotted against incident photon energy (figure from Gu 53).

terms, depending on the 16 different ways of choosing sets of polarization vectors. Thus,

$$\Phi = \Phi_0 + \Phi_1 + \Phi_2 + \Phi_3 + \Phi_4, \quad (II-4)$$

where  $\Phi_0$  is independent of polarizations,

$$\Phi_1 = \Phi_1(\xi^0) + \Phi_1(\xi) + \Phi_1(\zeta^0) + \Phi_1(\zeta), \quad (II-5)$$

$$\begin{aligned} \Phi_2 = & \Phi_2(\xi^0, \xi) + \Phi_2(\zeta^0, \zeta) + \Phi_2(\xi^0, \zeta^0) + \Phi_2(\xi, \zeta) \\ & + \Phi_2(\xi^0, \zeta) + \Phi_2(\xi, \zeta^0), \end{aligned} \quad (II-6)$$

and  $\Phi_3$ , and  $\Phi_4$  depend on 3 and 4 polarization vectors, respectively. Explicit expressions are given in Li 54a for all the  $\Phi_0, \dots, \Phi_4$ .

Thus far, the only experiments performed have involved not more than two polarizations. It is necessary then to average over unobserved initial polarizations and sum over unobserved final polarizations in order to obtain the cross section for some definite experiment. Since the states represented by  $-\xi$  and  $-\zeta$  are orthogonal to those represented by  $\xi$  and  $\zeta$ , the terms which are functions only of the unobserved polarizations will vanish in these averages and sums.

For the case of interest here the initial photon polarization  $\xi^0$  and the initial electron polarization  $\zeta^0$  are specified. For this case, (II-3) takes the form,

$$\begin{aligned} d\sigma(\xi^0, \zeta^0) = & 4r_0^2(k^2/k_0^2) \\ & \times [\Phi_0 + \Phi_1(\xi^0) + \Phi_1(\zeta^0) + \Phi_2(\xi^0, \zeta^0)] d\Omega. \end{aligned} \quad (II-7)$$

In this expression  $\Phi_0$  gives the usual Klein-Nishina formula independent of polarization,  $\Phi_1(\zeta^0) \equiv 0$ , and  $\Phi_1(\xi^0) = 0$  if no linear polarization of the gamma ray is present. Hence, with

$$d\sigma = d\sigma_0 + d\sigma_1 P \quad (II-8)$$

we have (To 56)

$$\begin{aligned} P d\sigma_1 = & 4r_0^2(k^2/k_0^2)\Phi_2(\xi^0, \zeta^0)d\Omega \\ = & -\frac{1}{2}Pr_0^2\left(\frac{k^2}{k_0^2}\right)\left(\frac{k_0}{k} - \frac{k}{k_0}\right)\cos\theta d\Omega. \end{aligned} \quad (II-9)$$

The electron polarization has been taken parallel (or antiparallel) to the direction of the incident photon,†† and  $P$  is the product of the polarizations of the photon and of the electron. ( $P$  is positive for a right circularly polarized gamma ray and an electron spin parallel to the direction of the incident photon.) Equation (II-9) is given in Gu 53. If an integration is performed over  $d\Omega$ , the part of the total cross section dependent on polarization becomes

$$\frac{\sigma_1}{2\pi r_0^2} = \frac{1+4k_0^2+5k^2}{k_0(1+k_0)^2} - \frac{1+k_0}{2k_0^2} \ln(1+2k_0). \quad (II-10)$$

with  $k_0$  in units of  $m_0c^2$ .

The ratio of the differential cross sections  $d\sigma_1/d\sigma_0$  is plotted as a function of  $\cos\theta$  for several energies in Fig. 4. This graph shows the difference in the sign of the response to polarization in the forward and backward quadrants. In general, also, the response at a given angle increases with increasing energy. The polarization-dependent total cross section  $\sigma_1$  is presented as a function of energy in Fig. 5. The change in sign of  $\sigma_1$  at  $E = 1.25m_0c^2 = 0.65$  Mev arises as a result of the difference in sign of  $d\sigma_1$  for forward and backward directions together with the fact that the forward Compton scattering becomes more dominant at higher energies.

†† This condition is easily removed (see Gu 53 and Li 54a).

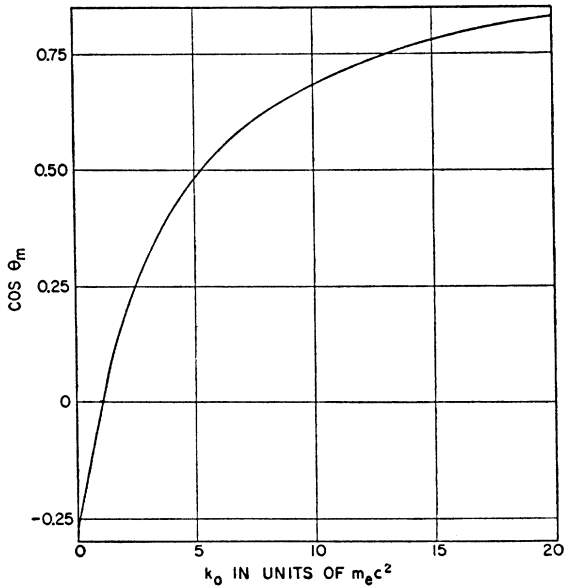


FIG. 6. Cosine of the Compton scattering angle which yields the maximum relative azimuthal anisotropy due to circular polarization, plotted as a function of the incident photon energy. In this case the circular polarization is perpendicular to the electron polarization (figure from Be 57).

This discussion has led to expressions applicable to the case in which circularly polarized gamma rays are scattered from electrons polarized parallel or antiparallel to the initial direction of propagation of the gamma ray. This is the case most used so far in experiments on circular polarization of gamma rays. Virtually all of these experiments detect the difference in the intensity of gamma rays transmitted through, or scattered forward, from magnetized iron, when the magnet is turned on and when it is turned off or reversed.

Recently Beard and Rose (Be 57) have suggested the use of the case in which the circularly polarized gamma rays are scattered from electrons polarized perpendicular to the initial direction of gamma-ray propagation. This case offers the advantage of determining an azimuthal asymmetry from two simultaneous measurements at opposite azimuthal scattering angles in the plane of the electron spin and photon propagation vector. Beard and Rose show<sup>††</sup> that at a certain scattering angle  $\theta = \theta_m$ , the relative azimuthal anisotropy  $J_1/J_0$  is a maximum. Figure 6 gives a graph of  $\cos \theta_m$  as a function of photon energy  $k_0$ . In Fig. 7,  $J_1/J_0$  at  $\theta = \theta_m$  is shown as a function of the energy of the incident photon. For completely polarized electrons,  $J_1/J_0$  reaches a maximum value of 0.33 at 0.511 Mev.

The most significant practical limitation involved in applying the above cases to an experiment is the fact that only about 2 electrons of the 26 in an iron atom are polarized. Thus in all of the experiments performed

<sup>††</sup> The cross section may be obtained in the manner that led to (II-9) except that the electron polarization is taken perpendicular to the direction of the incident photon.

on forward scattering and transmission of circularly polarized photons, the possible effects amount at most to only a few percent. In the case treated by Beard and Rose, even at 0.511 Mev where  $J_1/J_0$  is maximum, there will be only a 5% effect (for complete photon polarization and ideal geometry).

## B. Photodisintegration of the Deuteron

At gamma-ray energies below 20 Mev, and particularly below 10 Mev, the existing theory for the photodisintegration of the deuteron is satisfactory. This is the region of interest since we are concerned only with the polarization of gamma rays of nuclear origin. The threshold energy for the photodisintegration of the deuteron, 2.225 Mev (Be 56), places a definite lower limit on the energy of a nuclear gamma ray whose polarization can be studied using this mechanism. In the energy region of interest (2.225 to 20 Mev) the disintegration proceeds almost entirely by an electric dipole or magnetic dipole interaction. The former is sensitive to polarization, while the latter is not.

The cross section for the photodisintegration of the deuteron in the form derived by Bethe and Longmire (Be 50 and Be 56), assuming a central force potential, is expected to be valid below about 10 Mev. The differential cross section for electric dipole disintegration, the one that is polarization-sensitive is given by

$$d\sigma^e = 2 \left( \frac{e^2}{hc} \right) \left[ \frac{\gamma k^3}{(\gamma^2 + k^2)^3} \right] \left( \frac{1}{1 - \gamma r_{0i}} \right) \cos^2 \alpha d\Omega, \quad (\text{II-11})$$

where  $\alpha$  is the angle between the direction of polarization of the gamma ray and the direction of motion of the proton (or neutron), and  $r_{0i}$  is the effective neutron-

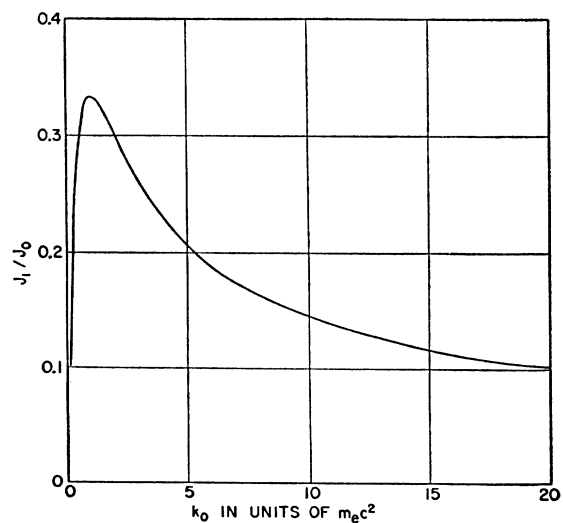


FIG. 7. Maximum relative azimuthal anisotropy  $J_1/J_0$  resulting from Compton scattering of incident circularly polarized photons, plotted as a function of incident photon energy. The circular polarization is perpendicular to the electron polarization (figure from Be 57).

proton range in the triplet state. The parentheses containing  $r_0$  represents a correction to the zero-range approximation for the cross section, which is given by the rest of the expression. The quantities  $\gamma$  and  $k$  can be obtained from the expressions

$$E = h\nu - W_1 = \hbar^2 k^2 / M \quad (\text{II-12})$$

$$W_1 = \hbar^2 \gamma^2 / M, \quad (\text{II-13})$$

where  $h\nu$  is the energy of the gamma ray,  $W_1$  the binding energy of the deuteron, and  $M$  the mass of the nucleon. That the angular distribution of the photoprotons varies as  $\cos^2\alpha$  has been experimentally confirmed by Wilkinson (Wi 52) using the completely polarized gamma rays from the reaction  $D_2(p, \gamma)He^3$ .

Since it is usually the azimuthal distribution of photoprotons or photoneutrons that is observed in determining the polarization of a gamma ray, the more useful form of (II-11) is

$$d\sigma_{\phi} = \frac{2e^2}{\hbar c} F(\gamma, k) \sin^2\theta \cos^2\phi d\Omega, \quad (\text{II-14})$$

where  $\theta$  and  $\phi$  are the usual polar coordinates. The direction of propagation of the gamma ray is given by  $\theta=0$ , and its direction of polarization by  $\theta=90^\circ$ ,  $\phi=0$ . The geometrical relationship of  $\theta$ ,  $\phi$ , and  $\alpha$  is illustrated in Fig. 1.

If the photodisintegration proceeded entirely by an electric dipole transition, the reaction would produce an ideal response to polarization in the sense defined above, namely that  $R = d\sigma_{90}/d\sigma_0 = 0$ .<sup>§§</sup> Over a large part of the energy range of interest this is nearly the case. However, as the gamma-ray energy is decreased to the threshold value the reaction proceeds increasingly

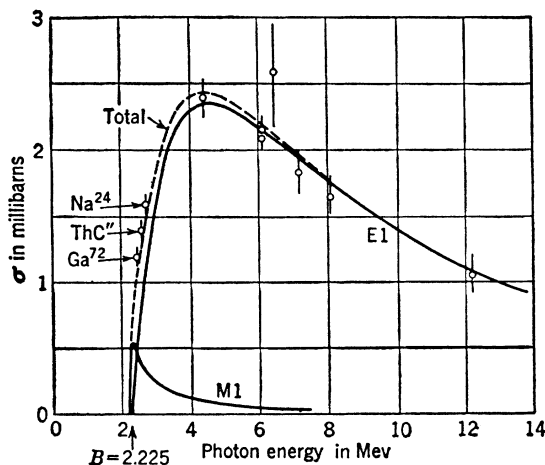


FIG. 8. Total cross section for the photodisintegration of the deuteron as a function of incident photon energy. Solid curves show the electric dipole and magnetic dipole cross sections as labeled, and dashed curve shows their sum. Points show representative experimental data (figure from Ev 55).

<sup>§§</sup> In the Compton effect we have  $R = \infty$  for an ideal response.

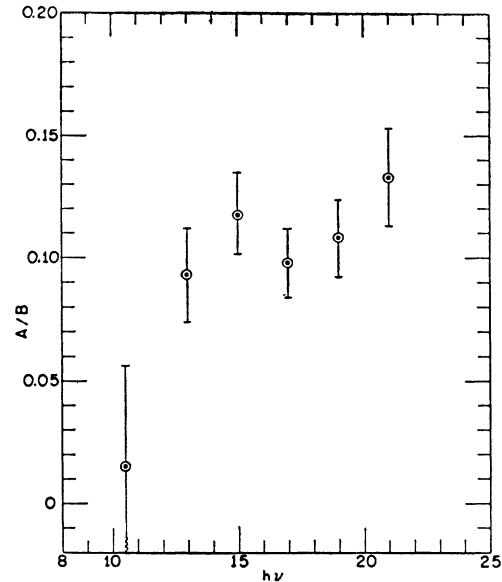


FIG. 9. The ratio  $A/B$  as a function of energy in Mev. This ratio is a measure of the isotropic term in the cross section for the photodisintegration of the deuteron. A noticeable effect starts at about 10 Mev (figure from Wh 58).

by the magnetic dipole interaction which yields an isotropic distribution of photoprotons. The total cross section for this process is given by (Se 53 and Be 50)

$$\sigma^m = \frac{2\pi e^2}{3 \hbar c} \left( \frac{\hbar}{Mc} \right)^2 (\mu_n - \mu_p)^2 \frac{k\gamma[\gamma - 1/a_s]^2}{(k^2 + \gamma^2)(k^2 + 1/a_s^2)} R(E), \quad (\text{II-15})$$

where  $\mu_n$  and  $\mu_p$  are the magnetic moments of the neutron and proton, respectively,  $a_s$  is the singlet scattering length, and  $R(E)$  is a correction for the nonzero range of the neutron-proton force, which has been derived by Salpeter (Sa 51).

Since the presence of the magnetic dipole interaction diminishes the polarization sensitivity of the reaction as a whole, it is of interest to compare the total cross sections for the magnetic and electric processes as a function of the gamma-ray energy. The total cross section for the electric dipole process, obtained by integrating (II-11) over  $\theta$  and  $\phi$ , is

$$\sigma^e = \frac{8\pi}{3} \left( \frac{e^2}{\hbar c} \right) \left[ \frac{\gamma k^3}{(\gamma^2 + k^2)^3} \right] \left( \frac{1}{1 - \gamma r_0} \right). \quad (\text{II-16})$$

The two cross sections in the zero-range approximation (i.e., without the range correction given by the last factor in each expression) are compared in Fig. 8 (Ev 55). The sum of the two cross sections is also shown as are several experimental points which agree fairly well with the curve and indicate the extent of validity of the zero-range approximation.

Other effects, which generally tend to diminish the ideal polarization sensitivity of the electric dipole dis-

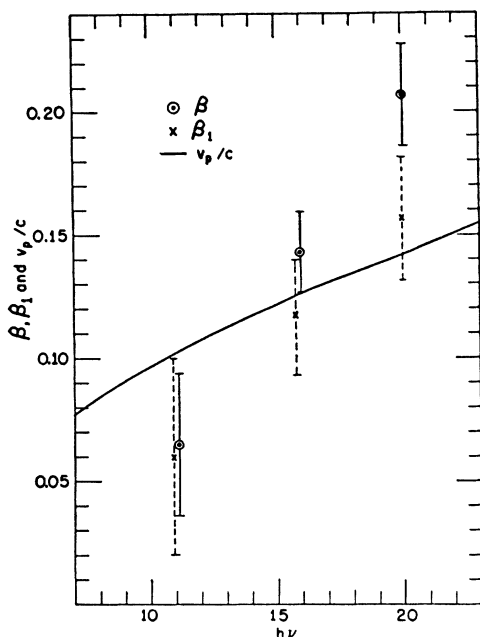


FIG. 10. The asymmetry coefficients  $\beta$  and  $\beta_1$ , as defined by (II-17) and (II-18), as a function of incident photon energy. Values of  $\beta$  and  $\beta_1$  are obtained after first determining  $A/B$ . For comparison the theoretical prediction  $v/c = [(h\nu - W_1)/Mc^2]^{1/2}$  (Ma 49) is plotted (figure from Wh 58).

integration, arise at energies above 10 Mev, and especially above 20 Mev. Since the nature of these effects is under current theoretical discussion, (Hu 57a) we confine attention to the empirical situation. The cross section is given in either one of the following forms (Wh 58):

$$d\sigma/d\Omega = A + B \sin^2\theta(1 + 2\beta \cos\theta), \quad (\text{II-17})$$

$$d\sigma/d\Omega = (A + B \sin^2\theta)(1 + 2\beta_1 \cos\theta). \quad (\text{II-18})$$

The term in  $\beta$  or  $\beta_1$  is attributed to the onset of the electric quadrupole interaction. In the recent experimental work by Whetstone and Halpern (Wh 58), values of  $A/B$  and  $\beta$  or  $\beta_1$  have been determined as shown in Figs. 9 and 10. These values of  $A/B$ , along with those of Allen (Al 55), are in good agreement with the recent calculations of de Swart and Marshak (De 58).

All these expressions are given in the center-of-mass system. Thus, in addition to the forward asymmetry which appears at higher energies, a forward asymmetry arises experimentally in the laboratory system because of the forward momentum of the gamma ray. This effect is illustrated in Fig. 11 which gives the laboratory angle corresponding to  $90^\circ$  in the center-of-mass system. In the range of interest the shift is not large.

The magnetic dipole reaction and the deviations from the  $\cos^2\alpha$  dependence above 10 Mev constitute the only significant effects that diminish the efficiency for detection of polarization in the energy region of interest here. In fact, from about 4 to 12 Mev the asymmetry

ratio  $R = d\sigma_{90}/d\sigma_0$  is less than 0.04. Perhaps the only serious drawback to the use of the photodisintegration of the deuteron in the detection of polarization is the relatively low total cross section ( $\sim 10^{-27}$  cm $^2$ ; see Fig. 8).

### C. Photoelectric Effect

The earliest measurements of polarization in the kev range made use of the photoelectric effect. Experiments using polarized photons having energies less than 40 kev (Wi 23, Bu 24, Ki 31) confirmed the basic theoretical prediction (Au 27, So 30) that the distribution of photoelectrons should vary approximately as  $\cos^2\alpha$ . As in the case of the photodisintegration of the deuteron, this distribution in terms of polar angles is  $\sin^2\theta \cos^2\phi$ , where  $\alpha$ ,  $\theta$ , and  $\phi$  are defined in the same way as before (Fig. 1).

The distribution has been calculated for electrons ejected from the  $K$  shell. Correspondingly, almost all the work dealing with the polarization sensitivity of the photoelectric effect has been concerned with emission from the  $K$  shell, ||| since it constitutes about 80% of the total emission for the energies of interest here (below about 1 Mev).

Fischer (Fi 31) and Heitler (He 44) have given the differential cross section in a nonrelativistic form (good to energies of about  $\frac{1}{2}m_0c^2$ ):

$$d\sigma_\phi = r_0^2 Z^5 \frac{(32)^{1/2} \left(\frac{m_0c^2}{k_0}\right)^{7/2}}{137^4} \times \frac{\sin^2\theta \cos^2\phi}{[(1 + k_0/2m_0c^2)^2 - \beta \cos\theta]^4} d\Omega, \quad (\text{II-19})$$

where  $\beta = v/c$  and  $Z$  is the atomic charge. Sauter (Sa 31, Sa 55) using relativistic considerations and assuming  $\beta \sim 1$  and  $Z/137 \ll 1$  obtains

$$\begin{aligned} d\sigma_\phi &\sim C(A + B \cos^2\phi) d\Omega, \\ A &= (\epsilon^2/4)(1 - \beta \cos\theta), \\ B &= (1 - \beta^2)^{1/2} - (\epsilon/2)(1 - \beta \cos\theta) \\ C &= (1/\epsilon)^4 (1 - \beta^2)^{1/2} \beta^2 \sin^2\theta / (1 - \beta \cos\theta)^4, \end{aligned} \quad (\text{II-20})$$

where  $\epsilon$  is the kinetic energy of the photoelectrons in units of  $m_0c^2$ .

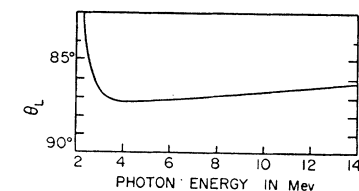


FIG. 11. Energy dependence of the angle in the laboratory system which corresponds to  $90^\circ$  in the center-of-mass system, in the photodisintegration of the deuteron (data from Wi 51a).

||| A nonrelativistic calculation by Schur (Sc 30) gives an azimuthal distribution for the electrons ejected from the  $L_I$  level similar to the nonrelativistic  $K$ -shell distribution. However, the emissions from the  $L_I$  shell represent only a small fraction of those emissions (20%) which are not from the  $K$  shell.

In these expressions there is a pronounced forward asymmetry in the angular distribution which increases as the energy of the gamma ray is increased. This effect is illustrated in Fig. 12 which gives theoretical curves for the photoelectron distribution as a function of  $\theta$  for several energies. In the nonrelativistic case the response to polarization is ideal, i.e.,  $R = d\sigma_{90}/d\sigma_0 = 0$ . In the relativistic case, however, the response is decreased by the fractional amount  $A/B$ . Another effect predicted by (II-20) is that the favored direction of emission of the photoelectron changes by  $90^\circ$  as the gamma-ray energy passes through 0.51 Mev. This is shown in Fig. 13. ¶¶ Accordingly, above 0.51 Mev the photoelectron would be emitted preferentially normal to the direction of polarization of the gamma ray.

A series of measurements with polarized photons ( $>40$  kev) designed to investigate this and other features of Sauter's expression has been carried out by Hereford and co-workers. Hereford (He 51, He 51a) studied the azimuthal distribution of the photoelectrons ejected from lead by the polarized radiation from positron-electron annihilation, and found a much greater asymmetry in the azimuthal distribution than predicted by (II-20). In a revised experiment Hereford and Keuper (He 53) obtained a result in rough agreement with that predicted by Sauter, if his equation, which is valid chiefly for low  $Z$ , is applied to the case of lead. McMaster and Hereford (Mc 54) continued the experiments by measuring the azimuthal asymmetry using photons (from  $\text{Co}^{60}$ ) which had been polarized by Compton scattering. By changing the angle of scattering they were able to obtain polarized gamma rays of different energies. Their measured values of  $R$  fell below unity above about 0.55 Mev, showing fair agreement with the theoretical curve in Fig. 13.

Brini *et al.* (Br 57) recently repeated the experiment

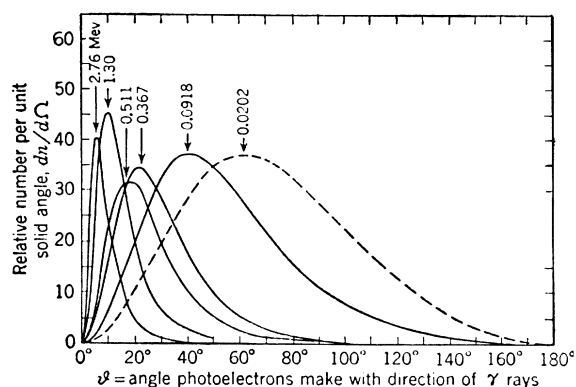


FIG. 12. Differential cross sections for photoelectrons ejected from the  $K$  shell, plotted against the angle of emission. The curves for the different photon energies are not normalized with respect to each other. Solid curves are calculated from Sauter's relativistic formula (Sa 31), the dashed curve from Fischer's non-relativistic formula (Fi 31) (figure from Ev 55).

¶¶ In this figure it is the reciprocal of  $R$  (as previously defined) that is plotted.

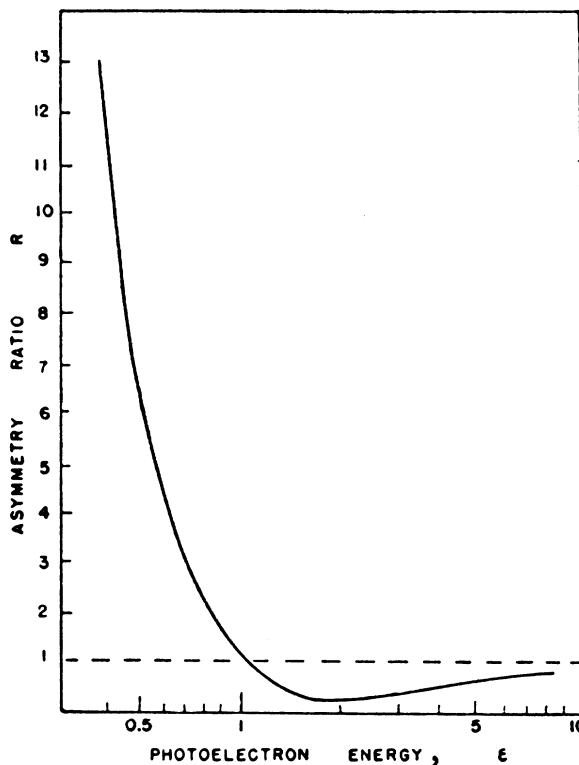


FIG. 13. Asymmetry ratio  $R = d\sigma_0/d\sigma_{90}$  for photoelectrons ejected from the  $K$  shell by linearly polarized photons for  $\theta = 90^\circ$ , as calculated from Sauter's formula (Sa 31). The abscissa is the incident photon energy in units of  $m_0c^2$  (figure from Mc 54).

of McMaster and Hereford, but did not find the  $90^\circ$  shift in the polarization response. Their data agree better with a theoretical curve of Archibald as given in Br 57. Apparently the knowledge of the polarization sensitivity of the photoelectric effect at higher energies is still somewhat uncertain. However, it is clear that the reaction can be used for gamma-ray energies which are well below 0.5 Mev.

The primary disadvantage of the photoelectric effect as an analyzer of polarization is that it requires detection of the photoelectron. Low-energy electrons are somewhat more difficult to detect than are the gamma rays in a typical Compton process. Furthermore, the scattering of low-energy electrons will present a serious problem.

## D. Other Polarization-Sensitive Processes

### (a) Pair Production

Berlin and Madansky (Be 50a) have investigated the possibility of using pair production as a polarization analyzer. Assuming a perfectly plane polarized incident photon they have calculated the expected asymmetry ratio  $R = d\sigma_{90}/d\sigma_0$  for several different experimental cases. They prefer the experimental arrangement in which all pairs in a particular plane are counted re-

ardless of angle or energy. For this case  $R=1.23$ ; i.e., the pair emission is a maximum in a plane perpendicular to the polarization.

However, Wick (Wi 51) pointed out that the conditions specified by Berlin and Madansky are practically impossible to realize experimentally, since they specify that the plane of the pair contains exactly the direction of the incident quantum. Accordingly, Wick suggests removing the restriction on the angle between the direction of propagation of the photon and the plane of the pair. He then finds that this experimental situation yields a polarization sensitivity comparable to those obtained by Berlin and Madansky. However, in Wick's case the plane of the pair prefers to be parallel to the polarization vector.

Pair production has not been used as a polarization analyzer for gamma rays of nuclear origin. This can be attributed primarily to the fact that, at the higher energies at which the reaction would prove most useful, the small angle between the pairs, the relatively small expected asymmetry ratio, and the scattering difficulties make it less desirable than the photodisintegration of the deuteron as a polarization analyzer.

#### (b) Nuclear Photoeffect

Although the general treatment of the angular distribution and polarization of reaction products (Bl 51, Si 53) is applicable to photonuclear reactions, Agodi (Ag 57) has given a specific treatment of the polarization sensitivity of photonuclear reactions. Without using a model for the nucleus for the photonuclear reaction, Agodi shows on quite general grounds (conservation of parity and angular momentum) that the azimuthal dependence of the differential cross section assumes a form proportional to  $(1+\alpha \cos^2\phi)$ , where  $\phi$  is the azimuthal angle as defined in Fig. 1. This result is quite general regardless of whether a single or mixed multipole transition is involved in the photonuclear process. In the case in which a single multipole is responsible for the transition, the value of  $\alpha$  for a completely polarized incoming gamma ray can be determined from the angular distribution (in  $\theta$ ) coefficient, if it is known. Such is not generally the case, however, when two or more multipoles contribute to the transition.

Apart from the photodisintegration of the deuteron, the most promising of all the known photonuclear reactions is the reaction  $\text{Be}^9(\gamma, n)\text{Be}^8$ . Since the threshold energy is about 1.66 Mev and the cross section at 9.5 Mev is about 1.6 mb, this reaction could compete with the photodisintegration of the deuteron as an effective analyzer of polarization for gamma rays if the value of  $\alpha$  were large enough.

#### (c) Photofission

Winhold and Halpern (Wi 56), Katz *et al.* (Ka 58), and others have shown experimentally that certain nuclei subject to photofission exhibit anisotropy in the

angular distribution of the fission fragments. Two such nuclei, the even-even nuclei,  $\text{Th}^{232}$  and  $\text{U}^{238}$ , for example, show angular distributions of the form  $(a+b \sin^2\theta)$ . Although the form of the distribution remains the same over the energy range studied (5 to 20 Mev), the ratio  $b/a$  varies from values of the order of 10 near threshold (just above 5 Mev) to values of the order of 0.1 in the vicinity of 20 Mev. The anisotropic distribution is assumed to result from an electric dipole interaction. Consequently, although the azimuthal distribution produced by polarized photons has not yet been studied, the foregoing angular distribution implies a polarization sensitivity proportional to  $b/a$ . Other nuclei, such as the odd- $A$  nuclei,  $\text{U}^{235}$  and  $\text{Pu}^{239}$ , have essentially isotropic angular distributions and thus are not expected to manifest any sensitivity to polarization.

Although the photofission cross sections in the energy region of interest here are of the order of 10 mb, the fact that appreciable anisotropy in the angular distribution is confined to the region roughly 2 to 3 Mev above threshold places some limitation on the potential use of photofission as a polarization analyzer. In addition, if neutron-induced fission or spontaneous fission is present, the detection of the photofission might become very difficult.

### III. MEASUREMENTS OF POLARIZATION OF NUCLEAR GAMMA RAYS

The following discussion is organized primarily on the basis of the type of polarization-sensitive mechanism involved. Attention has been given to chronological order only insofar as it lends itself to a logical development. The development of technique has also been a consideration in selecting experiments for discussion. A complete listing and outline of the experiments is attempted in Table XIII at the end of Part III. Since this discussion is primarily devoted to experiments on nuclear gamma rays, the polarization experiments on annihilation radiation and bremsstrahlung are not discussed except for the earliest annihilation experiments.

#### A. Measurement of Plane Polarization by Means of the Compton Effect

Not only the earliest, but also the most utilized, of the polarization sensitive reactions has been the Compton effect. This is due to the fact (Part II) that the reaction has a relatively high cross section along with a reasonable sensitivity to polarization over an energy range which includes many nuclear gamma rays of interest.

In general, a polarimeter that uses the Compton effect consists of a scatterer and an analyzer which detects the scattered radiation. The elements of such a polarimeter are shown in Fig. 14. Here the polarimeter consists of the elements  $B$  and  $C$ . Gamma rays from the source impinge on the Compton scatterer  $B$  and the scattered radiation is detected by the analyzing element



*C*. As a general rule *B* and *C* are crystals of scintillation counters and coincidence between *B* and *C* are measured. This makes it considerably easier to isolate and detect the desired Compton events. A polarization measurement is made by determining  $N_0/N_{90}$  (often called  $N_{||}/N_{\perp}$ ), the ratio of the coincidence counting rate when *C* is placed at  $\phi=0^\circ$  to that when it is placed at  $90^\circ$ . In principle, *B* could be merely a piece of scattering material, and the polarization measurement would depend only on the single counting rate in *C* at the  $0^\circ$  and  $90^\circ$  positions. However, in this case the shielding (and electronic discrimination) would have to be exceedingly good to prevent direct radiation from the source being recorded in *C*. See Sec. (a).

Except in the earliest experiments, a polarimeter has generally consisted of an organic scintillator for the scatterer and a sodium-iodide crystal for the detector of the scattered gamma ray. An organic scintillator, a material of low *Z*, makes a good scatterer because it permits fairly free escape of the scattered photons. Naturally, sodium iodide is the best analyzing crystal because of its high efficiency and good resolution for the detection of gamma rays. The objection to the use of sodium iodide for this purpose in the earliest experiments was the long decay time of its pulses. Development of suitable electronic techniques has greatly diminished this difficulty.

Circular polarization experiments utilizing the Compton effect are discussed in the last section of this part.

#### (a) Early Experiments on Annihilation Radiation

Although this paper deals mainly with the polarization of gamma rays of nuclear origin, for convenience and historical interest we begin with a brief discussion of the first measurements of polarization, those performed in order to detect the mutually perpendicular polarizations of the two quanta resulting from the annihilation of a positron and an electron. This prediction of the pair theory was pointed out by Wheeler (Wh 46). Assuming that two Compton polarimeters would be used to detect the polarizations, Pryce and Ward (Pr 47) and Snyder *et al.* (Sn 48) calculated the expected azimuthal distribution of one scattered quantum relative to the other. This is an example of a polarization-polarization correlation with the angle between the two polarimeters fixed at  $180^\circ$ .

FIG. 14. Schematic diagram of experimental arrangement of scintillating crystals in an apparatus designed to measure a direction-polarization correlation. Crystals *B* and *C* constitute the polarimeter; crystal *A* is the directional counter (figure from Me 50).

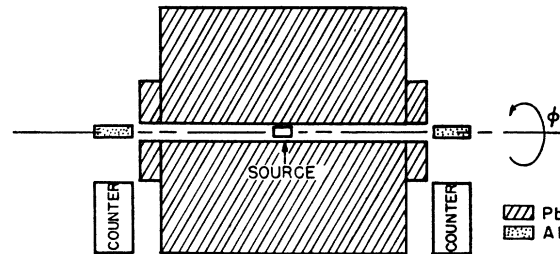
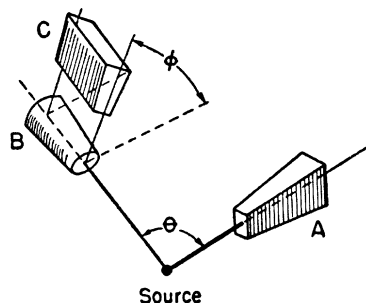


FIG. 15. Schematic diagram of typical experimental arrangement for study of linear polarization of annihilation radiation. In this illustration the scatterers are made of aluminum. The counters are in the parallel ( $||$ ) position.

The essential features of the experimental arrangement are shown in Fig. 15. The positron source ( $\text{Na}^{22}$  or  $\text{Cu}^{64}$ ) is placed at the center of a hole about  $\frac{3}{8}$  in. in diameter bored through the center of a lead block with dimensions approximately  $6 \times 6 \times 6$  in. The oppositely directed annihilation radiation beams emerging from the openings then impinge upon cylindrical scatterers (not detectors in this case) about 1 in. long. The detectors of the scattered radiation are placed so that the mean scattering angle is about  $82^\circ$ , the angle at which the Compton effect exhibits optimum sensitivity to polarization for this gamma-ray energy. (Fig. 2.) The experiment then consists in determining  $N_{\perp}/N_{||}$ , the ratio of the coincidence counting rate when the axes of the two detectors are at right angles to each other to that when they are parallel.

Bleuler and Bradt (Bl 48) using G-M counters with end-windows as detectors confirmed the predicted correlation, although their results have a relatively large margin of error. They obtained  $N_{\perp}/N_{||} = 1.9 \pm 0.3$  as compared to the theoretically predicted ratio of  $\sim 1.7$  for their geometry. Shortly thereafter, Hanna (Ha 48a) performed the experiment using G-M tubes and obtained values of  $N_{\perp}/N_{||}$  which were consistently lower than the theoretical values. Vlasov and Dzheleпов (Vl 49) obtained  $1.7 \pm 0.2$ . However, the approximations used in obtaining the theoretically expected ratio for their geometry were sufficiently rough that essentially there was only qualitative agreement with the theory. Wu and Shakhov (Wu 50) repeated the experiment using anthracene scintillation counters and obtained a value of  $N_{\perp}/N_{||} = 2.04 \pm 0.08$ , which compares well with the theoretical value of 2.00 for their geometry.

#### (b) Direction-Polarization Correlation

The arrangement of the scintillation crystals for a direction-polarization correlation experiment is shown in Fig. 14, in which *A* is the crystal of the counter which is insensitive to polarization and records only the direction of one gamma ray and *B* and *C* are the crystals of the Compton polarimeter which measures the linear polarization of the other gamma ray. The phototubes associated with the three crystals are em-

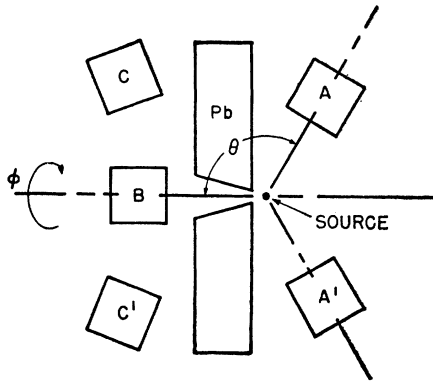


FIG. 16. Schematic diagram of apparatus of Metzger and Deutsch. Two additional counters are used to increase the yield in the measurement of the direction-polarization correlation. In the position shown,  $\phi=0$  (after Me 50).

ployed in a triple-coincidence circuit. Thus, a measurement of the polarization is obtained from the ratio of the triple-coincidence yields with crystal  $C$  at  $\phi=0^\circ$  and at  $\phi=90^\circ$ . The direction-polarization correlation is then obtained by determining this ratio as a function of the correlation angle  $\theta$ . The ratio of the counting rates is  $N_0/N_{90}$  from which one obtains the true polarization ratio  $J_0/J_{90}$  discussed in Part I.

Thorough consideration must be given to the possibility of recording "false" coincidences as a result of radiation being counted and scattered among the three crystals in combinations different from the one desired. Usually a good shield is placed in front of counter  $C$  to diminish the amount of direct radiation from the source or scattered radiation from  $A$  arriving at  $C$ . This shield diminishes the chance that one gamma ray goes to  $A$  while the other one goes to  $C$  and is then scattered to  $B$ , or that one gamma ray goes to  $B$  while the other goes to  $A$  and is scattered to  $C$ .

As mentioned in Part I, there is little to be gained (Ha 48) by putting a polarimeter at  $A$  as well as at  $B, C$ . Furthermore, if the corresponding direction-direction correlation is known it is only necessary in virtually all cases to measure the direction-polarization correlation at a single angle. This angle is usually selected so as to maximize the effect and it is often  $90^\circ$ .

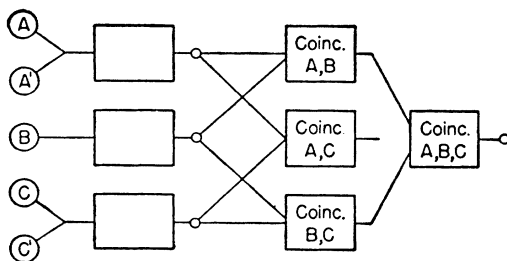


FIG. 17. Block diagram of the electronic circuits associated with the experimental arrangement shown in Fig. 16. Empty blocks represent appropriate stages of amplification, etc. (figure from Me 50).

Metzger and Deutsch (Me 50) first used the technique of the direction-polarization correlation in the study of several gamma-gamma cascades. The method has been extended by others to the study of correlations in which the radiation whose polarization is not analyzed is some other type of particle, either emitted or absorbed.

### (c) Experiments of Metzger and Deutsch

The classic experiments of Metzger and Deutsch (Me 50) exemplify the techniques involved in the measurement of direction-polarization correlations. Figure 16 is a schematic diagram of the experimental arrangement. Naphthalene was used for all of the crystals in this arrangement, but Metzger and Deutsch suggest the use of anthracene would be an improvement.

Counters  $A'$  and  $C'$  add to the original coincidence combination  $ABC$  three more equivalent (theoretically

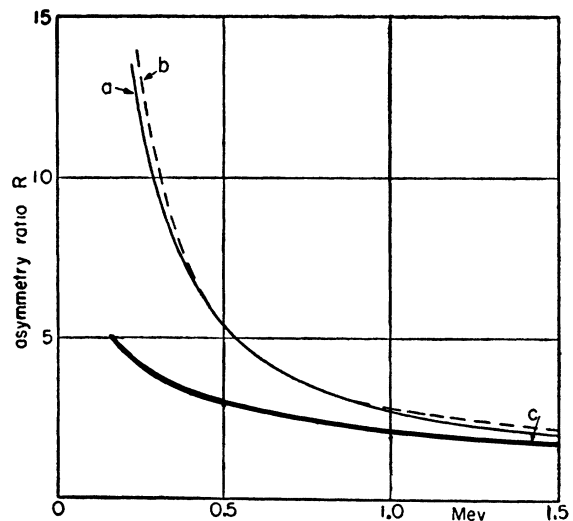


FIG. 18. Asymmetry ratio  $R$  as a function of gamma-ray energy in Mev for different geometries: (a)  $\theta_c=80^\circ$ , ideal geometry; (b)  $\theta_c=(\theta_c)_{\max}$ , ideal geometry; (c)  $\theta_c=80^\circ$ ,  $\Delta\theta_c=55^\circ$ ,  $\Delta\phi=60^\circ$  (figure from Me 50).

and experimentally) combinations  $ABC'$ ,  $A'BC$ ,  $A'BC'$ , so that the real coincidence yield is increased by a factor of four. The addition of  $C'$  also, to a first approximation, cancels the effect of any small asymmetry resulting from a possible misalignment of the axis of the polarimeter.

Figure 17 gives a block diagram of the electronics associated with the five counters. This system makes it possible to count double coincidences separately, which it is necessary to do in order to monitor the triple-coincidence rate properly and to determine the accidental rate. An arrangement such as this, or its equivalent, has been an important feature of all Compton polarimeters.

Metzger and Deutsch distinguish three polarization parameters:  $p=J_0/J_{90}$ , which describes the state of polarization of the gamma ray incident upon the

polarimeter;  $R$ , the asymmetry ratio, which is a measure of the polarization sensitivity of the polarimeter taking into consideration nonideal geometry; and  $N_0/N_{90}$ , the ratio of the triple-coincidence counting rates with the polarimeter set at  $\phi=0$  and  $\phi=90^\circ$ . These three parameters are related through the expression

$$N_0/N_{90} = (p+R)/(pR+1). \quad (\text{III-1})$$

For the case of ideal geometry (Part II)  $R$  is simply the ratio of two differential cross sections for Compton scattering, i.e.,  $R=d\sigma_{90}/d\sigma_0$ . There is an angle of scattering\*\*\*  $\theta_c = (\theta_c)_{\text{max}}$  at which  $R$  is a maximum for ideal geometry. The dependence of  $R$  on the energy of the initial photon, as calculated by Metzger and Deutsch, is given as curve  $b$  in Fig. 18 for  $\theta_c = (\theta_c)_{\text{max}}$ . Curve  $a$  shows the dependence of  $R$  for  $\theta_c = 80^\circ$ , which Metzger and Deutsch chose as a mean value. In order

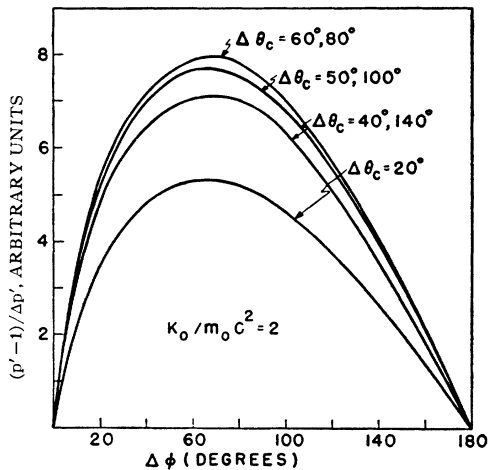


FIG. 19. Figure of merit of a Compton polarimeter as a function of the spread in the angle  $\phi$ , for various spreads in  $\theta_c$ . Incident photon energy equal to 1 Mev, and  $p=1.2$ . The curves do not differ significantly from those in Me 50.

to obtain statistically significant counting rates, however, it is necessary to use angular spreads  $\Delta\theta_c$  and  $\Delta\phi$ , which are considerably greater than zero, so that  $R$  is appreciably reduced. Metzger and Deutsch use  $(p'-1)/\Delta p'$  as a figure of merit for a polarimeter, where  $p'$  is the observed polarization ratio, and  $\Delta p'$  its error. This quantity is given as a function of the angular spreads in Figs. 19 to 22 for two gamma-ray energies. For angular spreads of  $60^\circ$ - $70^\circ$ , the figure of merit is a maximum over a wide range of energy. Hence, it is possible to design an efficient polarimeter of considerable versatility.

The actual spreads used by Metzger and Deutsch were  $\Delta\theta_c = 55^\circ$  and  $\Delta\phi = 60^\circ$ . That these were the effective values was determined experimentally in the following way. The partially polarized radiation result-

\*\*\* Here,  $\theta_c$  is used for the scattering angle to distinguish it from the correlation angle  $\theta$ .

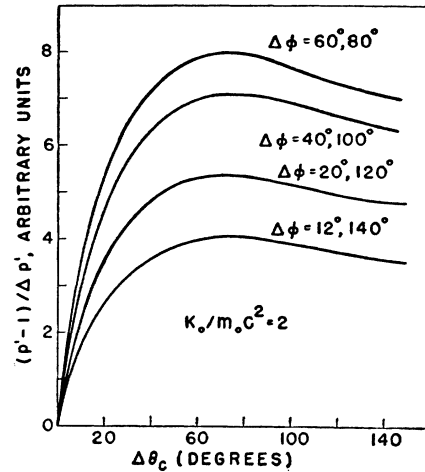


FIG. 20. Figure of merit of a Compton polarimeter as a function of the spread in the angle  $\theta_c$ , for various spreads in  $\phi$ . Incident photon energy equal to 1 Mev, and  $p=1.2$ . The curves do not differ significantly from those in Me 50.

ing from the Compton scattering of a collimated beam of gamma rays from a strong  $\text{Co}^{60}$  source impinged on the scattering crystal of the polarimeter. The degree of polarization  $p$  of this radiation is known through the Klein-Nishina formula. A measurement of  $N_0/N_{90}$  then determines  $R$  through the use of (III-1). With this value of  $R$ , the angular spreads  $\Delta\theta_c$  and  $\Delta\phi$  are obtained for the energy appropriate to the scattered quanta. With these values of  $\Delta\theta_c$  and  $\Delta\phi$ , the curve for  $R$  as a function of energy was then constructed and is given as curve  $c$  in Fig. 18.

With the equipment and techniques discussed, Metzger and Deutsch measured the direction-polarization correlations in the decays of  $\text{Sc}^{46}$ ,  $\text{Co}^{60}$ ,  $\text{Rh}^{106}$ , and  $\text{Cs}^{134}$ . Essentially as a check on the experimentally known direction-direction correlations (Br 48) and to elucidate the method, the polarizations were measured as a function of  $\theta$ . For each nucleus, possible direction-polarization correlations were calculated from the known coefficients of the direction-direction correlation. Thus, for the cascade  $j_1(L_1)j(L_2)j_2 \rightarrow 4(2)2(2)0$ , the

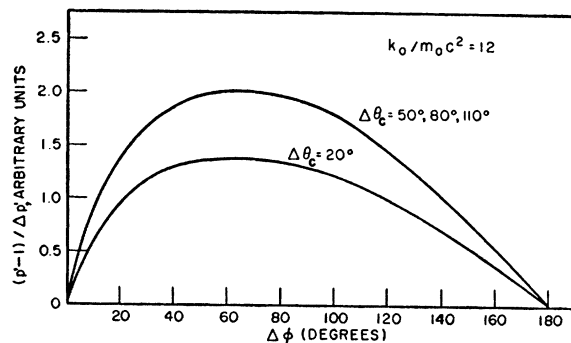


FIG. 21. Figure of merit of a Compton polarimeter as a function of the spread in  $\phi$ , for various spreads in  $\theta_c$ . Photon energy equal to 6 Mev, and  $p=1.2$ .

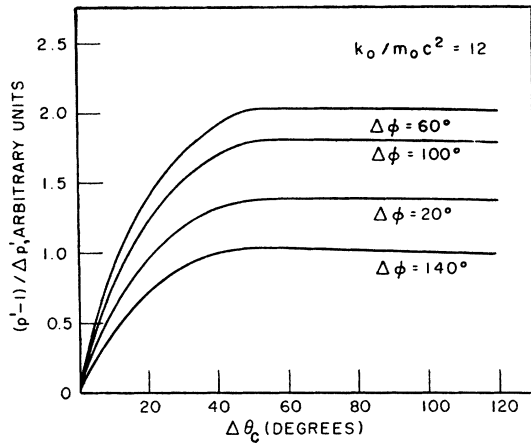


FIG. 22. Figure of merit of a Compton polarimeter as a function of the spread in  $\theta_c$ , for various spreads in  $\phi$ . Photon energy equal to 6 Mev, and  $p=1.2$ .

direction-direction correlation is

$$W(\theta) = 1 + (1/8) \cos^2\theta + (1/24) \cos^4\theta.$$

The direction-polarization correlation can be written down from Table III(b). At  $\theta=90^\circ$ , for example

$$W(90, \gamma) = 1 \pm \cos 2\gamma (1/8 + 1/24).$$

The sign is + or - according as the radiation is electric or magnetic. This expression applies if the first gamma ray goes to the directional counter and the second to the polarimeter, or if the gamma-ray paths are interchanged. In the experiment, both processes were observed indistinguishably with about equal efficiencies. Hence (at  $\theta=90^\circ$ ),

$$p = \frac{J_0}{J_{90}} = \frac{2 + (\pm)L_1 0.17 + (\pm)L_2 0.17}{2 - (\pm)L_1 0.17 - (\pm)L_2 0.17}$$

and  $p=1.40, 1$ , or  $0.71$  depending on whether the gamma rays in the cascade are  $(E2, E2)$ ,  $(E2, M2)$  or  $(M2, E2)$ , or  $(M2, M2)$ . The complete correlation can be worked out in similar fashion.

Figure 23 gives the three curves modified by the efficiency of the polarimeter, with the aid of (III-1). The data are those obtained in the decay of  $\text{Sc}^{46}$ . The experimental points fit the curve corresponding to an  $(E2, E2)$  cascade in  $\text{Ti}^{46}$ . Thus, the polarization measurement clearly selects the correct parity assignment. The situation for the cascade in  $\text{Ni}^{60}$  resulting from the decay of  $\text{Co}^{60}$  is entirely similar. In the  $\text{Rh}^{106}$  decay the calculated direction-direction coefficients for a  $0(2)2(2)0$  scheme were twice as large as the experimental ones. Without an explanation for this discrepancy, Metzger and Deutsch were only able to show that the direction-polarization measurement was consistent with the direction-direction measurement. The experimental result was interesting in that the polarization changes direction at  $\theta \approx 120^\circ$ , attaining large values on either

side of this angle. In the case of  $\text{Cs}^{134}$ , the possible participation of other coincident gamma rays in the correlation made a unique assignment impossible. Again the direction-polarization correlation was consistent with the direction-direction correlation, and the result was not unlike that for  $\text{Sc}^{46}$  and  $\text{Co}^{60}$ .

#### (d) Other Measurements with Radioactive Sources

Since the Metzger-Deutsch experiments, there have been many other measurements of direction-polarization correlations in a variety of nuclei. The same basic techniques are common to all. Naturally, there have been modifications and improvements to fill the needs of each new experiment. Accordingly, in the review of the remaining experiments using the Compton polarimeter only those techniques which represent relatively distinctive additions to the art are discussed.

Shortly after the work of Metzger and Deutsch, Williams and Wiedenbeck (Wi 50) using a similar experimental arrangement verified the results on  $\text{Rh}^{106}$  and  $\text{Co}^{60}$ . In the case of  $\text{Rh}^{106}$  the factor of two between the theoretical and experimental coefficients could be explained according to Spiers (Sp 50) by assuming the participation of another state close to the second excited state in  $\text{Pd}^{106}$ . Williams and Wiedenbeck also studied  $\text{Cs}^{134}$ , but found an isotropic direction-polarization correlation.

Stump (St 52) measured a beta-gamma direction-polarization correlation in the decay of  $\text{Sb}^{124}$ . The source and the beta detector were enclosed in a vacuum container in order to minimize beta scattering. The beta

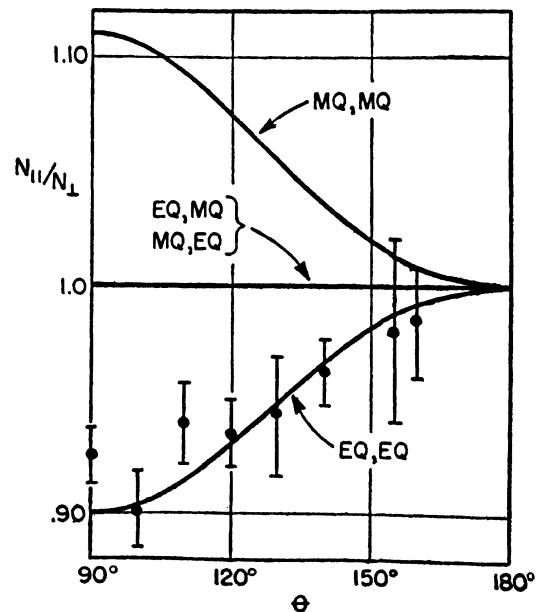


FIG. 23. Gamma-gamma direction-polarization correlation in the decay of  $\text{Sc}^{46}$ . The ratio  $N_{11}/N_1$  is plotted against  $\theta$ . The three curves correspond to the different parity assignments in the spin sequence 4-2-0 (figure from Me 50).

detector consisted of a thin crystal of anthracene mounted on the end of a light pipe leading to a photomultiplier tube outside the vacuum chamber. The polarimeter was considerably improved in efficiency by using an anthracene crystal as the scattering crystal and two oppositely placed sodium-iodide crystals as detectors of the scattered gamma rays. Since the angular correlation coefficients were already known (St 51) and quadrupole radiation is involved, it was necessary to take measurements only with the polarimeter at  $90^\circ$  to the beta counter. Stump found a value of about 1.1 for the ratio  $N_0/N_{90}$ . This datum, used in conjunction with the correlation coefficient, led to the conclusion that no parity change occurred in the gamma transition.

Further work on the radioactive nuclei  $\text{Co}^{60}$ ,  $\text{Cs}^{134}$ , and  $\text{Sb}^{124}$  was done by Klopper *et al.* (Kl 52). Plastic scintillators and type 5819 phototubes were used. The phototubes were shielded from magnetic fields in order to reduce the spurious dependence of the coincidence rate upon counter position. Residual effects were investigated by comparing the triple-coincidence rate to the single-channel counting rates at the various positions. In addition to monitoring the single rates, the various double-coincidence combinations, and the resolving time, the instrument was checked with observations at  $\theta = \pi$ , where  $N_0/N_{90}$  must equal 1.0. The gamma-gamma direction-polarization correlation for  $\text{Co}^{60}$  was measured to establish the reliability of the instrument. The result agreed with the earlier measurements (Me 50, Wi 50).

The polarization measurements on  $\text{Cs}^{134}$  agreed with the results of Metzger and Deutsch (Me 50), but not with those of Williams and Wiedenbeck (Wi 50). It was pointed out that both the direction-polarization and the direction-direction correlations could be explained with a  $4(E2)2(E2)0$  decay scheme, provided a 35% isotropic component is assumed to be present in both correlations.

In the case of  $\text{Sb}^{124}$  the gamma-gamma directional and polarization correlations were essentially isotropic. The authors suggested a  $3(10\% E2; 90\% M1)2(E2)0$  decay scheme. The beta-gamma direction-polarization correlation was also studied with this source. The measurement agreed with the result of Stump (St 52) confirming the  $E2$  nature of the radiation.

Additional work on the decay of  $\text{Cs}^{134}$  was done by Robinson and Madansky (Ro 52) who measured a polarization-polarization correlation for the gamma rays. The experiment was quite similar to the investigations on annihilation radiation (see Fig. 15). In fact, Robinson and Madansky first performed the experiment with annihilation radiation in order to determine experimentally the effective solid angle corrections. The signals from the two scattering crystals (stilbene) went to a coincidence circuit ( $7 \times 10^{-8}$  sec), the output of which triggered an oscilloscope. The pulses from the two analyzing crystals (NaI) were delayed, one more than the other, and displayed on the (triggered) oscilloscope. A coincidence analysis could be made by visual inspection

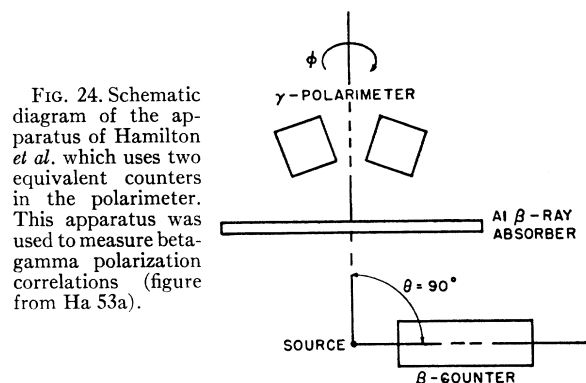


FIG. 24. Schematic diagram of the apparatus of Hamilton *et al.* which uses two equivalent counters in the polarimeter. This apparatus was used to measure beta-gamma polarization correlations (figure from Ha 53a).

of the photographs of the oscilloscope traces. The ratio of the number of coincidences with analyzing counters perpendicular to the number with the counters parallel was  $0.91 \pm 0.08$ . This result is not in disagreement with assignments of spins and parities made from the other correlation experiments on this nucleus (Wa 50, Pe 51, Ro 51).

A study of the direction-polarization correlation for the cascade involving the first two excited states of  $\text{Pb}^{208}$  in the  $\text{ThC}''$  decay was made by Kraushaar and Goldhaber (Kr 53). Again, a polarimeter of the Metzger-Deutsch type was used and a value for the efficiency was obtained by observing the polarization of scattered  $\text{Co}^{60}$  radiation. However, a more realistic value for the efficiency of the polarimeter was obtained by measuring the already known direction-polarization correlations for  $\text{Co}^{60}$  and  $\text{Rh}^{106}$  sources. For the measurement in the  $\text{Pb}^{208}$  cascade, a value of  $N_0/N_{90} = 0.958 \pm 0.3$  was obtained. This result, in conjunction with the result of Petch and Johns (Pe 50) on the direction-direction correlation, indicates an assignment of  $4(E2)2(E2)0$  to the cascade in  $\text{Pb}^{208}$ .

Direction-polarization correlations in the beta-gamma decay from  $\text{K}^{42}$ ,  $\text{As}^{76}$ ,  $\text{Rb}^{86}$ ,  $\text{Sb}^{124}$ , and  $\text{Cs}^{134}$  were studied by Hamilton *et al.* (Ha 53a). They used a two-counter polarimeter having stilbene crystals placed symmetrically with respect to the polarimeter axis, as shown in Fig. 24, so that each counter played a dual role as scatterer and analyzer. The aluminum plate prevented beta particles from reaching the counters of the polarimeter. The entire apparatus was surrounded by an aluminum can which served as a light shield and contained a helium atmosphere in order to reduce electron scattering. Hamilton *et al.* discuss thoroughly the dependence on angle of the spurious triple-coincidence rates associated with the various possible scattering combinations. The single and double rates, as in previous experiments, were determined quite accurately as a check on the proper operation of the instrument.

In the case of  $\text{Sb}^{124}$ ,  $\text{Cs}^{134}$ , and  $\text{As}^{76}$  there are additional beta-gamma cascades involving beta particles whose energies are lower than in the cascades under study. In these cases an aluminum absorber was intro-

TABLE XI. Values of the polarization correlation coefficient  $C(\text{obs})$  and  $C(\text{pred})$ , as observed by Ha 53a and as predicted (on basis of no parity change for the gamma) from the directional correlation coefficient  $Q_2+Q_4$  reported by other workers for similar beta-energy discrimination conditions. (Table from Ha 53a).

Nucleus	$Q_2+Q_4$	$C(\text{pred})$	$C(\text{obs})$
Cs <sup>134</sup>	0.00±0.01	0.00±0.003	0.009±0.013
Rb <sup>86</sup>	0.13±0.01	-0.068±0.005	-0.060±0.025
As <sup>76</sup>	0.07±0.02	-0.067±0.018	-0.114±0.035
K <sup>42</sup>	-0.06±0.02	0.022±0.007	-0.007±0.016
Sb <sup>124</sup>	-0.27±0.04	0.151±0.022	0.142±0.010

duced to absorb all but the desired high-energy beta particles. The effect of spurious triple coincidences caused by gamma rays reaching the beta crystal was determined by making runs with absorbers of various thickness, but all thick enough to absorb all beta particles.

In these experiments a quantity  $C$  is defined which is the coefficient characterizing the angular variation of the intensity of triple coincidences as a function of azimuthal angle of the polarimeter. Thus

$$N_\phi = 1 + C \cos^2\phi, \quad (\text{III-2})$$

so that  $N_\phi/N_{90} = 1 + C$ . Table XI compares the values of  $C$  obtained experimentally with values derived from the direction-direction coefficients determined by other workers.††† At  $\theta = 90^\circ$ , the polarization ratio is [see Sec. (c)]

$$p = \frac{J_0}{J_{90}} = \frac{1 \pm (Q_2 + Q_4)}{1 \mp (Q_2 + Q_4)}$$

for pure dipole ( $Q_4 = 0$ ) or pure quadrupole radiation, the upper signs holding with no parity change, the lower ones with parity change. From (III-1), one obtains  $N_\phi/N_{90}$  and hence  $C$ . In the case of Cs<sup>134</sup>, an isotropic direction-polarization correlation is observed as predicted. For Rb<sup>86</sup>, As<sup>76</sup> and Sb<sup>124</sup>, the observed polarization agrees with that predicted for no parity change in the gamma transition from the first excited state. An essentially isotropic direction-polarization correlation is observed for K<sup>42</sup>.

Brazos and Steffen (Br 56) have studied the direction-polarization correlation of the 0.722–0.566-Mev gamma-ray cascade resulting from the decay of the 50-day In<sup>114</sup> isomer to Cd<sup>114</sup>. The oppositely placed analyzing crystals were rotated automatically about an axis through the scatterer and source once every hour to minimize the effect of possible electronic fluctuations. The measurement indicated a  $4(E2)2(E2)0$  cascade, which is also favored by the directional correlation measurements on this cascade (Br 56).

The direction-polarization correlation in the 1.24–

††† The directional correlation results used were the following: K<sup>42</sup> (Be 50b, St 51), As<sup>76</sup> (Wa 50a, Ri 52), Rb<sup>86</sup> (St 51, Ri 52), Sb<sup>124</sup> (Be50b), Cs<sup>134</sup> (Be 50b, St 50).

0.845-Mev gamma-ray cascade in the decay of Co<sup>56</sup> has been measured by Wood and Jastram (Wo 55). A liquid scintillator was used as the scattering counter. Using the direction-direction coefficients (Hu 55) and the polarization measurement on the 0.845-Mev gamma ray, it was established that this gamma ray was electric quadrupole (no parity change).

An investigation of the spins and parities of the first three excited levels in Ce<sup>140</sup> and the first two in Sr<sup>88</sup> was conducted by Bishop and Perez y Jorba (Bi 55) by means of direction-direction and direction-polarization correlations. They used scattering crystals (made of polystyrene activated with diphenyl tetrabutadiene) of two sizes, one for low the other for high-energy gamma rays, since too large a crystal at a given energy makes double scattering too probable. They limited the double scattering to 15% in their experiments. Single-channel pulse-height analyzers were used in the channels of both the directional counter and the scattering counter. In the case of the scattering counter, energy discrimination is desirable since the polarimeter is in effect a crude Compton spectrometer. Thus, the window of the pulse-height analyzer selects the pulses from Compton recoil electrons in the scattering crystal corresponding to a gamma ray of a given energy scattered at a given (approximately) angle. Figure 25 shows a pulse-height spectrum obtained this way for the gamma rays from Sr<sup>88</sup> following the beta decay of Y<sup>88</sup>.

The decay scheme in Ce<sup>140</sup>, following beta decay of La<sup>140</sup>, is fairly complex as shown by the level diagram in Table XIII. Bishop and Perez y Jorba measured the direction-polarization correlation with the 1.60-Mev gamma ray going to the directional counter and either the 0.329-, 0.487-, or 0.815-Mev gamma ray going to the polarimeter. The experimental value of  $N_\phi/N_{90}$  (1.077±0.022) was consistent with assignments of  $3^-4^+-2^+$  or  $3^+-4^-2^-$  for the first three excited states taken in descending order. However, on the basis of the Goldhaber-Sunyar rule, giving  $2^+$  for the first excited state, and on considering transition probabilities in the beta decay to these states, the first possibility was naturally chosen. Again, in the case of the simple cascade in Sr<sup>88</sup> the measurements were most consistent with the possibilities  $3^-2^+-0^+$  or  $3^-1^+-0^+$  for the first two excited states and the ground state. The first possibility was chosen since it agrees best with internal-conversion data (Pe 48, Me 52a).

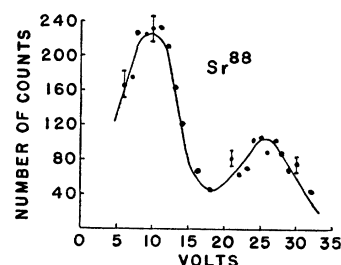


FIG. 25. Pulse-height spectrum of recoil electrons (in the scatterer) which are in coincidence with scattered gamma rays detected by the analyzing counters of the polarimeter. The gamma rays are from Sr<sup>88</sup> produced in the decay of Y<sup>88</sup> (figure from Bi 55).

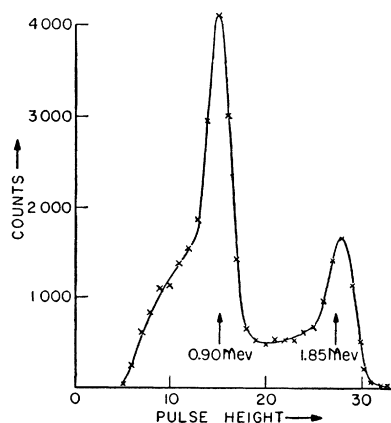
The  $\text{Sr}^{88}$  gamma rays were also studied by Coleman (Co 56). His Compton polarimeter was used as a pulse-height analyzer by summing the pulse from the scattered electron in the scattering scintillator with that from the scattered gamma in the analyzing counter. With this technique the analyzing counter can subtend a large solid angle at the scattering scintillator without loss of resolution. The pulse-height spectrum obtained with this "total absorption" polarimeter is presented in Fig. 26. Separate polarization measurements were made on each member of the 0.91–1.85-Mev cascade in  $\text{Sr}^{88}$ . The results show that the parities of the 1.85- and 2.75-Mev levels are even and odd, respectively, in agreement with the results of Bishop and Perez y Jorba (Bi 55).

Later, using the same equipment, Coleman (Co 56a) studied the polarization correlation of the 0.99–1.33-Mev gamma-ray cascade in  $\text{Ti}^{48}$  produced in the decay of  $\text{V}^{48}$ . He discusses the problem of ambiguity arising from a multipole mixture when the result of a direction-direction correlation is used to determine level assignments. Brazos and Steffen (Br 56) showed in their work on the  $\text{Cd}^{114}$  levels that the ambiguity could be reduced by measuring the direction-polarization correlation. In addition, the mixing ratio may be determined when both correlations are known. This problem is illustrated in Part I. For the cascade in  $\text{Ti}^{48}$ , pure quadrupole radiation was established giving the assignment  $4(E2)2(E2)0$ .

The gamma-gamma direction-polarization correlations in the  $\text{Co}^{60}$  and  $\text{Na}^{24}$  decays were studied by Estulin *et al.* (Es 56). The experimental arrangement used was similar to that of Metzger and Deutsch. The measurements on  $\text{Co}^{60}$  were made to determine the reliability of those on  $\text{Na}^{24}$ . In each case the value of  $N_0/N_{90}$  indicated an  $(E2, E2)$  transition in the cascade, leading to assignments of positive parity for the first two excited states in  $\text{Ni}^{60}$  and  $\text{Mg}^{24}$ .

Stelson and McGowan (St 57) have measured the direction-polarization correlation in the 133–482-keV cascade in  $\text{Ta}^{181}$ . They used  $\text{NaI}(\text{Tl})$  crystals, 3 in. thick and 3 in. in diameter, in the counters of the correlation arrangement except in the Compton scatterer

FIG. 26. Pulse-height spectrum of gamma rays from the same decay as in Fig. 25, observed using a "total absorption" polarimeter (figure from Co 56).



which was an anthracene scintillator,  $1\frac{1}{2}$  in. thick by  $\frac{3}{4}$  in. in diameter. The output of a fast-slow triple-coincidence circuit gated a 20-channel pulse-height analyzer on which was displayed the pulse-height spectrum from the analyzing counter of the polarimeter. The effectiveness of the polarimeter had been determined by measuring the polarization of gamma rays resulting from the Coulomb excitation of  $2^+$  levels in even-even nuclei (see next section). The direction-direction measurements (Mc 54a, Pa 55, He 55) had indicated two possible assignments for the 133–482-keV decay:  $5/2(E2)9/2(E2+M1)7/2$  and  $1/2(E2) \times 5/2(E2+M1)7/2$ . The experimental value of  $N_0/N_{90}$  obtained in the polarization measurement clearly agreed with the latter assignment with even parities for the levels. The direction-polarization correlation was measured with both liquid and solid  $\text{Hf}^{181}$  sources as a check on possible systematic errors. It was estimated that the 4% contribution of 136.82-keV radiation from the decay of the 618.9-keV state just above the 615-keV state, did not significantly affect the results.

#### (e) Measurements on Gamma Rays from Nuclear Reactions and Coulomb Excitation

French and Newton (Fr 52) applied these methods to an alpha-gamma direction-polarization correlation in the  $\text{F}^{19}(p, \alpha)\text{O}^{16}(\gamma)\text{O}^{16}$  reaction. This experiment was exceptional in that an octupole transition (Ar 50, Ba 50) is involved and complete polarization is expected at an angle of  $118^\circ$  with respect to the coincident  $\alpha$  particle as seen in Part I. Furthermore the gamma-ray energy was 6.13 MeV. Even though both the crystal absorption and the polarization sensitivity of the Compton process are low at this gamma-ray energy, a Compton polarimeter was still used successfully. Figure 2 shows that  $R=1.27$  at this energy. After correcting for the angular spreads in the apparatus, the authors obtain values of 0.84 and 1.19 for the asymmetry ratio for magnetic and electric octupole radiation, respectively. Since the experimental ratio was  $1.14 \pm 0.06$ , it was concluded that the radiation is electric octupole. This gave an assignment of odd parity to the 6.13-MeV state in  $\text{O}^{16}$ , and even parity to the compound state in  $\text{Ne}^{20}$  and the ground state of  $\text{F}^{19}$ , assuming that the ground state of  $\text{O}^{16}$  is even.

McGowan and Stelson (Mc 58) have measured the polarization of gamma rays resulting from the Coulomb excitation of several odd- $A$  nuclei. In general, these gamma-rays are from mixed  $M1+E2$  transitions. Sometimes, a measurement of the direction-direction correlation between the gamma rays and the incident beam will determine the ratio  $E2/M1$  in addition to specifying the spin of the excited state which is involved. However, the value of  $E2/M1$  or of the spin often remains ambiguous. Such ambiguities can usually be resolved by a direction-polarization measurement.

The equipment and the techniques were essentially

the same as those used by these workers in their study of the gamma rays from  $Ta^{181}$  discussed in the preceding section. The only basic change is that the bombarding beam and target replace the directional counter and source, since the correlation in this case is between bombarding particle and gamma ray. With this method ambiguities in  $E2/M1$  for the gamma-ray transitions or uncertainties in the spin of the first excited states of the following nuclei have been resolved:  $Mo^{95}$ ,  $Rh^{103}$ ,  $Ag^{107}$ ,  $Ag^{109}$ ,  $Cd^{111}$ ,  $Cd^{113}$ ,  $Au^{197}$ ,  $Tl^{203}$ , and  $Tl^{205}$  (see Table XIII).

Litherland and Gove (Li 58) have measured the polarizations of the 1.64-, 0.94-, and 1.37-Mev gamma rays from the  $C^{12}(He^3, p)N^{14}$ ,  $O^{16}(He^3, p)F^{18}$ , and  $Mg^{24}(p, p'\gamma)$  reactions, respectively. The measurements on the 1.64-Mev gamma ray showed that the 3.95-Mev level in  $N^{14}$  had the same parity (positive) as the first excited state. Similarly the 0.94-Mev level in  $F^{18}$  had the same parity (positive) as the ground state. The measurements on  $Mg^{24}$  were performed at the 2.01- and 2.40-Mev resonances and in both cases very large polarizations were found for the gamma rays emitted at  $90^\circ$ . The results also indicate that the first excited state of  $Mg^{24}$  has the same parity (positive) as the ground state.

#### (f) Measurements on Gamma Rays from Aligned Nuclei

Of the several possible methods used for orienting nuclei,††† the two that have been used the most in the experiments with gamma-ray polarization are the Bleaney method (nuclear alignment) and the Rose-Gorter method (nuclear polarization). Either one or both of these methods was used in the gamma-ray polarization experiments now to be described. The method of Rose and Gorter (Go 48, Ro 49) takes advantage of the nuclear polarization produced by magnetic hyperfine coupling in paramagnetic ions which have been polarized by an external magnetic field. In Bleaney's method (Bi 51a) no external field is used. Instead, the internal crystalline field is used to produce the nuclear alignment, through the magnetic hyperfine coupling in paramagnetic ions. In any nuclear orientation method the very low temperatures which are required are produced by adiabatic demagnetization.

The gamma rays emitted by aligned nuclei are linearly polarized. In fact, all the phenomena and the nomenclature which are associated with the direction-polarization correlation have their counterpart in the alignment-polarization correlation.

Bishop *et al.* (Bi 52), using Bleaney's method, made polarization measurements on the gamma rays emitted from aligned sources of  $Co^{58}$  and  $Co^{60}$ . After adiabatic demagnetization, values of  $N_{11}/N_1$  were measured with a Compton polarimeter as a function of  $1/T^*$  by letting the source warm up (Fig. 27). The magnetic temperature  $T^*$  is obtained by measuring the susceptibility

††† Extensive discussions of the methods of orienting nuclei are given in St 57a and Bi 57.

and applying Curie's law. The polarization of both gamma rays together in the 4-2-0 cascade in  $Ni^{60}$  and of the 805-keV gamma ray from  $Fe^{58}$  showed that all these quadrupole transitions (established in the case of  $Fe^{58}$  by Da 52) were electric.

Bishop *et al.* (Bi 54) in a later experiment measured the linear polarization of the gamma rays from aligned  $Mn^{54}$  nuclei. This was done both by Bleaney's method and by that of Rose and Gorter, a greater gamma-ray polarization being obtained with the latter technique. Since the Rose-Gorter method uses an external magnetic field, the scintillation crystals of the polarimeter were mounted on the ends of light pipes, and the photomultipliers were magnetically shielded. With each method the values of  $N_{11}/N_1$  (obtained as a function of  $1/T^*$ ) showed that the radiation from the first excited state of  $Cr^{54}$  at 835 keV had positive parity and was therefore electric quadrupole (Gr 54).

Again using Bleaney's method, Bishop *et al.* (Bi 55a) measured the polarization of the 123-keV radiation from the 137-keV level of  $Fe^{57}$  in the decay of  $Co^{57}$ . This work was accompanied by a measurement of the alignment-direction correlation. It was known (Al 54) that the 123-keV transition is predominantly dipole. The measurement of  $N_{11}/N_1$  as a function of  $1/T^*$  indicated that the transition is predominantly magnetic, thus confirming the suggested parity assignments to the 14- and 137-keV levels (Le 55). From the polarization measurements and the directional correlation a value of  $(E2/M1)^{\frac{1}{2}} = +0.19 \pm 0.02$  was obtained.

Cacho *et al.* (Ca 55), using Bleaney's method, found a value for  $N_{11}/N_1$  of 1.58 at  $1/T^* = 40$  for radiation from the 145-keV first excited state of  $Pr^{141}$  in the  $Ce^{141}$  decay. This led to the conclusion that the transition is predominantly magnetic dipole. The polarization study in conjunction with the directional correlation (Ca 55, Am 56) gave  $(E2/M1)^{\frac{1}{2}} = 0.08 \pm 0.02$ .

The linear polarizations of the quadrupole (Hu 56a) gamma rays, coming from the 6-4-2-0 cascade in  $Cr^{52}$ , following the decay of  $Mn^{52}$  were investigated by Huiskamp *et al.* (Hu 57) using the Rose-Gorter method. The Compton polarimeter which they used also served as a Compton spectrometer [see Sec. (d)] to analyze the

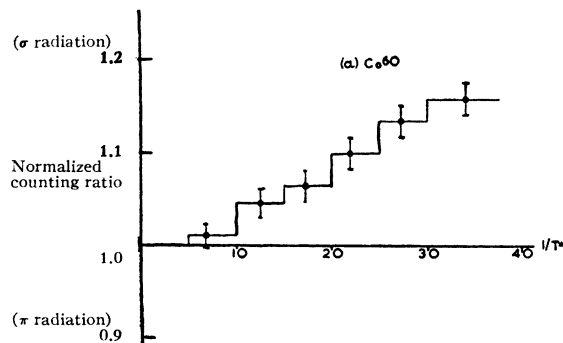


FIG. 27. Linear polarization of the gamma rays from an aligned  $Co^{60}$  source as a function of  $1/T^*$  (figure from Bi 52).



0.73-, 0.94- and 1.46-Mev gamma rays in the cascade. The energy resolution was sufficient to determine the polarization of each of the three gamma rays. In each case, the radiation was found to be electric.

The same apparatus and method also were used by Diddens *et al.* (Di 58) to polarize  $\text{Co}^{56}$  nuclei in the study of the levels in  $\text{Fe}^{56}$ . The Compton polarimeter used as a spectrometer displayed sufficient resolution (14% at 2.76 Mev, 25% at 1.2 Mev) so that the linear polarizations of five gamma rays (0.845, 1.24, 1.75, 2.61, and 3.25 Mev) could be measured satisfactorily. As in the work on  $\text{Mn}^{52}$  a plastic scintillator was used as the scatterer in the polarimeter instead of  $\text{NaI(Tl)}$  because it was found that pair production in the  $\text{NaI}$  with its resulting annihilation radiation produced a serious background for the more energetic gamma rays. The authors also investigated the alignment-direction correlations for the above and other gamma rays produced in the decay of  $\text{Co}^{56}$ . From all their measurements and with the work of others (Sa 55a) they obtained spins and parities for the 0.845-, 2.08-, 3.45-, 3.84-, and 4.10-Mev levels (see Table XIII). Also the 0.845-, 1.24-, and 3.25-Mev gamma rays were found to be electric quadrupole, whereas the 1.75- and 2.61-Mev gamma rays were magnetic dipole.

### B. Measurement of Plane Polarization by Means of the Photodisintegration of the Deuteron

Next to the Compton effect, photodisintegration of the deuteron has proved the most useful polarization-sensitive reaction for gamma rays. In Part II, it was shown that the electric dipole photodisintegration serves as an ideal polarization-sensitive mechanism for gamma rays of energies ranging from about 4 Mev to about 12 Mev. The main disadvantages of the reaction are its low cross section ( $\sim 10^{-27}$  cm<sup>2</sup>) and the fact that the presence of the isotropic magnetic interaction makes it unsuitable for gamma rays whose energies are much below 4 Mev. It can however be used well above 12 Mev without serious loss of sensitivity.

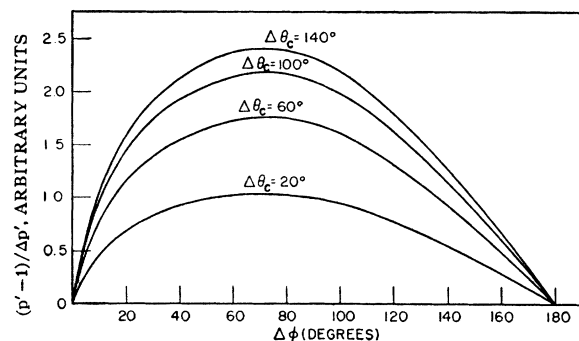


FIG. 28. Figure of merit of a polarimeter using the photodisintegration of the deuteron, plotted as a function of the spread in the angle  $\phi$ , for various spreads in  $\theta_c$  (computed for  $p=1.2$ ).

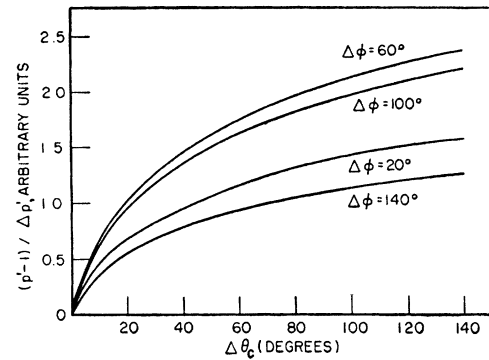


FIG. 29. Figure of merit of a polarimeter using the photodisintegration of the deuteron, plotted as a function of the spread in angle  $\theta_c$ , for various spreads in  $\phi$  (computed for  $p=1.2$ ).

#### (a) Experimental Considerations

Two methods of utilizing the polarization sensitivity of the deuteron are apparently feasible. One method would be very similar to the Compton polarimeter. The gamma rays would impinge on a "scatterer" containing deuterium, and the photoneutrons would be detected in one (or two) side counters. Almost all the discussion of the Compton polarimeter can be applied to this case. Thus, the advantage of making the "scatterer" itself a detector is obvious. In this case the photoproton would be detected. A very serious drawback to such a polarimeter would be the very high background of events from Compton scattering and pair production. This difficulty might be overcome with modern techniques such as the use of time-of-flight to isolate the neutrons. The advantage of the method over the Compton polarimeter would be its increased sensitivity to polarization at high gamma-ray energy. Its advantage over the emulsion technique, described in the following, would be its possible use in a direction-polarization measurement requiring the detection of co-incident radiations. Figures 28 and 29 show the figure of merit for such a polarimeter for various angular spreads. The conditions are the same as in the corresponding calculations for the Compton polarimeter, Figs. 19 to 22, except that here the energy is not an important parameter as long as the electric dipole disintegration is dominant (as assumed in Figs. 28 and 29). That the polarization sensitivity is practically independent of  $\theta_c$  is reflected in the continued rise of the curves as  $\Delta\theta_c$  increases in Fig. 29. The curves in Figs. 28 and 29 can be used in the analysis of data obtained in the emulsion technique.

The simplest polarimeter using the photodisintegration of the deuteron, and the one used in all the experiments performed so far, consists of a nuclear emulsion impregnated with heavy water ( $\text{D}_2\text{O}$ ). The emulsions are mounted so that the plane of the emulsion is normal to the direction of propagation of the gamma rays. In this position the maximum number of photoprotons will

lie in the emulsion since the angular distribution of the photoprotons goes essentially as  $\sin^2\theta$  about the direction of propagation of the gamma ray. The emulsion can then serve as a polarimeter by comparing the density of tracks at  $\phi=0^\circ$  with that at  $\phi=90^\circ$ .

The technique of loading the emulsion was first used by Goldhaber (Go 51) in studies of the angular distribution of the protons from the photodisintegration of deuterons. In the experiments described below, either Ilford C2 or G5 emulsions were soaked in  $D_2O$  to saturation at some fixed temperature between  $10^\circ C$  and  $20^\circ C$ . Although the grain density of proton tracks is considerably diminished under these conditions, satisfactory range definition can be obtained in Ilford C2 emulsions with appropriate developing techniques. Better definition can be achieved using Ilford G5 emulsions but in this case precautions must be taken to reduce fogging if low-energy gamma or x-radiation is present.

The amount of water absorbed by a saturated emulsion increases with increasing temperature. However, the emulsion generally becomes too soft to use at temperatures much above  $20^\circ C$ . Saturation of the plates is desirable in order to attain a uniform distribution of water throughout the emulsion. If range determinations are to be made, it is essential for the proton range for a given energy to be constant throughout the emulsion. A uniform distribution of the water is important also in making depth measurements in the emulsion. If the expansion of the emulsion on soaking and the subsequent shrinkage on development do not take place uniformly, it is not possible to obtain accurate measurements on the vertical range of a track. A depth measurement depends on a knowledge of the shrinkage factor (ratio of emulsion thickness before and after development). For most purposes an adequate measurement of the shrinkage factor can be obtained with a micrometer, although more elegant techniques are possible. While the emulsions are being exposed they are kept in watertight containers at a controlled temperature. Usually one plate in an exposure is saturated with  $H_2O$  to provide a background measurement.

#### (b) Experiments Using Nuclear Emulsions

Emulsions soaked in  $D_2O$  were first used in a polarization experiment by Wilkinson (Wi 52) in a study of the gamma rays from the  $H^2(p,\gamma)He^3$  reaction. In this nonresonant reaction, the energy of the gamma ray is greater than 5.5 Mev by an amount which depends on the energy of the bombarding protons. Since the directional distribution is given by  $\sin^2\theta$  (Fo 49), the gamma rays are expected to be essentially completely polarized (Part I).

Ilford C2 emulsions  $100\ \mu$  thick were soaked in  $D_2O$  and placed about 7 cm from a  $D_3PO$  target. Although the reaction was weak, 120 usable proton tracks were found in the emulsion after a five-hour exposure with a

$50\text{-}\mu$  proton beam (1.1 Mev). Wilkinson adopted some simple range and depth criteria to insure the counting of desired events. Since the polarization sensitivity is independent of the polar angle, only the azimuthal angle is recorded. Figure 30 shows the azimuthal distribution of proton tracks projected on the plane of the emulsion. It confirms that the gamma rays are electric dipole and are essentially perfectly polarized. On the other hand, if it is assumed from other evidence (Fo 49) that the gamma rays are completely polarized, then the experiment serves to confirm the ideal polarization sensitivity of the photodisintegration of the deuteron for gamma rays of about 6 Mev.

Fagg and Hanna (Fa 53) used the photodisintegration process to measure the polarization of the 6.13-, 6.9-, and 7.1-Mev gamma rays from the  $F^{19}(p,\alpha)O^{16}(\gamma)O^{16}$  reaction, at  $E_p=0.874$  Mev. Ilford C2 emulsions  $400\ \mu$  thick were soaked to saturation in  $D_2O$  and placed 4 cm from a thin target, with the plane of the emulsion normal to the gamma rays emitted at  $90^\circ$ . Several exposures of about  $250\ \mu$ a-hours each were made. Complete resolution of the 6.9-, and 7.1-Mev gamma rays could not be expected but it was essential to isolate the strong 6.13-Mev radiation from the other two. This could be done in a simple manner which permitted (relatively) rapid counting, with the result shown in Fig. 31. In essence, a single depth criterion was adopted: an acceptable proton track must be in sharp focus along its complete range. The utility of the technique is seen by writing the photoproton distribution, (II-14), in terms of projected range  $p=R\sin\theta$ :

$$d\sigma \sim p^2(R^2 - p^2)^{-1/2} dp.$$

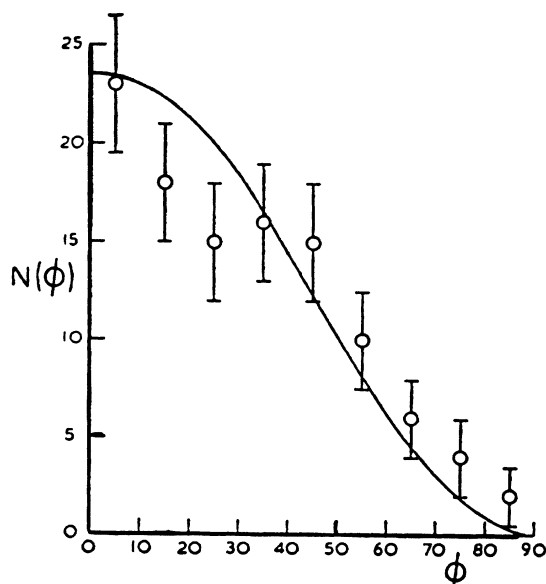


Fig. 30. Linear polarization of gamma rays from  $H^2(p,\gamma)He^3$ , demonstrated by photodisintegration of deuterons in impregnated emulsion. The azimuthal distribution of photoproton tracks projected onto the plane of the emulsion is shown (figure from Wi 52).

This distribution is plotted as the dotted line in Fig. 31. Experimentally, it gives a very pronounced peaking at  $p=R$ . The cutoff at  $p_c$  is of course established by the depth criterion. In this case  $p_c$  was chosen to resolve the 6.13-Mev gamma ray. The resolution could be improved, by increasing  $p_c$ , without greatly decreasing the total number of accepted tracks.

With this technique enough resolution was obtained to give qualitatively the polarizations of the 6.9- and 7.1-Mev gamma rays. This qualitative information was used along with the measured polarization ratio and the directional distribution coefficient (Sa 52) for the unresolved group to deduce the parities of the 6.91- and 7.12-Mev states in  $O^{16}$ . These parities (plus and minus, respectively) agreed with those given by Seed and French (Se 52). No assignment could be made for the 6.13-Mev level since the corresponding polarization distribution was essentially isotropic, in agreement with the isotropy observed by Sanders (Sa 52) in his directional distribution measurement.

Nuclear emulsions impregnated with heavy water were also used by Hughes and Sinclair (Hu 56) in their study of the polarization of the gamma radiation from the reactions  $Al^{27}(p,\gamma)Si^{28}$ ,  $Mg^{26}(p,\gamma)Al^{27}$ , and  $Na^{23}(p,\gamma)Mg^{24}$ . Ilford G5 emulsions (300  $\mu$  and 400  $\mu$  thick) were used in order to give well-defined tracks and to avoid fading of the tracks during the long exposures. A copper absorber  $\frac{1}{8}$  in. thick was effective in

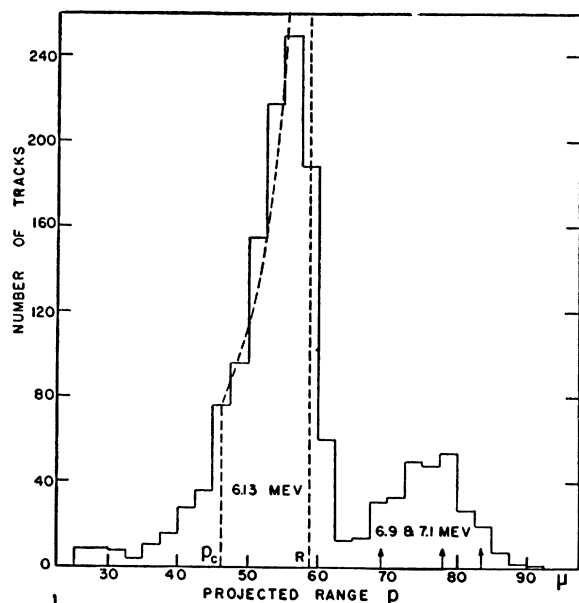


FIG. 31. Projected range distribution of the photoprotons produced by the 6.13-, 6.91-, and 7.12-Mev gamma rays from the  $F^{19}(p,\alpha)O^{16}(\gamma)O^{16}$  reaction. The photoprotons are produced in emulsions impregnated with  $D_2O$ . Dashed curve is the theoretical distribution for the projected range, assuming an empirical cutoff at  $P_c$ .  $R$  is range of photoproton resulting from the 6.13-Mev gamma ray. Arrows in the vicinity of 80 microns mark expected ranges of photoprotons from the 6.91- and 7.12-Mev gamma rays (figure from Fa 53).

preventing low-energy x-rays from blackening the plates. The targets used were thin enough so that in each bombardment a single resonance was isolated. Both the horizontal and vertical projection of each proton track was measured in the microscope and the range was calculated from these values. The following gamma rays were investigated: the 7.5- and 10.4-Mev gamma rays from  $Si^{28}$ , the 7.6- and 8.6-Mev gamma rays from  $Al^{27}$ , and the 7.2-, 8.1-, and 10.8-Mev gamma rays from  $Mg^{24}$ . A definite polarization was observed in the case of the 10.4-, 7.6-, and 10.8-Mev radiations, all of which were found to be electric in character. The 10.4-, 7.6-, and 10.8-Mev radiations had each been shown to be dipole in character in Ru 54, Ru 56, and Gr 55, respectively. The character of the radiation was used to assign even parity to the ground state and first excited state of  $Al^{27}$  (in agreement with Da 53) and to the ground state of  $Na^{23}$ . For the remainder of the gamma rays no polarization was observed. Hughes and Sinclair also include in an appendix a range-energy relation for protons up to 5 Mev in wet emulsions.

### C. Measurements of Plane Polarization by Means of the Photoelectric Effect

In Part II it was shown that the usefulness of the photoelectric effect for detection of gamma-ray polarization is rather doubtful. The experiments which have been performed have been primarily motivated by a desire to elucidate the photoelectric effect rather than to measure polarization. With an arrangement very similar to Fig. 15, Hereford (He 51) used two photoelectric polarimeters to observe the cross-polarization of annihilation radiation. In an improved experiment Hereford and Keuper (He 53) substituted a Compton polarimeter for one of the photoelectric detectors. These investigations were followed by the experiments of McMaster and Hereford (Mc 54) and of Brini *et al.* (Br 57) in which the polarization produced in Compton scattering was used to investigate the photoelectric effect, with the discordant results already noted in Part II.

### D. Measurement of Circular Polarization by Means of the Compton Effect

Recently, considerable interest has been exhibited in the measurement of circular polarization of gamma rays. This interest has been stimulated primarily by the fundamental reformulation of the law of conservation of parity in weak interactions and the resultant introduction and confirmation of the two-component neutrino theory (Le 56, Le 57). The developments in the measurements of the circular polarization of gamma rays have progressed at a rapid rate. It is the aim here to bring together the methods and techniques of the various investigations and to collect the results which have appeared.

TABLE XII. Sign of the circular polarization effect  $R$  for right circular polarization, for the conditions listed.

Sign of $R$	Transmission	Scattering
-	$E_\gamma < 0.63$ Mev	$\theta_c < 90^\circ$
+	$E_\gamma > 0.63$ Mev	$\theta_c > 90^\circ$

(a) *Experimental Considerations*

A discussion of the Compton scattering of circularly polarized gamma rays by polarized electrons has been given in Part II. The most convenient source of polarized electrons is a ferromagnet. Experimentally the circular polarization of gamma rays is detected by observing the difference in the scattering from electrons in magnetized iron when the magnetization is reversed or when it is removed. This may be done by observing (1) the gamma rays transmitted through the magnetized iron, (2) those scattered from the iron at same appropriate angle, or (3) the electrons ejected forward from the surface of the iron. Although a considerable effect (change in the counting rate with change in magnetic field) could be expected for perfectly polarized gamma rays and electrons at certain angles and energies (Figs. 4 and 5), in practice the effect is greatly diminished by the fact that only about 2 electrons of the 26 in each iron atom can be polarized by magnetization. Therefore, the polarization effect is at most only a few percent; and quite often it is less than one percent, if the gamma-ray polarization is small.

For any one of the above methods, let  $N_+$  denote the experimental yield of gamma rays when the magnetization of the analyzer is directed toward the source, and  $N_-$  the yield when it is directed away from the source. The experimental effect is given by

$$R = 2 \frac{N_+ - N_-}{N_+ + N_-} \quad (\text{III-3})$$

The sign of the effect is of great importance. It is determined by the sign of the polarization-sensitive cross section (Figs. 4 and 5) and the sense of the photon polarization. For ready reference the sign of  $R$  is given in Table XII for right circular polarization (see definition in Part I, C) and for four experimental conditions. The sign of  $R$  is reversed for left circular polarization. Hence, from the sign of the effect, one may determine the sense of the circular polarization and so also of the polarized emitting nucleus. This much alone has led to very important discoveries.

In accordance with the theoretical definition (Part I, C), the degree of circular polarization is

$$P_3 = \frac{J_r - J_l}{J_r + J_l} \quad (\text{III-4})$$

where  $J_r$  and  $J_l$  are the number of right and left circularly polarized photons. Let  $J_r^0$  and  $J_l^0$  be the initial

intensities and  $J_r^\pm$  and  $J_l^\pm$  the transmitted intensities corresponding to (+) or (-) magnetization. Then

$$J_r^\pm = J_r^0 \exp\{-nt(\sigma_0 z \pm \sigma_1 \nu)\}$$

$$J_l^\pm = J_l^0 \exp\{-nt(\sigma_0 z \mp \sigma_1 \nu)\}.$$

With  $N_\pm = J_r^\pm + J_l^\pm$ , we obtain for (III-3)

$$R = 2P_3 \tanh(-n\sigma_1 \nu), \quad (\text{III-5})$$

where  $n$  is the number of iron atoms per unit volume,  $t$  is the effective thickness of the iron analyzer, and  $\nu$  is the number of polarized electrons per iron atom, equal to 2.06 at saturation (Ar 53). In using this formula to obtain  $P_3$  from a measurement of  $R$ , it is necessary to find appropriate values for  $t$  and  $\nu$ . Alternatively, the analyzer may be calibrated with a source of known polarization.

For the differential cross section we can write

$$d\sigma = d\sigma_0 \pm fP_3 d\sigma_1, \quad (\text{III-6})$$

where  $d\sigma_1$  is the polarization-sensitive cross section shown in Fig. 4 for the case in which the electron polarization is parallel to the photon momentum. The circular polarization  $P_3$  and the electron polarization  $f$  are displayed explicitly. At saturation  $f \cong 2/26$ . Since, in an analysis by scattering, the observed intensity is simply proportional to the differential cross section, we can write§§§

$$R = 2 \frac{d\sigma_+ - d\sigma_-}{d\sigma_+ + d\sigma_-} = 2fP_3 \frac{d\sigma_1}{d\sigma_0}, \quad (\text{III-7})$$

where  $d\sigma_1/d\sigma_0$  is the ratio of the two differential cross sections. In order to use this expression it is important to have a value for  $f$  that applies to the iron in the region of the scattering. When large solid angles are used, it is also necessary to integrate the cross sections over the angular spreads. In practice the efficiency of the analyzer is often checked with radiation of known polarization.

Since long runs usually are necessary in order to obtain statistically significant results, the changes in the magnetic field are usually made at frequent, periodic intervals in order to minimize the effect of possible electronic drifts. Changes in the counting rate of the detector produced by the changes in the magnetic field are avoided by magnetically shielding the counter and by removing it from the influence of the field by use of a light pipe. If the experimental arrangement is such that changes in magnetic field do affect the counting rate, the effect can be controlled in the beta-gamma coincidence experiments by normalizing the coincidence rate to the gamma-ray singles rate.

§§§ If there is a component of linear polarization in the gamma radiation, the normalization of this expression is changed (Wh 55).

(b) *Measurements on Gamma Rays from Polarized Nuclei (Parity Conserving)*

The first experiment dealing with the circular polarization of gamma rays was performed by Clay and Herford (Cl 52) who attempted to measure the circular polarization of annihilation radiation by detecting Compton electrons ejected in the forward direction from magnetized iron. The effects they observed are now believed to be instrumental in origin (To 56).

Using the apparatus shown in Fig. 32 Wheatley *et al.* (Wh 55) studied circularly polarized gamma rays of nuclear origin in their investigation of the gamma rays emitted from  $\text{Co}^{60}$  nuclei which had been polarized by the Rose-Gorter method. After adiabatic demagnetization the cryostat containing the source was inserted into the position shown in Fig. 32 (which shows one half of the symmetrical apparatus). It is recalled that the circular polarization is a maximum for gamma rays emitted along the axis of the nuclear polarization, and that the circular polarization changes sign if the axis is reversed. It was convenient therefore to perform the experiment by reversing the nuclear polarization (instead of the electron polarization) which is controlled by the inner magnet  $M_p$  (which shares a yoke with the outer magnet  $M_s$ ). Except for the features associated with the nuclear polarization, especially in the design of the magnet, the polarimeter itself is a forerunner of

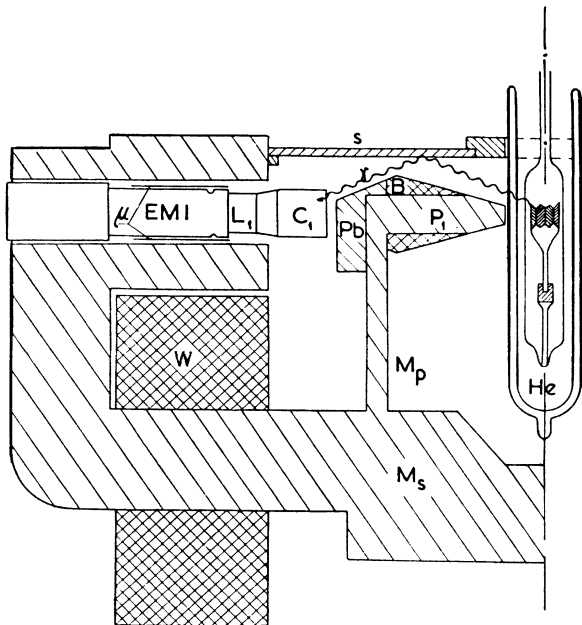


FIG. 32. Diagram of apparatus used by Wheatley *et al.* for producing and measuring circularly polarized gamma rays. A change in the differential Compton cross section is measured by changing the direction of circular polarization of the gamma rays, emitted from polarized nuclei in the cryostat, relative to the direction of magnetization in the scattering iron  $S$ . Magnet  $M_p$  (with coil  $B$ ) determines the direction of polarization of the nuclei; Magnet  $M_s$  (with coil  $W$ ) determines the direction of magnetization of  $S$  (figure from Wh 55).

more recent analyzers using the scattering method. Direct radiation is shielded from the detector, but gamma rays scattered (at angles between  $45^\circ$  and  $70^\circ$ ) from the magnetized strip  $S$  (Armco iron) are recorded. The magnetization in  $S$  is produced by the magnet  $M_s$ . The degree of circular polarization achieved was as high as 75% at the lowest temperature,  $0.006^\circ\text{K}$ . The observed fractional change in counting rate upon changing the direction of polarization of the nuclei was at most 3%. In this experiment the circular correlation function has the form (Part I, C)

$$P_3 = [A_1 P_1(\cos\theta) + A_3 P_3(\cos\theta)] / W(\theta),$$

where  $A_1$ ,  $A_3$ , and the coefficients in the directional function  $W(\theta)$  are functions of the degree of orientation and so of the temperature. For temperatures in the region  $1/T < 60$ , Wheatley *et al.* obtain excellent agreement with the theoretical correlation function. For lower temperatures the observed deviation may be due to imperfect knowledge of the hyperfine coupling. As we have seen the sign of the effect alone makes possible a determination of the sign of the magnetic moment of the emitting nucleus. In this case the sign of the magnetic moment of the  $\text{Co}^{60}$  nucleus was found to be positive.

Trumpy (Tr 57) using the apparatus shown in Fig. 33 studied the circular polarization of the gamma rays resulting from the capture of polarized neutrons by the following nuclei:  $\text{S}^{32}$ ,  $\text{Ca}^{40}$ ,  $\text{Ti}^{48}$ ,  $\text{Cr}^{53}$ ,  $\text{Fe}^{57}$ ,  $\text{Ni}^{58}$ ,  $\text{Zn}^{64}$ , and  $\text{W}^{182}$ . The emitting compound nucleus receives its polarization from the captured neutron. Again, the maximum circular polarization occurs for gamma rays emitted along the axis of polarization. Trumpy selected the transmission method for the analysis of circular polarization. Thermal neutrons emerge from a neutron collimator and pass through a neutron polarizer, consisting of a small iron block mounted in the gap of a magnet in which a field of 14 900 oe is produced. The polarized neutrons impinge on a target and the capture gamma rays, emerging along the directions parallel and antiparallel to the polarization, reach two sodium iodide detectors after being transmitted through the two analyzing magnets. The path through each magnet core is 8 cm long. The heavy shielding of lead and boron carbide reduces the intense background of radiation arising chiefly from neutron capture in the polarizing iron block. Particular gamma rays could be selected for study by means of energy discrimination in the detectors. The experiment was performed by recording the counts in both detectors as a function of the direction of magnetization in the analyzers and the direction of polarization of the neutrons as determined by the polarizing magnet.

Trumpy uses an explicit formula given by Biedenharn *et al.* (Bi 51) for the capture of totally polarized thermal neutrons followed by pure multipole emission. In the correlation  $A_1 P_1(\cos\theta)$ , which measures the degree of

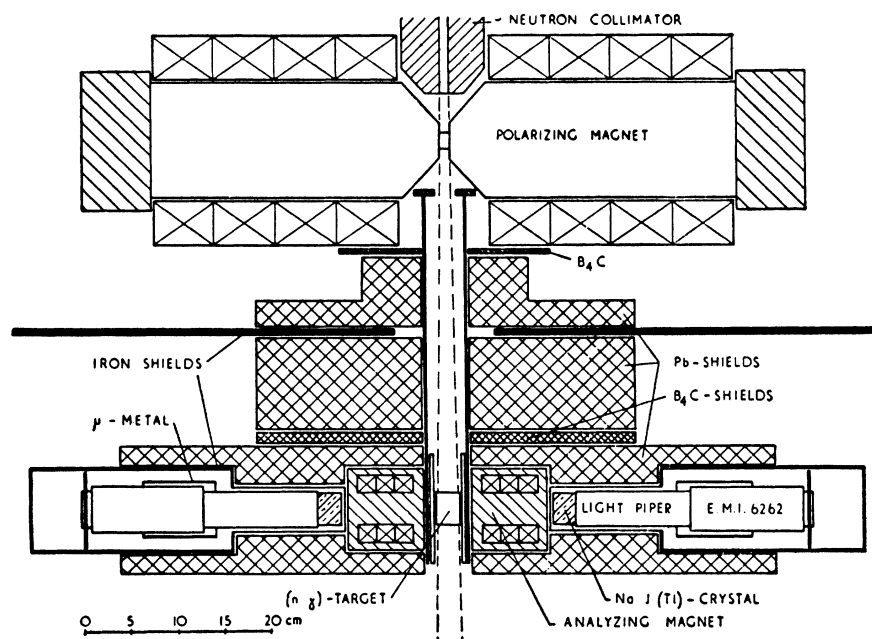


FIG. 33. Top view of experimental arrangement used by Trumpy to detect circular polarization following capture of polarized neutrons. Circular polarization is detected by measurement of the transmission through magnetized iron (figure from Tr 57).

right circular polarization, the coefficient  $A_1$  is given by

$$A_1 = 2(j - j_1) \frac{L(L+1) + j(j+1) - j_2(j_2+1)}{L(L+1)(2j_1+1)}, \quad (\text{III-8})$$

where  $j_1$ ,  $j$  and  $j_2$  are the spins of target nucleus, compound nucleus and final nucleus, respectively, and  $L$  is the multipole order of the gamma-ray transition. This is equivalent to the result obtained in Part I, C. Since one or more of the angular momenta in (III-8) are often known and  $j = j_1 \pm \frac{1}{2}$ , a measurement of  $A_1$  can yield definite assignments of spin (and parity). For example, if  $j_1 = 0$ ,  $j = \frac{1}{2}$ , and  $L = 1$ , then  $A_1 = 1$  or  $-\frac{1}{2}$  for  $j_2 = \frac{1}{2}$  or  $\frac{3}{2}$ , respectively.

The theoretical value of the circular polarization, given by  $A_1$ , is reduced in practice because of the incomplete polarization of the neutron beam (19%). The efficiency of the analyzer was determined in a manner equivalent to (III-5). In the case of  $S^{33}$  the spin of the 3.15-Mev level was found to be  $\frac{3}{2}$ . In  $Ca^{41}$  the spin of the 1.98-Mev level also was determined as  $\frac{3}{2}$ . The measurements on the 6.41- and 6.75-Mev gamma rays from  $Ti^{49}$  were consistent with spins of  $\frac{1}{2}$  and  $\frac{3}{2}$  for the 1.70- and 1.35-Mev states, respectively. Trumpy's results for  $Cr^{54}$  in conjunction with his angular correlation work (Tr 57a) indicated a  $1(1)2(2)0$  decay scheme for the 9.72-, 0.84- and 0-Mev levels. Also both the 9.72- and 8.88-Mev gamma rays are  $E1$ . Contrary to shell-model predictions, the results on  $Fe^{57}$  indicated that its ground state is  $\frac{1}{2}^-$ . A spin of  $\frac{3}{2}$  was confirmed for the ground state of  $Ni^{59}$ , and either  $\frac{3}{2}$  or  $\frac{5}{2}$  for the ground state of  $Zn^{65}$ . The spins and multipolarity involved in the decay of the 6.18-Mev state in  $W^{183}$  were known from other work. Consequently the measurement on this

nucleus constituted a verification of the direction and order of magnitude of the expected circular polarization.

In another part of their work, discussed in Part III, A(f), Huiskamp *et al.* (Hu 57) measured the circular polarization of the three unresolved gamma rays of  $Cr^{52}$  (0.73, 0.94, 1.43 Mev) resulting from the decay of  $Mn^{52}$ . The  $Mn^{52}$  nuclei were polarized by the Rose-Gorter method. The arrangement for the circular polarization measurement was identical to that in the experiment of Wheatley *et al.* (Wh 55) shown in Fig. 32. The range of forward scattering angles defined by the geometry and the energy bias of the detector were such that all three gamma rays could be counted. The degree of circular polarization found for the  $Mn^{52}$  gamma rays as a function of  $1/T^*$  is shown in Fig. 34. No attempt was made to determine the intensity contributed by each gamma ray to the total since all three radiations were expected to have the same degree of circular polarization. Thus it was clearly possible to determine the sign of the effect which was all that was desired. As in the case of the experiment of Wheatley *et al.* (Wh 55), the sign of the effect indicated that the sign of the magnetic moment of  $Mn^{52}$  is positive.

Discovery of nonconservation of parity in weak interactions prompted Wilkinson (Wi 58) to re-examine the extent to which parity is conserved in the strong interactions. He tested the conservation of parity in strong interactions by three classes of experiments. One of these involves a search for circular polarization of gamma rays from a nuclear reaction in the initial state of which all particles are unpolarized. Wilkinson looked for circular polarization of the 2.14- and 7.12-Mev gamma rays from the  $B^{11}(p,p')B^{11*}(\gamma)B^{11}$  and  $F^{19}(p,\alpha)O^{16*}(\gamma)O^{16}$  reactions, respectively. He used

transmission through magnetized iron as the method of analysis for circular polarization. Since very small effects, if any, were expected, considerable precautions were taken to eliminate systematic errors resulting, for instance, from the influence of magnet reversals on the photomultipliers or from electronic drifts. The scintillating crystal was mounted at the end of a light pipe either two or four feet long. The two-foot pipe was used with the  $F^{19}(p,\alpha)O^{16*}$  reaction for which greater resolution was needed. The photomultiplier was surrounded not only with a mu-metal shield but also with two coaxial iron pipes. To prevent the degraded radiation emerging from the magnet from masking the effect under study, the bias of the electronic apparatus was set to accept only the very high-energy end of the spectrum. Since the search was for such small effects, over five-hundred runs were made on each reaction. The results of the runs were carefully averaged in different ways to eliminate the possible influence of systematic errors. Average values of  $N+/N- = 1.00025 \pm 0.00026$  and  $1.00003 \pm 0.00024$  were found for the boron and fluorine reactions, respectively, where  $N+/N-$  is the ratio of the counting rate with the magnetic field in one direction to that in the other. Thus, within the aforementioned limits, there is no circular polarization and no nonconservation of parity.

### (c) Beta-Gamma Circular Polarization Correlation

The measurement of circular polarization in beta-gamma decay was one of the early experiments performed after the discovery of nonconservation of parity in weak interactions (Le 56) and the revival of the two-component theory of the neutrino (Le 57). The

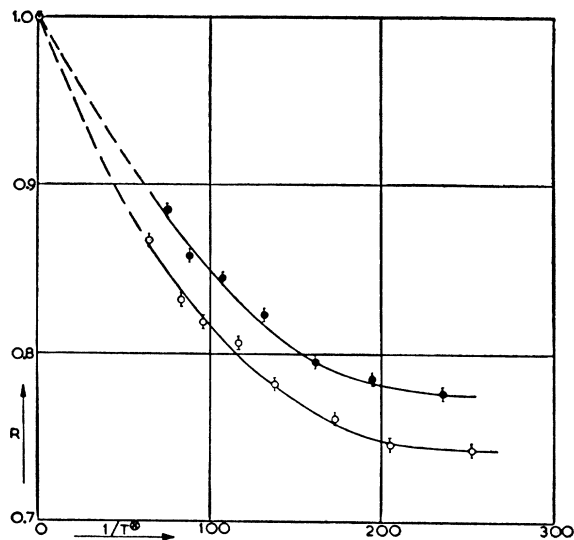


FIG. 34. Circular polarization of gamma rays emitted from a polarized  $Mn^{52}$  source. Ordinate  $R$  is the counting rate normalized to unity at  $T=1^\circ K$ . Open circles correspond to the polarizing field and the induction in the scattering iron being parallel, while closed circles correspond to their being antiparallel (figure from Hu 57).

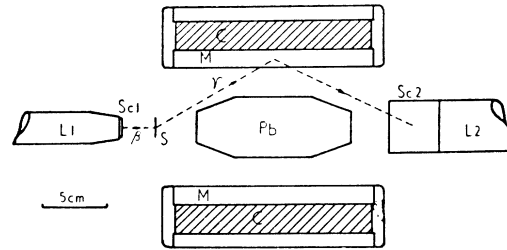


FIG. 35. Experimental arrangement used by Schopper for the beta-gamma circular-polarization correlation. Sc 1 is the beta counter using a plastic scintillator; Sc 2 is the gamma counter with a NaI(Tl) crystal; L1 and L2 are light guides; S is the source; and M is a cylindrical magnet with magnetizing coils (figure from Sc 57).

experiments have since been carried forward and have provided valuable information on the nature of beta decay. The aim of the measurements is to determine the asymmetry coefficient  $A_1 = -(v/c)A$  in the circular polarization correlation (Part I, C),

$$P_3 = (v/c)A \cos\theta, \quad (\text{III-9})$$

which gives the degree of right circular polarization as a function of the angle between the beta particle and the gamma ray. Both the scattering method and the transmission method have been used to good advantage in this work, the polarizations being obtained by (III-5) and (III-7) or their equivalent. The beta-gamma circular polarization measurement provides the same information as does a knowledge of the electron distribution from polarized nuclei. The former technique has the advantage, however, of being feasible for a large number of different nuclei.

Schopper (Sc 57) first performed such a correlation experiment in the decay of  $Co^{60}$  and of  $Na^{22}$ . These nuclei have allowed  $\parallel \parallel \parallel \beta$  transitions with  $\Delta J=1$  followed by pure multipole radiation. The experimental arrangement (Fig. 35) is designed to study the circular polarization of the gamma rays emitted at an angle close to  $180^\circ$  measured with respect to the direction of the beta particles. The average forward scattering angle was  $55^\circ$ , which is about optimum for circularly polarized gamma rays of the energies used in the experiment ( $\sim 1.25$  Mev). Electronic discrimination in the circuits was provided in order to avoid counting backscattered gamma rays, annihilation radiation, and stray beta particles. Although light pipes were used in the detectors, possible variations in the coincidence rate produced by the changes in the magnetic field were eliminated by using the ratio of the coincidence rate to the product of the singles rates.

In the decay of  $Co^{60}$  two gamma rays are emitted in a 4-2-0 cascade, but the gamma rays can be treated as one since in this special case the polarization of the second gamma ray is the same as that of the first

$\parallel \parallel \parallel$  All of the beta transitions discussed in this section are allowed unless otherwise specified.

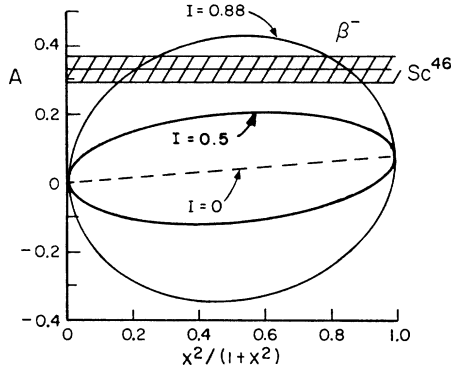


FIG. 36. Asymmetry coefficient in the beta-gamma circular polarization for a  $4^+(\beta)4^+(\gamma)2^+(\gamma)0^+$  transition. The experimental value for  $\text{Sc}^{46}$  is indicated. Theoretical curves for  $I = I_{\text{max}} = 0.88$ ,  $I = 0.5$  and  $I = 0$  are shown;  $I$  is the interference term that enters into  $A$ . If  $I > 0$ , the upper branch of the theoretical curve refers to the choice of  $x = a^{\frac{1}{2}} M_{GT}/M_F > 0$  and the lower branch to the case  $x < 0$ . If  $I < 0$  the opposite assignment is true. The figure shows that a large value for  $I$  is required to fit the experimental data (figure from Bo 58).

(To 53). Schopper found  $A = +0.39 \pm 0.08$  and  $-0.41 \pm 0.07$  for  $\text{Na}^{22}$  and  $\text{Co}^{60}$ , respectively. These results can be compared to theoretical values of  $+\frac{1}{3}$  and  $-\frac{1}{3}$  respectively. The result on  $\text{Co}^{60}$  is in accord with the experiment of Wu *et al.* (Wu 57) which measured the electron distribution from polarized  $\text{Co}^{60}$  nuclei. The opposite signs for  $\text{Co}^{60}$  and  $\text{Na}^{22}$  indicate opposite circular polarizations and show that the antineutrino emitted in negatron decay and the neutrino emitted in positron decay have opposite helicity. In a note added in proof in his paper Schopper reports a result leading to a value of  $A = -0.07 \pm 0.05$  for  $\text{Na}^{24}$ .

Boehm and Wapstra (Bo 57, Bo 58) using a very similar experimental arrangement have studied the circular-polarization correlations in many beta-gamma decays. Their first experiments were performed on  $\text{Co}^{60}$ ,  $\text{Au}^{198}$  and  $\text{Hg}^{203}$ , the latter two of which have first-forbidden beta transitions to the 0.411- and 0.279-Mev states in  $\text{Hg}^{198}$  and  $\text{Tl}^{203}$ , respectively. A refined expression for the efficiency of the analyzer was calculated by Alder,

$$\epsilon = 2.90k(1 + 0.13k)/(1 + 0.36k + 0.09k^2),$$

where  $\epsilon$  would be the experimental effect (in percent) for a completely circularly polarized gamma ray of energy  $k$  (in units of  $m_0c^2$ ). Measurements on the circularly polarized bremsstrahlung created by the beta-particles from  $\text{P}^{32}$  and  $\text{Tm}^{170}$  were made partly to check this formula and partly to establish the  $v/c$  law for the polarization of electrons emitted in beta decay. The experimental results found for  $\text{P}^{32}$  and  $\text{Tm}^{170}$  were consistent with both the formula and the  $v/c$  law. In the circular-polarization measurement performed on  $\text{Co}^{60}$  a value of  $A = -0.41 \pm 0.08$  was found, in agreement with Schopper's value. The value of  $A = 0.52 \pm 0.16$  that was found for  $\text{Au}^{198}$  is consistent with a

spin of 2 and rules out a spin of 3 for the ground state of  $\text{Au}^{198}$ . With the value of  $A = -0.06 \pm 0.22$  for  $\text{Hg}^{203}$  (Bo 58) it was not possible to exclude a spin of  $\frac{5}{2}$  for the ground state of  $\text{Hg}^{203}$  but the measurement is consistent with a spin of  $\frac{3}{2}$ .

Boehm and Wapstra studied further the above  $J$ - $J$  transition in  $\text{Au}^{198}$  along with those in  $\text{Co}^{58}$  (Bo 57a, Bo 58) and  $\text{Sc}^{46}$  (Bo 57b, Bo 58). The  $J$ - $J$  transitions are of great interest because of the mixed nature of the beta transition. Thus the decay scheme of  $\text{Sc}^{46}$  is  $4^+(\beta)4^+(2)2^+(2)0$  and differs from the  $\text{Co}^{60}$  case only in that  $\Delta J = 0$  instead of 1. For this decay scheme, Boehm and Wapstra write the asymmetry coefficient in compact form (Part I, C) as

$$A = (0.0834x^2 + 0.745a^{\frac{1}{2}}Ix)/(1+x^2), \quad (\text{III-10})$$

where  $x = a^{\frac{1}{2}} M_{GT}/M_F$ ,  $a = (C_{GT}/C_F)^2 = 1.3$  (Ko 56) and  $I$  is the interference factor whose numerator is equal to  $S_1$  for  $LL' = 01$  in Table X. If  $I = 0$ ,  $A$  varies from 0 to 0.083, as  $x$  goes from 0 to  $\infty$ . If  $Ix > 0$ , then  $A > 0$ , but if  $Ix < 0$ , then  $A < 0$  except when  $|Ix| < 0.098x^2$ . Finally, if the two-component neutrino theory with invariance under time reversal is valid, the maximum value of  $|I|$  is given by  $a^{-\frac{1}{2}} = 0.88$ . These properties are illustrated in Fig. 36 which gives curves for three values of  $|I|$ , namely 0, 0.5 and the maximum 0.88. The experimental result for  $\text{Sc}^{46}$ ,  $A = 0.33 \pm 0.04$ , is shown on the graph. The experimental value indicates a large value of  $|I|$ . Boehm and Wapstra give  $|I| \geq 0.5$  with a statistical uncertainty of 1%. Since the dominant term  $\Re(C_S C_T'^* + C_S' C_T^* - C_V C_A'^* - C_V' C_A^*)$  in  $I$  is  $\Re(C_S C_T'^* + C_S' C_T^* - C_V C_A'^* - C_V' C_A^*)$ , this large value of  $|I|$  rules out a pure  $V$ ,  $T$  or a pure  $S$ ,  $A$  interaction in this beta decay. If the maximum interference is assumed, a value of 2.2 is found for  $|M_{GT}/M_F|$ . For  $\text{Co}^{58}$ , Boehm and Wapstra found  $A = -0.14 \pm 0.07$ , and since the pure  $GT$  value is  $-0.083$ , no conclusion could be drawn concerning the interference term. The assumption of maximum interference, as suggested by the  $\text{Sc}^{46}$  result, leads to  $|M_{GT}/M_F| > 8$ . The value of  $A$  obtained for  $\text{Au}^{198}$  (first forbidden) agreed with the earlier result and was consistent with the maximum theoretical value.

In a complete report (Bo 58), Boehm and Wapstra add to the treatment of  $\text{Sc}^{46}$ ,  $\text{Au}^{198}$ , and  $\text{Co}^{58}$  a discussion of their work on  $\text{Sc}^{44}$ ,  $\text{V}^{48}$ , and  $\text{Na}^{24}$ . In the case of  $\text{Sc}^{44}$  and  $\text{V}^{48}$ , the values of  $A = -0.02 \pm 0.04$  and  $+0.06 \pm 0.05$  indicate some interference since they are greater than the pure  $GT$  values of  $-0.17$  and  $-0.083$ , respectively. If, as in the case of  $\text{Sc}^{46}$ , the maximum interference is assumed,  $|M_{GT}/M_F| \cong 5$  for both nuclei. For  $\text{Na}^{24}$  a value of  $A = +0.07 \pm 0.04$  is obtained as compared to the pure  $GT$  value of 0.08. If maximum interference is assumed,  $|M_{GT}/M_F| > 25$ . Interference between the  $GT$  and  $F$  interactions was also found by Boehm (Bo 58a) in the decay of  $\text{Mn}^{52}$ . In this example,  $A = -0.16 \pm 0.05$ , and the pure  $GT$  value is  $-0.056$ .

¶¶¶ The other term in  $I$  has a maximum value  $\cong 0.12$ .



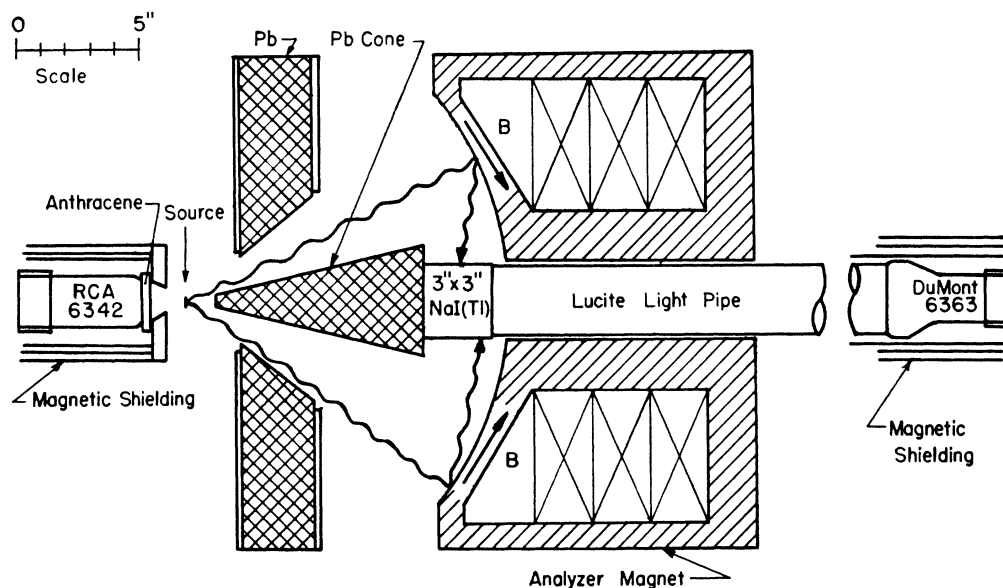


FIG. 37. Experimental arrangement of Steffen utilizing the method in which the electron polarization is perpendicular to the circular polarization (figure from St 58a).

Among the other early investigators in this field were Lundby *et al.* (Lu 57) who also made measurements on  $\text{Co}^{60}$ . Since it was felt the energy discrimination would be improved, they used the method of transmission through magnetized iron instead of the forward-scattering technique. They found a value of  $A = -0.32 \pm 0.07$ . In a note added in proof a value of  $A = +0.34 \pm 0.14$  for  $\text{Na}^{22}$  also is given.

DeBrunner and Kündig (De 57) using the method of scattering also measured the anisotropy coefficient for  $\text{Co}^{60}$  and found  $A = -0.344 \pm 0.09$  in good agreement with other values and with the theoretical value of  $-\frac{1}{3}$ . Shortly thereafter Berthier *et al.* (Be 57a) using the same equipment studied  $\text{Au}^{198}$ , the decay of which is first forbidden. It was found that  $A = 0.34 \pm 0.09$  which is somewhat smaller than the value above (Bo 58).

Again using the forward scattering from magnetized iron, Appel and Schopper (Ap 57) measured the circular-polarization correlations in  $\text{Co}^{60}$ ,  $\text{Zr}^{95}$ , and  $\text{Sb}^{124}$ . The measurement on  $\text{Co}^{60}$  was primarily to test the reliability of the apparatus, but they give a value of  $A = -0.35 \pm 0.05$  for this nucleus. In the case of the decay of  $\text{Zr}^{95}$ , the measurements were made on the unresolved 0.722- and 0.754-Mev radiations from  $\text{Nb}^{95}$ . By comparing the experimental value of  $A = -0.46 \pm 0.09$  with possible theoretical values in the manner discussed in the foregoing (Al 57), Appel and Schopper conclude that there is probably present an  $ST$  or  $VA$  interference term. The measurements made with  $\text{Sb}^{124}$ , which has a first-forbidden transition to the 0.605-Mev state in  $\text{Te}^{124}$ , yielded a value of  $A = -0.13 \pm 0.06$ . This is smaller in absolute value than the value of  $A = -\frac{1}{3}$  calculated (Al 57) on the basis of a simple once-forbidden transition.

In an effort to determine whether or not parity breakdown is a maximum, Appel *et al.* (Ap 58) remeasured more accurately the beta-gamma circular-polarization correlations in  $\text{Co}^{60}$  and  $\text{Na}^{22}$ . The measurement of the polarization correlation seems favorable for this purpose since all the necessary corrections can be calculated accurately and systematic errors can be kept small. They found  $A = -0.340 \pm 0.035$  and  $A = +0.295 \pm 0.054$  for  $\text{Co}^{60}$  and  $\text{Na}^{22}$ , respectively. These values compare favorably with the corresponding theoretical values of  $-\frac{1}{3}$  and  $+\frac{1}{3}$  for the case when nonconservation of parity and noninvariance under charge conjugation are maximum.

Steffen (St 58) also studied the circular polarization of the gamma rays from  $\text{Co}^{60}$  and  $\text{Sc}^{46}$ . He verified the dependence of the degree of circular polarization on  $v/c$  [Eq. (III-9)] and that the angular distribution varies as  $\cos\theta$ . For  $\text{Co}^{60}$  and  $\text{Sc}^{46}$ , values of  $A = -0.34 \pm 0.02$  and  $A = +0.24 \pm 0.02$  were found. Although the  $\text{Sc}^{46}$  value is smaller than that given by Bo 58, it verifies the presence of a large interference between  $GT$  and  $F$  interaction. If maximum interference between  $V$  and  $A$  interactions is assumed,  $|M_{GT}/M_F| \simeq 4.0$ . With these nuclei Steffen (St 85a) has also used the method (Be 57) in which the electron polarization is perpendicular to the circular polarization. His experimental arrangement is shown in Fig. 37.

In a beautiful experiment by Goldhaber *et al.* (Go 58) on the 80-kev isomer of  $\text{Eu}^{152}$ , it was shown that the neutrino is left handed (negative helicity).  $\text{Eu}^{152}$  decays by electron capture to the 961-kev state in  $\text{Sm}^{152}$ . The experiment was performed by measuring the circular polarization of the 961-kev gamma rays which are subsequently resonant scattered from  $\text{Sm}^{152}$ . The ex-

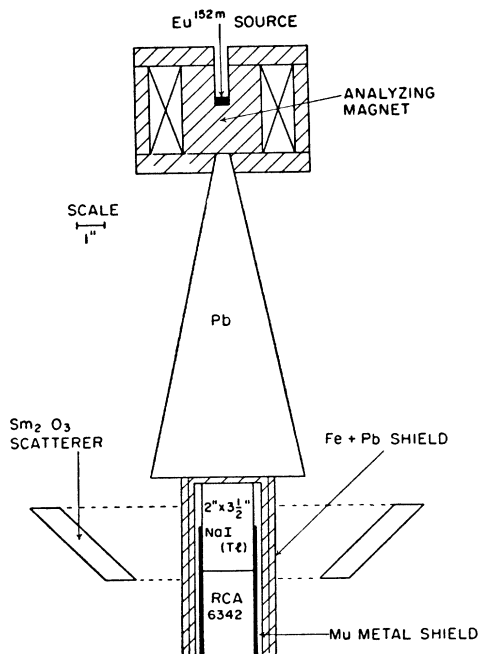


FIG. 38. Experimental arrangement for measurement of circular polarization of resonant scattered gamma rays. This arrangement was used by Goldhaber *et al.* to determine helicity of neutrinos (figure from Go 58).

perimental arrangement is shown in Fig. 38. Through conservation of energy and momentum the requirement of resonant scattering selects those gamma rays which are emitted opposite to the neutrino emitted in the electron capture. The magnetic analyzer determines the circular polarization (helicity) of the gamma rays. The helicity of the neutrino is then determined since a gamma ray emitted in the direction opposite to the neutrino will have the same helicity by conservation of angular momentum. The measurement gave negative helicity for the gamma ray and thus also for the neutrino.

### E. Tabulation of Polarization Experiments on Nuclear Gamma Rays

The methods and results of the experiments discussed in the text are summarized in Table XIII. An explanation of the notation used and how the entries were made in the various columns of the table is given below.

**Column I. Nucleus.**—In all cases the nucleus given in this column is the nucleus emitting the gamma ray whose polarization is being measured. The experiments are listed in order of increasing mass number  $A$ .

**Column II. Source of reaction.**—In this column is given a level diagram of the radioactive decay or nuclear reaction used in each experiment. Frequently one diagram is applicable to several experiments and so is not repeated. The level diagrams given in the table are not complete. Only those levels which directly feed the gamma-ray transitions under study and those between the contributing levels and the ground state are shown in the diagram. Secondly, the level diagrams show only those transitions in the daughter or residual nucleus which give rise to the polarizations which were measured. Thirdly, only those beta transitions which lead directly to the gamma ray or cascade of gamma rays under

study are given by solid arrows. Dashed arrows denote the fact that other beta transitions *may* be contributing to the intensity of the gamma ray under study but not through the particular cascade under study. Decay by positron emission, electron emission, or electron capture are designated by  $\beta^+$ ,  $\beta^-$ , or  $EC$ , respectively.

In the case of the reactions in this table, the neutron, proton, or alpha particle is denoted by  $n$ ,  $p$ , or  $\alpha$ , respectively. In the case of resonant reactions, the resonant level is shown by a solid line. Nonresonant reactions show a dashed line, whereas in thick-target reactions a bracket is shown in place of all the "levels" reached in the compound nucleus. The bombarding energy is given as a dashed line in the initial nucleus. Neutron-capture reactions are shown with the "state" of the compound nucleus at the same height as that of the initial nucleus since thermal capture is involved in all cases. Coulomb excitation is denoted by a doubled-lined arrow.

Energy levels below 10 Mev are given to three significant figures, some of those above 10 Mev are given to four. The energies of the levels are given immediately to the right of the level, whereas the spins, when known, are given to the left. Gamma-ray energies are given between the level values either to the right or left, whichever is convenient. When the level scheme is sufficiently complicated, arrows are used to indicate the energy of the gamma ray. All energies and spins are the most recent given by the Nuclear Data Group, National Research Council (Mc 58a).

**Column III. Polarization technique.**—The letters given in this column denote the basic polarization technique used in each of the experiments. They are as follows:

$C$  = Compton polarimeter detecting linear polarization.

$C_f$  = Compton magnetic polarimeter detecting circular polarization by forward scattering.

$C_t$  = Compton magnetic polarimeter detecting circular polarization by transmission.

$D$  = Photodisintegration of the deuteron, detecting linear polarization by use of nuclear emulsions soaked in  $D_2O$ .

**Column IV. Experimental conditions.**—Three essential experimental conditions are given in this column. In order from top to bottom, as given with each experiment, they are as follows. (1) The physical entity which establishes the direction of quantization in the polarization correlation. Thus, if the direction is established by the propagation vector of an alpha particle, the entry  $\alpha$  is made; if by a magnetic field, the entry "mag. field" is made, etc. In cases where the direction of propagation of a gamma ray in a cascade establishes the direction, the gamma ray is specified by energy when it is known. If there has been no clear discrimination between which gamma ray establishes the direction and which is accepted by the polarimeter, only the symbol  $\gamma$  is placed in this position. It should be noted in cases where Bleaney's method of alignment is used, that the words "crystal electric field" have been used primarily for convenience and do not in general mean that this field direction is the alignment direction. In general the alignment direction is established as the result of the coupling between the crystal electric field and the atomic orbital motion which in turn is coupled to the spins. Thus different alignment directions may occur depending on the crystal used. (2) Below entry (1) is given the angle between the axis of quantization and the axis of the polarimeter. When a complete direction-polarization correlation function is determined, the range of angles is indicated by an arrow between the extremes of the angular range. (3) Below entry (2) is specified the gamma ray whose polarization is being measured. When there is more than one gamma ray being analyzed and energy discrimination is made between each, a semicolon is placed between them. When the gamma rays are not resolved, a comma is placed between them and a ( $n$ ) is inserted at the end. When there is discrimination available, but it is not specified which of the gamma rays is being analyzed, an "or" is placed between the gamma-ray entries.

**Column V. Summary of results.**—In the case of linear polarization measurements, the gamma rays studied are usually listed

first in vertical order with their multiplicities. The multiplicity is given even though additional evidence outside of the experiment listed usually is required to deduce it. In the case of the circular polarization measurements the anisotropy coefficient  $A$  is given for each gamma ray listed. In two instances  $N_+/N_-$  is used to indicate the ratio of counting rates before and after reversing the magnetic field.

The parity of a state is listed when it is of special interest, usually as designated by the author. The parity is determined, of

course, only relative to other assumed or known parities. Other information such as spins, the sign of a magnetic moment, etc., is frequently given also when it is considered a significant part of the author's conclusions. As a general rule, the chief conclusion of the author is the one given.

A colon is used to connect an item given in the column with the results of the measurements made on it, e.g., "cascade:  $4(E2)2(E2)0$ ."

A reference is made to other work (usually a measurement of

TABLE XIII. Summary of experiments. An explanation of the various entries is given in Sec. E of Part III.

Nucleus	Source or Reaction	Polarization Technique	Experimental Conditions	Summary of Results	Reference
$\text{He}^3$		D	p $90^\circ$ $\sim 6.3\gamma$	6.3 $\gamma$ : E1, $\sim 100\%$ polarized; agrees with Fo49	Wi52
$\text{B}^{11}$		Ct	p $0^\circ$ 2.14 $\gamma$	2.14 $\gamma$ : no circ. pol.; $N_+/N_- = 1.00025 \pm$ 0.00026, parity con- served	Wi58
$\text{N}^{14}$		C	$\text{He}^3$ $90^\circ$ 1.64 $\gamma$	1.64 $\gamma$ : M1 or E2, 3.95 state parity: +	Li58
$\text{O}^{16}$		C	$\alpha$ $118^\circ$ 6.14 $\gamma$	6.14 $\gamma$ : E3; $\text{Ne}^{20}$ exc. state and $\text{F}^{19}$ gnd. state parities: + (Ar50, Ba50)	Fr52
		D	p $90^\circ$ 6.14 $\gamma$ ; 6.91 $\gamma$ ; 7.12 $\gamma$	6.14 $\gamma$ : unpolarized, 6.91 $\gamma$ : E2, 7.12 $\gamma$ : E1; agrees with Se52 (Sa52)	Fa53

TABLE XIII (continued).

Nucleus	Source or Reaction	Polarization Technique	Experimental Conditions	Summary of Results	Reference
$O^{16}$		$C_t$	p $0^\circ$ 7.12 $\gamma$	7.12 $\gamma$ : no circ. pol. $N_+/N_- = 1.00003 \pm 0.00024$ parity conserved	W158
$F^{18}$		C	$He^3$ $90^\circ$ 0.94 $\gamma$	0.94 $\gamma$ : M1 or E2, 0.94 state parity: +	Li58
$Ne^{22}$		$C_f$	$\beta$ 152 $^\circ$ 1.28 $\gamma$	1.28 $\gamma$ : $A = -0.39 \pm 0.08$ ; additional proof of nonconservation of parity.	Sc57
$Mg^{24}$		D	p $90^\circ$ 10.8 $\gamma$	1.28 $\gamma$ : $A = -0.340 \pm 0.055$ ; accurate indication that nonconservation of parity and noninvariance under charge conjugation are maximum	Ap58
$Mg^{24}$		C	$\gamma$ 100 $^\circ$ 1.37 $\gamma$ or 2.75 $\gamma$	10.8 $\gamma$ : E1, $Na^{23}$ gnd.state parity: + (Gr55)	Hu56
$Mg^{24}$				1.37 $\gamma$ : E2, 2.75 $\gamma$ : E2; 1.37 $\gamma$ or 2.75 $\gamma$ agrees with B152	Es56

TABLE XIII (continued).

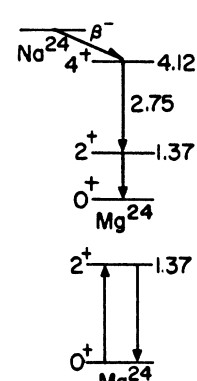
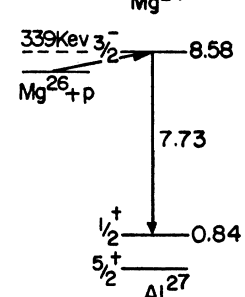
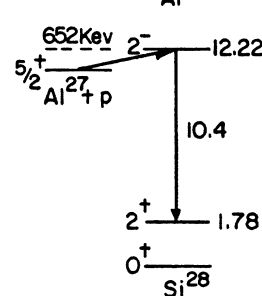
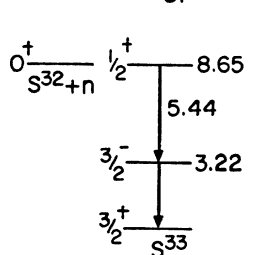
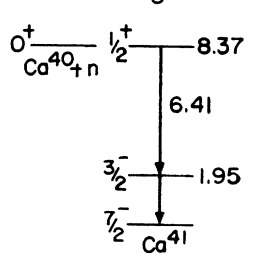
Nucleus	Source or Reaction	Polarization Technique	Experimental Conditions	Summary of Results	Reference
$Mg^{24}$		Cf	$\beta$ $152^\circ$ $1.37\gamma, 2.75\gamma(u)$	$1.37\gamma, 2.75\gamma(u): A = -0.068 \pm 0.047$	Sc57 Ap57
		Cf	$\beta$ $159^\circ$ $1.37\gamma, 2.75\gamma(u)$	$1.37\gamma, 2.75\gamma(u): A = +0.07 \pm 0.04;$ if max. interference assumed, $ M_{GT}/M_T  > 25$	Bo58
		C	p $90^\circ$ $1.37\gamma$	$1.37\gamma: E2$	Li58
$Al^{27}$		D	p $90^\circ$ $7.73\gamma$	$7.73\gamma: E1,$ $0.84$ state parity: + agrees with Da53 (Ru56)	Hu56
$Si^{28}$		D	p $90^\circ$ $10.4\gamma$	$10.4\gamma: E1,$ $Al^{27}$ gnd. state parity: - (Ru54)	Hu56
$S^{33}$		Ct	n polarization $0^\circ, 180^\circ$ $5.44\gamma$	$3.22$ state: $3/2,$ $3.22\gamma: E1$ (Ho53, Br54)	Tr57
$Ca^{41}$		Ct	n polarization $0^\circ, 180^\circ$ $6.42\gamma$	$1.95$ state: $3/2,$ $1.95\gamma: E2$ (Ho53, Br54)	Tr57

TABLE XIII (continued).

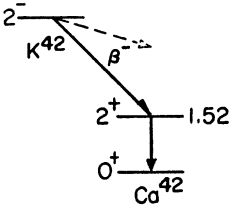
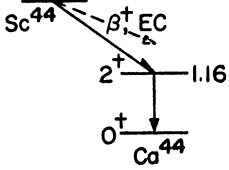
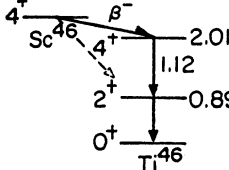
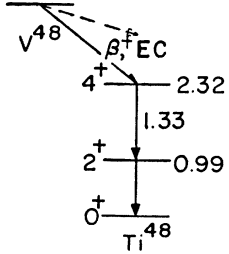
Nucleus	Source or Reaction	Polarization Technique	Experimental Conditions	Summary of Results	Reference
Ca <sup>42</sup>		C	$\beta$ 90° 1.52 $\gamma$	1.52 $\gamma$ : unpolarized (Be50b, St51)	Ha53a
Ca <sup>44</sup>		C <sub>f</sub>	$\beta$ 159° 1.16 $\gamma$	1.16 $\gamma$ : A = -0.02 ± 0.04; if max.interference assumed,  M <sub>GT</sub> /M <sub>FP</sub>   ≈ 5	Bo58
Ti <sup>46</sup>		C	$\gamma$ 90° → 180° 0.89 $\gamma$ , 1.12 $\gamma$ (u)	0.89 $\gamma$ : E2, 1.12 $\gamma$ : E2. cascade: 4(E2)2(E2)0 (Br48)	Me50
		C <sub>f</sub>	$\beta$ 159° 0.89 $\gamma$ , 1.12 $\gamma$ (u)	0.89 $\gamma$ , 1.12 $\gamma$ (u): A = 0.33 ± 0.04; large interference be- tween GT and F cou- plings; if max.in- terference assumed,  M <sub>GT</sub> /M <sub>FP</sub>   ≈ 2.2	Bo57b Bo58
		C <sub>f</sub>	$\beta$ ~155° 0.89 $\gamma$ , 1.12 $\gamma$ (u)	0.89 $\gamma$ , 1.12 $\gamma$ (u): A = 0.24 ± 0.02; verifies large inter- ference between GT and F couplings; if max.in- terference assumed,  M <sub>GT</sub> /M <sub>FP</sub>   ≈ 4	St58
Ti <sup>48</sup>		C <sub>f</sub>	$\beta$ 159° 0.99 $\gamma$ , 1.33 $\gamma$ (u)	0.99 $\gamma$ , 1.33 $\gamma$ (u): A = 0.06 ± 0.05; if max.interference assumed,  M <sub>GT</sub> /M <sub>FP</sub>   ≈ 5	Bo58
		C	1.33 $\gamma$ ; 0.99 $\gamma$ 105° 0.99 $\gamma$ ; 1.33 $\gamma$	0.99 $\gamma$ : E2 133 $\gamma$ : E2 cascade: 4(E2)2(E2)0	Co56a

TABLE XIII (continued).

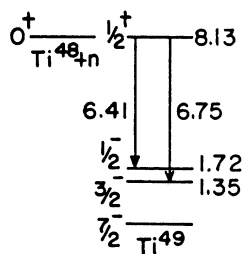
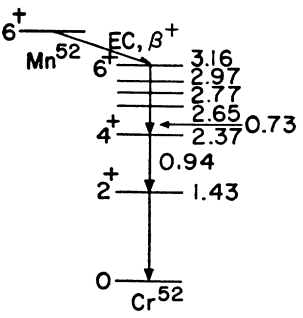
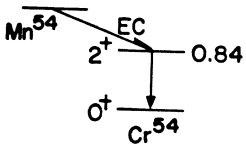
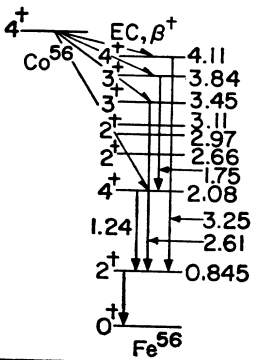
Nucleus	Source or Reaction	Polarization Technique	Experimental Conditions	Summary of Results	Reference
Ti <sup>48</sup>		Ct	n polarization 0°, 180° 6.41γ; 6.75γ	1.72 state: 1/2, 1.35 state: 3/2, 1.35γ: E2 (Ho53, Br54)	Tr57
Cr <sup>52</sup>		C	mag. field 90° 0.73γ; 0.94γ; 1.43γ	0.73γ: E2, 0.94γ: E2, 1.43γ: E2; agrees with Ke54	Hu57
		Cf	mag. field 0°, 180° 0.73γ, 0.94γ, 1.43γ(u)	Mn52 mag. mom: +	Hu57
		Cf	β 159° 0.73γ, 0.94γ, 1.43γ(u)	0.73γ, 0.94γ, 1.46γ(u): A = -0.16 ± 0.05; interference between GT and F couplings	Bo58a
Cr <sup>54</sup>		C	mag. field 90° 0.84γ	0.84γ: E2	Bi54
		Ct	n polarization 0°, 180° 8.88γ; 9.72γ	8.88γ: E1, 9.72γ: E1; 8.88 - 0.84 cascade: 1(E1)2(E2)0	Tr57
Fe <sup>56</sup>		C	mag. field 90° 0.845γ; 1.24γ; 1.75γ; 2.61γ; 3.25γ	0.845γ: E2, 1.24γ: E2, 1.75γ: M1, 2.61γ: M1, 3.25γ: E2; 0.845, 2.08, 3.45, 3.84, and 4.10 levels: 2+, 4+, 3+, 3+, and 4+ resp. (Sa55a)	D158
		C	1.24γ 90° 0.845γ	0.845γ: E2 (Hu55)	Wo55

TABLE XIII (continued).

Nucleus	Source or Reaction	Polarization Technique	Experimental Conditions	Summary of Results	Reference	
Fe <sup>57</sup>		C	crystal electric field 90°	0.122γ: E2/M1 = +0.19 ± 0.02 (A154)	Bi55a	
		Ct	n polarization 0°, 180°	7.64γ	Fe <sup>57</sup> gnd.state: 1/2 (B153)	Tr57
Fe <sup>58</sup>		C	crystal electric field 90°	0.800γ: E2 (Da52)	Bi52	
		Ct	β 159°	0.800γ	0.800γ: A = -0.14 ± 0.07; if max.interference assumed,  M <sub>GT</sub> /M <sub>F</sub>   ≈ 2.8	Bo57a, Bo58
Ni <sup>59</sup>		Ct	n polarization 0°, 180°	9.00γ	Ni <sup>59</sup> gnd.state: 3/2; confirms Pr54	Tr57
Ni <sup>60</sup>		C	γ 90° → 180°	1.17γ: E2, 1.33γ: E2; 1.17γ, 1.33γ(u) 1.17 - 1.33 cascade: 4(E2)2(E2)0 (Br48)	Me50	
			γ 90° → 180°	1.17γ, 1.33γ(u)	1.17γ: E2, 1.33γ: E2; agrees with Me50	W150



TABLE XIII (continued).

Nucleus	Source or Reaction	Polarization Technique	Experimental Conditions	Summary of Results	Reference
$\text{Ni}^{60}$		C	$\gamma$ $90^\circ \rightarrow 180^\circ$ 1.17 $\gamma$ , 1.33 $\gamma$ (u)	1.17 $\gamma$ : E2, 1.33 $\gamma$ : E2; agrees with Me50 and Wi50	K152
		C	crystal elec- tric field $90^\circ$ 1.17 $\gamma$ , 1.33 $\gamma$ (u)	1.17 $\gamma$ : E2, 1.33 $\gamma$ : E2; agrees with Me50	Bi52
		C	$\gamma$ $100^\circ$ 1.17 $\gamma$ or 1.33 $\gamma$	1.17 $\gamma$ : E2, 1.33 $\gamma$ : E2; agrees with Me50	Es56
		Cf	mag. field $151^\circ$ 1.17 $\gamma$ , 1.33 $\gamma$ (u)	$\text{Co}^{60}$ mag. mom: +	Wh55
		Cf	$\beta$ $152^\circ$ 1.17 $\gamma$ , 1.33 $\gamma$ (u)	1.17 $\gamma$ , 1.33 $\gamma$ (u): A = -0.41 $\pm$ 0.07; $\nu$ in $\beta^+$ decay in oppo- site screw sense from $\nu^-$ in $\beta^-$ decay	Sc57
		Cf	$\beta$ $159^\circ$ 1.17 $\gamma$ , 1.33 $\gamma$ (u)	1.17 $\gamma$ , 1.33 $\gamma$ (u): A = -0.41 $\pm$ 0.08	Bo57 Bo58
		Ct	$\beta$ $180^\circ$ 1.17 $\gamma$ , 1.33 $\gamma$ (u)	1.17 $\gamma$ , 1.33 $\gamma$ (u): A = -0.32 $\pm$ 0.07	Lu57
		Cf	$\beta$ $153^\circ$ 1.17 $\gamma$ , 1.33 $\gamma$ (u)	1.17 $\gamma$ , 1.33 $\gamma$ (u): A = -0.35 $\pm$ 0.05	Ap57
				1.17 $\gamma$ , 1.33 $\gamma$ (u): A = +0.295 $\pm$ 0.054; accurate indication that nonconservation of parity and noninvari- ance under charge conju- gation are maximum	Ap58
		Cf.	$\beta$ $\sim 150^\circ$ 1.17 $\gamma$ , 1.33 $\gamma$ (u)	1.17 $\gamma$ , 1.33 $\gamma$ (u): A = -0.344 $\pm$ 0.09	De57
	Cf	$\beta$ $\sim 150^\circ$ 1.17 $\gamma$ , 1.33 $\gamma$ (u)	1.17 $\gamma$ , 1.33 $\gamma$ (u): A = -0.34 $\pm$ 0.02	St58	
$\text{Zn}^{65}$		Ct	n polarization $0^\circ, 180^\circ$ 7.88 $\gamma$	0.052 state: 3/2 (Cr54)	Tr57

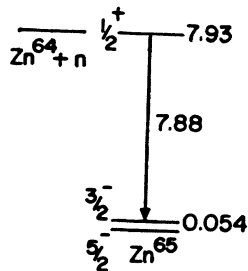


TABLE XIII (continued).

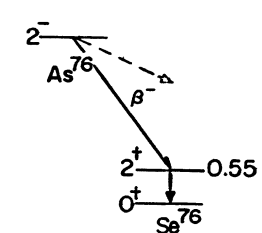
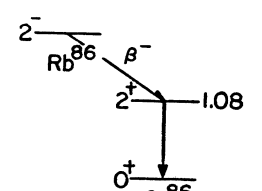
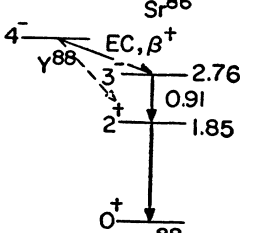
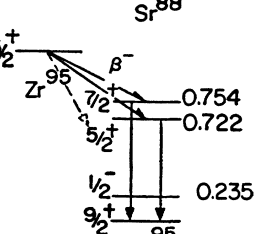
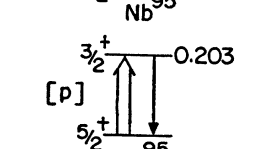
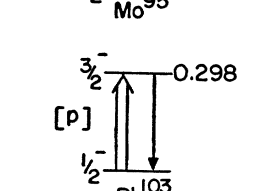
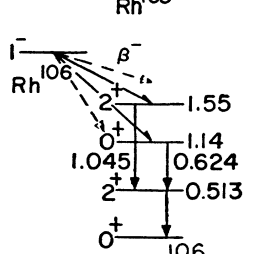
Nucleus	Source or Reaction	Polarization Technique	Experimental Conditions	Summary of Results	Reference
Se <sup>76</sup>		C	$\beta$ $90^\circ$ 0.55 $\gamma$	0.55 $\gamma$ : E2 (Ri52, Wa50a)	Ha53a
Sr <sup>86</sup>		C	$\beta$ $90^\circ$ 1.08 $\gamma$	1.08 $\gamma$ : E2 (St51, Ri52)	Ha53a
Sr <sup>88</sup>		C	1.85 $\gamma$ $90^\circ$ 0.91 $\gamma$	1.85 $\gamma$ : E2, 0.91 $\gamma$ : E1; cascade: 3(E1)2(E2)0 agrees with Pe48 and Me52a	Bi55
		C	1.85 $\gamma$ ; 0.91 $\gamma$ $90^\circ \rightarrow 180^\circ$ 0.91 $\gamma$ ; 1.85 $\gamma$	0.91 $\gamma$ : E1 1.85 $\gamma$ : E2 agrees with Bi55	Co56
Nb <sup>95</sup>		Cf	$\beta$ $153^\circ$ 0.722 $\gamma$ , 0.754 $\gamma$ (u)	0.722 $\gamma$ , 0.754 $\gamma$ (u): A = -0.46 $\pm$ 0.09; S,T or V,A interference is present	Ap57
Mo <sup>95</sup>		C	p $90^\circ$ 0.203 $\gamma$	0.203 $\gamma$ : $(E2/M1)^{1/2} =$ -0.58 $\pm$ 0.20	Mc58
Rh <sup>103</sup>		C	p $90^\circ$ 0.298 $\gamma$	0.298 $\gamma$ : $(E2/M1)^{1/2} =$ -0.17	Mc58
Pd <sup>106</sup>		C	$\gamma$ $90^\circ \rightarrow 180^\circ$ 0.513 $\gamma$ , 0.73 $\gamma$ (u)	0.513 $\gamma$ : E2, 0.73 $\gamma$ : E2: cascade: 0(E2)2(E2)0 tentatively (Br48)	Me50

TABLE XIII (continued).

Nucleus	Source or Reaction	Polarization Technique	Experimental Conditions	Summary of Results	Reference
Pd <sup>106</sup>		C	$\gamma$ 90° → 180° 0.513 $\gamma$ , 0.73 $\gamma$ (u)	0.513 $\gamma$ : E2; cascade: suggest 0(E2)2(E2)0 mixed with cascade from close lying 3rd exc. state (Sp50, K153, Kr53).	W150
Ag <sup>107</sup>		C	p 90° 0.324 $\gamma$	0.324 $\gamma$ : (E2/M1) <sup>1/2</sup> = -0.21	Mc58
Ag <sup>109</sup>		C	p 90° 0.309 $\gamma$	0.309 $\gamma$ : (E2/M1) <sup>1/2</sup> = -0.19	Mc58
Cd <sup>111</sup>		C	p 90° 0.342 $\gamma$	0.342 $\gamma$ : (E2/M1) <sup>1/2</sup> = 0.385	Mc58
Cd <sup>113</sup>		C	p 90° 0.300 $\gamma$	0.300 $\gamma$ : (E2/M1) <sup>1/2</sup> = 0.29	Mc58
Cd <sup>114</sup>		C	$\gamma$ 90° → 270° 0.566 $\gamma$ , 0.722 $\gamma$ (u) cascade: 4(E2)2(2E)0	0.566 $\gamma$ : E2 0.722 $\gamma$ : E2	Br56
Te <sup>124</sup>		C	$\beta$ 90° 0.605 $\gamma$	0.605 $\gamma$ : E2 (St51)	St52
		C	$\beta$ 90° → 180° 0.605 $\gamma$	0.605 $\gamma$ : E2 (K152)	K152
		C	$\gamma$ 90° → 180° 1.69 $\gamma$ , 0.605 $\gamma$ (u)	0.605 $\gamma$ : E2, 1.69 $\gamma$ : E2/M1 = 0.09, cascade: 3(E2, M1)2(E2)0	K152
		C	$\beta$ 90° 0.605 $\gamma$	0.605 $\gamma$ : E2 (Be50b)	Ha53a

TABLE XIII (continued).

Nucleus	Source or Reaction	Polarization Technique	Experimental Conditions	Summary of Results	Reference
Te <sup>124</sup>		C <sub>f</sub>	β 153° 0.605γ	0.605γ: A = 0.13 ± 0.06	Ap57
Ba <sup>134</sup>		C	γ 90° → 180° 0.563γ, 0.570γ, 0.605γ, 0.796γ(u)	polarization consistent with a composite correlation coefficient = 0.13	Me50
		C	γ 90° → 180° 0.563γ, 0.570γ, 0.605γ, 0.796γ(u)	γ: unpolarized; see K152 which agrees with Me50 (St55)	W150
		C	γ 90° → 180° 0.563γ, 0.570γ, 0.605γ, 0.796γ(u)	0.605γ: E2, 0.796γ: E2; 1.402 - 0.605 cascade: <b>4(E2)2(E2)0, (Ro51)</b>	K152
		C	γ polarimeter 180° 0.563γ, 0.570γ, 0.605γ, 0.796γ(u)	polarization - polarization correlation observed not in disagreement with Wa50, Pe51 and Ro51	Ro52
		C	β 90° 0.563γ, 0.570γ, 0.605γ, 0.796γ(u)	0.605γ, 0.796γ(u): unpolarized (Be50a, St50)	Ha53a
Ce <sup>140</sup>		C	1.60γ 90° 0.329γ, 0.487γ; 0.815γ	0.329γ: E1, 0.487γ: E2, 0.815γ: E1; cascade: <b>3(E1)4(E2)2(E2)0</b>	B155
Pr <sup>141</sup>		C	crystal electric field 90° 0.145γ	0.145γ: E2/M1 = 0.08 ± 0.02 (Ca55)	Ca55
Sm <sup>152</sup>		C <sub>t</sub>	ν 167° 0.960γ	0.960γ: neg. helicity, ν: neg. helicity; GT interaction is A,	Go58

TABLE XIII (continued).

Nucleus	Source or Reaction	Polarization Technique	Experimental Conditions	Summary of Results	Reference
Ta <sup>181</sup>		C	0.133 $\gamma$ 90° 0.482 $\gamma$	0.482 $\gamma$ : $(E2/M1)^{1/2} = 6.3$ ; 1.33 - 0.482 cascade: 1/2 <sup>+</sup> - 5/2 <sup>+</sup> - 7/2 <sup>+</sup> (Pa55, Me54a, He55)	St57
Au <sup>197</sup>		C	p 90° 0.280 $\gamma$	0.280 $\gamma$ : $(E2/M1)^{1/2} = -0.41$ $\pm 0.04$	Mc58
Hg <sup>198</sup>		C <sub>F</sub>	$\beta$ 159° 0.411 $\gamma$	0.411 $\gamma$ : A = +0.52 $\pm 0.09$ ; max. interference between different T (or A) and S (or V) matrix ele- ments	Bo57 Bo57a Bo58
		C <sub>F</sub>	$\beta$ ~150° 0.411 $\gamma$	0.411 $\gamma$ : A = 0.34 $\pm$ 0.05	Be57a
Tl <sup>203</sup>		C <sub>F</sub>	$\beta$ 159° 0.279 $\gamma$	0.279 $\gamma$ : A = -0.06 $\pm$ 0.22	Bo57 Bo58
		C	p 90° 0.279 $\gamma$	0.279 $\gamma$ : $(E2/M1)^{1/2} = 1.50$ $\pm 0.08$	Mc58
Tl <sup>205</sup>		C	p 90° 0.205 $\gamma$	0.205 $\gamma$ : $(E2/M1)^{1/2} = 1.46$ $\pm 0.16$	Mc58
Pb <sup>208</sup>		C	$\gamma$ 90° 0.583 $\gamma$ , 2.61 $\gamma$ (u)	0.583 $\gamma$ : E2, 2.61 $\gamma$ : E2; cascade: 4(E2)2(E2)0 (Pe50)	Kr53

TABLE XIII (addenda). Summary of experiments. An explanation of the various entries is given in Part III, E.

Nucleus	Method	Addenda. In the second column the letters have the same meaning as before. Result and reference
N <sup>14</sup>	D	Measurement of linear polarization of $\gamma$ ray in C <sup>13</sup> ( $\beta,\gamma$ )N <sup>14</sup> at $E_p=1.76$ Mev indicated no parity change in the transition to the ground state [Strassenburg, Hubert, Krone, and Prosser, Bull. Am. Phys. Soc. Ser. II, <b>3</b> , 372 (1958)].
Mg <sup>24</sup>	C <sub>f</sub>	Measurement of $\beta$ - $\gamma$ circular-polarization correlation in decay of Na <sup>24</sup> gave $A = +0.05 \pm 0.04$ in agreement with other results [R. M. Steffen and P. Alexander, reported in <i>Proceedings of the Rehoveth Conference on Nuclear Structure</i> (North-Holland Publishing Company, Amsterdam, 1958)].
P <sup>31</sup>	D	Linear polarization measured at three resonances in Si <sup>30</sup> ( $\beta,\gamma$ )P <sup>31</sup> . The 8.04-, 8.20-, and 8.24-Mev $\gamma$ rays are E1, M1, and E1, respectively (Tu 57).
S <sup>34</sup>	C	Measurement of $\gamma$ - $\gamma$ direction-polarization correlation in the 1.16-2.10-Mev cascade, with the $\gamma$ -rays resolved, confirmed the assignment of $2^+(M1,E2)2^+(E2)0^+$ and gave $\delta=0.13$ [C. G. Shute and P. S. Fisher, Phil. Mag. <b>3</b> , 726 (1958)].
Ti <sup>46</sup>	C <sub>t</sub>	Measurement of $\beta$ - $\gamma$ circular-polarization correlation in the decay of Sc <sup>46</sup> gave $A = +0.29 \pm 0.11$ in agreement with other results. [Lundby, Patro, and Stroot, quoted by M. A. Grace, Proc. Roy. Soc. (London) <b>A246</b> , 460 (1958)].
Ni <sup>60</sup>	C <sub>t</sub>	The $\beta$ - $\gamma$ circular-polarization correlation was measured as a function of $v/c$ . Circular polarizations greater than $\frac{1}{2}v/c$ were observed, especially for small values of $v/c$ [Page, Pettersson, and Lindqvist, Phys. Rev. (to be published)].
Sm <sup>152</sup>	C <sub>t</sub>	The experiment of Go 58 was repeated to show that the neutrino has negative helicity in the decay of Eu <sup>152</sup> [I. Marklund and L. A. Page, Nuclear Phys. <b>9</b> , 88 (1958)].
W <sup>183</sup>	C <sub>t</sub>	Measurement of circular-polarization of radiation following capture of polarized thermal neutrons indicated complete right circular polarization in agreement with spin assignments and the expected E1 character of the radiation. Result used by Tr 57 to establish the reliability of experimental arrangement.
Hg <sup>195</sup>	C <sub>f</sub>	Measurement of $\beta$ - $\gamma$ circular-polarization correlation on decay of Au <sup>198</sup> gave $A = 0.45 \pm 0.06$ for an electron energy range of 520-620 kev and $A = 0.38 \pm 0.10$ for a range of 620-850 kev (R. M. Steffen and P. Alexander, see Mg <sup>24</sup> above).
Hg <sup>198</sup>	C	The 411-kev $\gamma$ ray from Au <sup>198</sup> was resonant scattered by Hg <sup>198</sup> and the linear polarization of the scattered radiation was measured. A multipolarity of E2 was confirmed for the radiation [V. Knapp and B. S. Sood, Proc. Roy. Soc. (London) <b>A247</b> , 369 (1958)].
Pb <sup>208</sup>	C	Linear polarization measurements [G. T. Wood and P. S. Jastram, Phys. Rev. <b>100</b> , 1237(A) (1955)] along with directional measurements confirmed the assignments, of $0^+$ , $3^-$ , $5^-$ , $4^-$ , and $5^-$ to the first 5 states in Pb <sup>208</sup> [Elliott, Graham, Walker, and Wolfson, Phys. Rev. <b>93</b> , 356 (1954)].

the direction-direction correlation) if it seems particularly relevant or related to the polarization measurement. No attempt is made at completeness in the listing of relevant references.

*Column VI. Reference.*—The reference corresponding to each experiment listed in the table is given in this column.

#### ACKNOWLEDGMENTS

We would like to thank Dr. Joachim Ehrman for many helpful discussions and Dr. Francis E. Throw for his generous aid and advice in writing the manuscript. Dr. Phillip Malmberg, Mr. Ronald Fast, and Mr. Samuel Chappell were of great assistance in the search of the literature. Mr. Chappell also helped with some of the calculations. Mr. Ralph Klingler provided many of the calculations on which the tables are based. The Graphic Arts Branch of NRL supplied most of the figures and reproductions. We are grateful also to Dorothy Bodden for her careful preparation of the manuscript. One of us (SSH) would like to thank the Guggenheim Memorial Foundation for a fellowship which aided in the work.

#### BIBLIOGRAPHY

- Ag 57 A. Agodi, Nuovo cimento **5**, 21 (1957).  
 Al 54 D. E. Alburger and M. A. Grau, Proc. Phys. Soc. (London) **A67**, 280 (1954).  
 Al 55 L. Allen, Jr., Phys. Rev. **98**, 705 (1955).  
 Al 56 Alder, Bohr, Huus, Mottelson, and Winther, Revs. Modern Phys. **28**, 432 (1956).  
 Al 57 Alder, Stech, and Winther, Phys. Rev. **107**, 728 (1957).  
 Am 56 Ambler, Hudson, and Temmer, Phys. Rev. **101**, 196 (1956).  
 Am 57 Ambler, Hayward, Hoppes, and Hudson, Phys. Rev. **105**, 1413 (1957).  
 Ap 57 H. Appel and H. Schopper, Z. Physik **149**, 103 (1957).  
 Ap 58 Appel, Schopper, and Bloom, Phys. Rev. **109**, 2211 (1958).  
 Ar 50 W. R. Arnold, Phys. Rev. **80**, 34 (1950).  
 Ar 53 P. Argyres and G. Kittel, Acta Met. **1**, 241 (1953).  
 Au 27 P. Auger and F. Perrin, J. phys. radium **8**, 93 (1927).  
 Ba 50 Barnes, French, and Devons, Nature **166**, 145 (1950).  
 Be 50 H. A. Bethe and C. Longmire, Phys. Rev. **77**, 647 (1950).  
 Be 50a T. H. Berlin and L. Mandansky, Phys. Rev. **78**, 623 (1950).  
 Be 50b J. R. Beyster and M. L. Wiedenbeck, Phys. Rev. **79**, 728 (1950).  
 Be 56 H. A. Bethe and P. Morrison, *Elementary Nuclear Theory* (John Wiley and Sons, Inc., New York, 1956).  
 Be 57 D. B. Beard and M. E. Rose, Phys. Rev. **108**, 164 (1957).  
 Be 57a Berthier, Debrunner, Kündig, and Zwahlen, Helv. Phys. Acta **30**, 483 (1957).  
 Be 58 Benczer, Koller, Schwarzschild, Vise, and Wu, Phys. Rev. (to be published).  
 Bi 51 Biedenharn, Rose and Arfkin, Phys. Rev. **83**, 683 (1951).  
 Bi 52 Bishop, Daniels, Goldschmidt, Halban, Kurti, and Robinson, Phys. Rev. **88**, 1432 (1952).  
 Bi 53 L. C. Biedenharn and M. E. Rose, Revs. Modern Phys. **25**, 729 (1953).  
 Bi 54 Bishop, Daniels, Durand, Johnson, and Perez y Jorba, Phil. Mag. **45**, 1197 (1954).  
 Bi 55 G. R. Bishop and J. P. Perez y Jorba, Phys. Rev. **98**, 89 (1955).  
 Bi 55a Bishop, Grace, Johnson, Knipper, Lemmer, Perez y Jorba, and Scurlock, Phil. Mag. **46**, 951 (1955).  
 Bl 48 E. Bleuler and H. L. Bradt, Phys. Rev. **73**, 1398 (1948).  
 Bl 51 R. J. Blin-Stoyle, Proc. Phys. Soc. (London) **A64**, 700 (1951).  
 Bl 51a B. Bleaney, Proc. Phys. Soc. (London) **A64**, 315 (1951).  
 Bl 52 S. Bloom, Phys. Rev. **88**, 312 (1952).  
 Bl 53 C. F. Black, Phys. Rev. **90**, 381 (1953).  
 Bl 57 R. J. Blin-Stoyle and M. A. Grace, *Handbuch der Physik* (Springer Verlag, Berlin, 1957), Vol. **42**, p. 555.  
 Bo 57 F. Boehm and A. H. Wapstra, Phys. Rev. **106**, 1364 (1957).

- Bo 57a F. Boehm and A. H. Wapstra, Phys. Rev. **107**, 1462 (1957).  
 Bo 57b F. Boehm and A. H. Wapstra, Phys. Rev. **107**, 1202 (1957).  
 Bo 58 F. Boehm and A. H. Wapstra, Phys. Rev. **109**, 456 (1958).  
 Bo 58a F. Boehm, Phys. Rev. **109**, 1018 (1958).  
 Br 48 E. L. Brady and M. Deutsch, Phys. Rev. **74**, 1541 (1948).  
 Br 54 Bretscher, Alderman, Elwyn, and Shull, Phys. Rev. **96**, 103 (1954).  
 Br 56 J. N. Brazos and R. M. Steffen, Phys. Rev. **102**, 753 (1956).  
 Br 57 Brini, Peli, Rimondi, and Veronesi, Nuovo cimento **6**, 98 (1957).  
 Bu 24 F. W. Bubb, Phys. Rev. **23**, 137 (1924).  
 Ca 55 Cacho, Grace, Johnson, Knipper, Scurllock, and Taylor, Phil. Mag. **46**, 1287 (1955).  
 Ca 57 Cavanagh, Turner, Coleman, Gard, and Ridley, Phil. Mag. **21**, 1105 (1957).  
 Cl 52 F. P. Clay and F. L. Hereford, Phys. Rev. **85**, 675 (1952).  
 Co 53 F. Coester and J. M. Jauch, Helv. Phys. Acta **26**, 3 (1953).  
 Co 56 C. F. Coleman, Phil. Mag. **1**, 166 (1956).  
 Co 56a C. F. Coleman, Phys. Rev. **103**, 647 (1956).  
 Cr 54 B. Crasemann, Phys. Rev. **93**, 1034 (1954).  
 Da 52 Daniels, Grace, Halban, Kurti, and Robinson, Phil. Mag. **43**, 1297 (1952).  
 Da 52a C. M. Davission and R. D. Evans, Revs. Modern Phys. **24**, 79 (1952).  
 Da 53 Daniel, Koester, and Mayer-Kuchuk, Z. Naturforsch. **8a**, 447 (1953).  
 De 50 M. Deutsch and K. Siegbahn, Phys. Rev. **77**, 680 (1950).  
 De 57 P. Debrunner and W. Kundig, Helv. Phys. Acta **30**, 261 (1957).  
 De 57a S. Devons and L. J. B. Goldfarb, *Handbuch der Physik* (Springer Verlag, Berlin, 1957), Vol. 42, p. 362.  
 De 58 J. J. deSwart and R. E. Marshak, Phys. Rev. (to be published).  
 Di 58 Diddens, Huiskamp, Severiens, Miedema, and Steenland, Nuclear Phys. **5**, 58 (1958).  
 Es 56 Estulin, Popov, and Chukreev, Zhur. Eksptl. i Teort. Fiz. **30**, 1052 (1956).  
 Ev 55 R. D. Evans, *The Atomic Nucleus* (McGraw-Hill Book Company, Inc., New York, 1955).  
 Fa 48 D. L. Falkoff, Phys. Rev. **73**, 518 (1948).  
 Fa 49 U. Fano, J. Opt. Soc. Am. **39**, 859 (1949).  
 Fa 53 L. W. Fagg and S. S. Hanna, Phys. Rev. **92**, 372 (1953).  
 Fa 54 U. Fano, Phys. Rev. **93**, 121 (1954).  
 Fe 55 M. Ferentz and N. Rosenzweig, Argonne National Laboratory Report ANL-5324 (unpublished).  
 Fi 31 J. Fischer, Ann. Physik **8**, 821 (1931).  
 Fo 49 Fowler, Lauritsen, and Toolestrup, Phys. Rev. **76**, 1767 (1949).  
 Fr 38 W. Franz, Ann. Physik **33**, 698 (1938).  
 Fr 52 A. P. French and J. O. Newton, Phys. Rev. **85**, 1041 (1952).  
 Fu 50 E. G. Fuller, Phys. Rev. **79**, 303 (1950).  
 Ga 57 Yu. V. Capanov and V. S. Popov, Zhur. Eksptl. i Teort. Fiz. **33**, 256 (1957).  
 Go 34 C. G. Gorter, Physik. Z. **35**, 923 (1934).  
 Go 46 G. Goertzel, Phys. Rev. **70**, 897 (1946).  
 Go 48 C. J. Gorter, Physica **14**, 504 (1948).  
 Go 51 G. Goldhaber, Phys. Rev. **81**, 930 (1951).  
 Go 58 Goldhaber, Grodzins, and Sunyar, Phys. Rev. **109**, 1015 (1958).  
 Gr 54 Grace, Johnson, Kurti, Lemmer, and Robinson, Phil. Mag. **45**, 1192 (1954).  
 Gr 55 Grant, Rutherglen, Flack, and Hutchinson, Proc. Phys. Soc. (London) **A68**, 369 (1955).  
 Gr 55a T. P. Gray and G. R. Satchler, Proc. Phys. Soc. (London) **A68**, 349 (1955).  
 Gr 56 D. F. Griffing and J. C. Wheatley, Phys. Rev. **104**, 389 (1956).  
 Gu 53 S. B. Gunst and L. A. Page, Phys. Rev. **92**, 970 (1953).  
 Ha 40 D. R. Hamilton, Phys. Rev. **58**, 122 (1940).  
 Ha 48 D. R. Hamilton, Phys. Rev. **74**, 782 (1948).  
 Ha 48a R. C. Hanna, Nature **162**, 332 (1948).  
 Ha 51 O. Halpern, Phys. Rev. **82**, 753 (1951).  
 Ha 51a O. Halpern, Nature **168**, 782 (1951).  
 Ha 53 J. Halpern and E. V. Weinstock, Phys. Rev. **91**, 934 (1953).  
 Ha 53a Hamilton, Lemonik, and Pipkin, Phys. Rev. **92**, 1191 (1953).  
 He 44 W. Heitler, *The Quantum Theory of Radiation* (Oxford University Press, London, 1944).  
 He 51 F. L. Hereford, Phys. Rev. **81**, 482 (1951).  
 He 51a F. L. Hereford, Phys. Rev. **81**, 627 (1951).  
 He 53 F. L. Hereford and J. P. Keuper, Phys. Rev. **90**, 1043 (1953).  
 He 55 Heer, Ruetschi, Gimmi, and Kundig, Helv. Phys. Acta **28**, 336A (1955).  
 Ho 53 J. R. Holt and T. U. Marsham, Proc. Phys. Soc. (London) **A66**, 467, 565 (1953).  
 Hu 55 Hurley, Rudman, and Jastram, Phys. Rev. **98**, 1187(A) (1955).  
 Hu 56 I. S. Hughes and D. Sinclair, Proc. Phys. Soc. (London) **A69**, 125 (1956).  
 Hu 56a Huiskamp, Steenland, Miedema, Tolhoek, and Gorter, Physica **22**, 587 (1956).  
 Hu 57 Huiskamp, Diddens, Severiens, Miedema, and Steenland, Physica **23**, 605 (1957).  
 Hu 57a L. Hulthén and M. Sugawara, *Handbuch der Physik* (Springer Verlag, Berlin, 1957), Vol. 39, p. 129.  
 Ka 58 Katz, Kowalski, Brown, and Baerg, Bull. Am. Phys. Soc. Ser. II, **3**, 174 (1958).  
 Ke 54 G. L. Keister, Phys. Rev. **96**, 855(A) (1954).  
 Kh 55 G. P. Khutsishvili, J. Exptl. Teoret. Phys. (U.S.S.R.) **28**, 496 (1955).  
 Ki 31 P. Kirkpatrick, Phys. Rev. **38**, 1938 (1931).  
 Kl 29 O. Klein and Y. Nishina, Z. Physik **52**, 853 (1929).  
 Kl 52 Kloeper, Lennox, and Wiedebeck, Phys. Rev. **88**, 695 (1952).  
 Kl 53 E. D. Klema and F. K. McGowan, Phys. Rev. **92**, 1469 (1953).  
 Ko 56 O. Kofoed-Hansen and A. Winther, Kgl. Danske Videnskab. Selskab, Mat.-fys. Medd **30**, No. 20 (1956).  
 Kr 53 J. J. Kraushaar and M. Goldhaber, Phys. Rev. **89**, 1081 (1953).  
 Ku 35 N. Kurti and F. E. Simon, Proc. Roy. Soc. (London) **A149**, 152 (1935).  
 Le 55 Lemmer, Segault, and Grace, Proc. Phys. Soc. (London) **A68**, 701 (1955).  
 Le 56 T. D. Lee and C. N. Yang, Phys. Rev. **104**, 254 (1956).  
 Le 57 T. D. Lee and C. N. Yang, Phys. Rev. **105**, 1671 (1957).  
 Li 49 D. S. Ling and D. L. Falkoff, Phys. Rev. **76**, 1639 (1949).  
 Li 54 F. W. Lipps and H. A. Tolhoek, Physica **20**, 85 (1954).  
 Li 54a F. W. Lipps and H. A. Tolhoek, Physica **20**, 395 (1954).  
 Li 58 A. E. Litherland and H. E. Gove, Bull. Am. Phys. Soc. Ser. II, **3**, 200 (1958).  
 Ll 52 S. P. Lloyd, Phys. Rev. **88**, 906 (1952).  
 Lu 57 Lundby, Patro and Stroot, Nuovo cimento **6**, 745 (1957).  
 Ma 49 J. F. Marshall and E. Guth, Phys. Rev. **76**, 1879 (1949).  
 Ma 50 J. F. Marshall and E. Guth, Phys. Rev. **78**, 738 (1950).  
 Ma 51 J. E. MacDonald and D. L. Falkoff, Phys. Rev. **83**, 875 (1951).  
 Ma 58 F. Mandl, Proc. Phys. Soc. (London) **A71**, 177 (1958).  
 Mc 54 W. H. McMaster and F. L. Hereford, Phys. Rev. **95**, 723 (1954).  
 Mc 54a F. K. McGowan, Phys. Rev. **93**, 471 (1954).  
 Mc 58 F. K. McGowan and P. H. Stelson, Phys. Rev. **109**, 901 (1958).  
 Mc 58a C. L. McGinnis (private communication).  
 Me 50 F. Metzger and M. Deutsch, Phys. Rev. **78**, 551 (1950).  
 Me 52 F. R. Metzger, Phys. Rev. **86**, 435 (1952).  
 Me 52a F. R. Metzger and H. C. Amacher, Phys. Rev. **88**, 147 (1952).  
 Mo 57 M. Morita and R. S. Morita, Phys. Rev. **107**, 1316 (1957).  
 My 38 R. D. Myers, Phys. Rev. **54**, 361 (1938).  
 Ni 29 Y. Nishina, Z. Physik **52**, 869 (1929).  
 Pa 55 H. Paul and R. M. Steffen, Phys. Rev. **98**, 231 (1955).  
 Pe 48 W. C. Peacock and J. W. Jones, U. S. Atomic Energy Commission Declassified Document AEC-D 1812, March 1948 (unpublished).  
 Pe 50 H. E. Petch and M. W. Johns, Phys. Rev. **80**, 478 (1950).  
 Pe 51 C. L. Peacock and J. L. Braud, Phys. Rev. **83**, 484 (1951).  
 Po 49 R. V. Pound, Phys. Rev. **76**, 1410 (1949).  
 Po 54 O. J. Poppema, thesis, Groningen (1954).

- Po 57 Postma, Huiskamp, Miedema, Steenland, Tolhoek, and Gorter, *Physica* **23**, 259 (1957).
- Pr 47 M. H. L. Pryce and J. C. Ward, *Nature* **160**, 435 (1947).
- Pr 54 W. W. Pratt, *Phys. Rev.* **95**, 1517 (1954).
- Ri 52 S. L. Ridgway and F. M. Pipkin, *Phys. Rev.* **87**, 202 (1952).
- Ro 49 M. E. Rose, *Phys. Rev.* **75**, 213 (1949).
- Ro 51 B. L. Robinson and L. Madansky, *Phys. Rev.* **84**, 604 (1951).
- Ro 52 B. L. Robinson and L. Madansky, *Phys. Rev.* **88**, 1065 (1952).
- Ru 54 Rutherglen, Grant, Flack, and Deucbars, *Proc. Phys. Soc. (London)* **A67**, 101 (1954).
- Ru 56 Rutherglen, Deucbars, and Wallace (private communication in Hu 56).
- Sa 31 P. Sauter, *Ann. Physik* **11**, 454 (1931).
- Sa 51 E. E. Salpeter, *Phys. Rev.* **82**, 60 (1951).
- Sa 52 J. E. Sanders, *Phil. Mag.* **43**, 630 (1952).
- Sa 53 G. R. Satchler, *Proc. Phys. Soc. (London)* **A66**, 1081 (1953).
- Sa 54 G. R. Satchler, *Phys. Rev.* **94**, 1304 (1954).
- Sa 55 F. Sauter and H. O. Wuster, *Z. Physik* **141**, 83 (1955).
- Sa 55a M. Sakai, *J. Phys. Soc. Japan* **10**, 729 (1955).
- Sa 55b G. R. Satchler, *Proc. Phys. Soc. (London)* **A68**, 1041 (1955).
- Sc 30 G. Schur, *Ann. Physik* **4**, 433 (1930).
- Sc 50 L. I. Schiff, *Phys. Rev.* **78**, 733 (1950).
- Sc 57 H. Schopper, *Phil. Mag.* **2**, 710 (1957).
- Se 52 J. Seed and A. P. French, *Phys. Rev.* **88**, 1007 (1952).
- Se 53 E. Segre, *Experimental Nuclear Physics* (John Wiley & Sons, Inc., New York, 1956), Vol. I.
- Si 51 Simon, Rose, and Jauch, *Phys. Rev.* **84**, 1155 (1951).
- Si 53 A. Simon and T. A. Welton, *Phys. Rev.* **90**, 1036 (1953).
- Si 53a A. Simon, *Phys. Rev.* **92**, 1050 (1953).
- Sn 48 Snyder, Pasternak and Hornbostel, *Phys. Rev.* **73**, 440 (1948).
- So 30 A. Sommerfeld and G. Schur, *Ann. Physik* **4**, 409 (1930).
- Sp 50 J. A. Spiers, *Phys. Rev.* **78**, 75 (1950).
- St 50 R. Stump and S. Frankel, *Phys. Rev.* **79**, 243 (1950).
- St 51 D. T. Stevenson and M. Deutsch, *Phys. Rev.* **84**, 1071 (1951).
- St 51a R. M. Steffen, *Phys. Rev.* **83**, 166 (1951).
- St 52 R. Stump, *Phys. Rev.* **86**, 249 (1952).
- St. 52a N. R. Steenberg, *Proc. Phys. Soc. (London)* **A65**, 791 (1952).
- St 53 Steenberg, *Proc. Phys. Soc. (London)* **A66**, 391 (1953).
- St 53a N. R. Steenberg, *Proc. Phys. Soc. (London)* **A66**, 399 (1953).
- St 53b N. R. Steenberg, *Can. J. Phys.* **31**, 204 (1953).
- St 55 Stewart, Scharenberg, and Wiedenbeck, *Phys. Rev.* **99**, 691 (1955).
- St 56 R. M. Steffen and J. N. Brazos, *Phys. Rev.* **99**, 1646(A) (1956).
- St 57 P. H. Stelson and F. K. McGowan, *Phys. Rev.* **105**, 1346 (1957).
- St 57a M. J. Steenland and H. A. Tolhoek, *Progress in Low Temperature Physics* (North Holland Publishing Company, Amsterdam, 1957), Vol. II, p. 292.
- St 58 R. M. Steffen, *Bull. Am. Phys. Soc. Ser. II*, **3**, 205 (1958).
- St 58a R. M. Steffen (private communication).
- To 52 H. A. Tolhoek and J. A. M. Cox, *Physica* **18**, 357 (1952).
- To 52a H. A. Tolhoek, *Physica* **18**, 1257 (1952).
- To 53 H. A. Tolhoek and J. A. M. Cox, *Physica* **19**, 101 (1953).
- To 56 H. A. Tolhoek, *Revs. Modern Phys.* **28**, 277 (1956).
- Tr 57 G. Trumpy, *Nuclear Phys.* **2**, 664 (1957).
- Tr 57a G. Trumpy (to be published).
- Tu 57 Tutakin, Tzytco, Gonchar, Walter, and Lwov, USSR Conference on Low-Energy Nuclear Reactions, Moscow (1957).
- Va 56 J. H. Van Vleck, *Bull. Am. Phys. Soc. Ser. II*, **1**, 11 (1956).
- Vl 49 Vlasov, Dzhelepov, *Doklady Akad. Nauk.* **69**, No. 6, 777 (1949).
- Wa 50 Waggoner, Moon, and Roberts, *Phys. Rev.* **80**, 420 (1950).
- Wa 50a Walter, Huber, and Zunti, *Helv. Phys. Acta* **23**, 697 (1950).
- Wh 46 J. A. Wheeler, *Ann. N. Y. Acad. Sci.* **48**, 219 (1946).
- Wh 55 Wheatley, Huiskamp, Diddens, Steenland, and Tolhoek, *Physica* **21**, 841 (1955).
- Wh 58 A. Whetstone and J. Halpern, *Phys. Rev.* **109**, 2072 (1958).
- Wi 23 C. T. R. Wilson, *Proc. Roy. Soc. (London)* **A104**, 11 (1923).
- Wi 50 A. H. Williams and M. L. Wiedenbeck, *Phys. Rev.* **78**, 822 (1950).
- Wi 51 G. C. Wick, *Phys. Rev.* **81**, 467 (1951).
- Wi 51a M. Wiener, National Bureau of Standards Circular 515 (1951).
- Wi 52 D. H. Wilkinson, *Phil. Mag.* **43**, 659 (1952).
- Wi 56 E. J. Winhold and I. Halpern, *Phys. Rev.* **103**, 990 (1956).
- Wi 58 D. H. Wilkinson, *Phys. Rev.* **109**, 1610 (1958).
- Wo 49 L. Wolfenstein, *Phys. Rev.* **75**, 1664 (1949).
- Wo 55 G. T. Wood and P. S. Jastram, *Phys. Rev.* **98**, 1187(A) (1955).
- Wu 50 C. S. Wu and I. Shakhov, *Phys. Rev.* **77**, 136 (1950).
- Wu 57 Wu, Ambler, Hayward, Hoppes, and Hudson, *Phys. Rev.* **105**, 1413 (1957).
- Zi 50 I. Zinnes, *Phys. Rev.* **80**, 386 (1950).